

MINUTIAE-BASED PARTIAL FINGERPRINT RECOGNITION

by

Tsai-Yang Jea

A thesis submitted

to the Faculty of the Graduate School

of the University at Buffalo, the State University of New York

in partial fulfillment of the requirements

for the degree of Doctor of Philosophy

Department of Computer Science & Engineering

November 2005

Abstract

Although fingerprint matching based on minutia features is a well researched problem in the field of automatic fingerprint recognition, it is still an unsolved problem presenting many research challenges. Many algorithms have been proposed to match a pair of minutia templates of fingerprints. Most of these algorithms assume that the two templates are approximately of the same size. This assumption is no longer valid. The need for recognition of partial fingerprints is increasing in both forensic and civilian applications. In forensics, latent fingerprints lifted from crime scenes are often noisy and broken, thus the usable portions are small and partial. In civilian applications, the invention of small hand-held devices, such as mobile phones, PDAs, and miniaturized fingerprint sensors present considerable demands on partial fingerprints processing. Miniaturization of fingerprint sensors has led to small sensing areas varying from 1.0"x1.0" to 0.42"x0.42". However, fingerprint scanners with a sensing area smaller than 1.0"x1.0", which is considered to be the average fingerprint size (as required by FBI specifications), can only capture partial fingerprints.

Matching partial fingerprints against full pre-enrolled images in the database presents several problems: (i) the number of minutia points available in such partial fingerprints is few, thus reducing its discriminating power; (ii) loss of singular points (core and delta) is likely and therefore, a robust algorithm independent of these singularities is required; (iii)

uncontrolled impression environments result in unspecified orientations of partial fingerprints; and (iv) the skin elasticity and humidity can cause distortions which increase the ambiguity between genuine and imposter samples.

Generally, a fingerprint based biometrics system is considered as highly secure, and is equivalent to a long password system. However, with the decreasing number of features on a small fingerprint and the non-exact matching nature, the security strength of a partial fingerprint recognition reduces. The relation between the acquired fingerprint size and the security strength plays a key role in designing a fingerprint recognition system and is needed to be studied.

In this dissertation, we present: (i) two novel minutiae based fingerprint matching methods to overcome the challenges encountered by partial fingerprint recognition and (ii) a study of the security vulnerability of partial fingerprint recognition systems.

Contents

1	Introduction	1
1.1	Problem of Matching Partial fingerprints	2
1.2	Security Issues of Partial Fingerprint Matching	2
1.3	Previous Work	4
1.4	Proposed Approach	6
1.5	Thesis Outline	7
2	Background	8
2.1	Fingerprint Representation	8
2.1.1	Image-based representation	9
2.1.2	Global Ridge Pattern	11
2.1.3	Local Ridge Detail	11
2.1.4	Intra-ridge Detail	13
2.2	Minutiae-Based Fingerprint Recognition	13
2.3	Fingerprint Image Enhancement	14

2.4	Minutia Extraction	19
2.4.1	Binarization-based Minutiae Extraction	20
2.4.2	Direct Gray-scale Minutiae Extraction	25
2.5	Minutiae-Based Matching	28
3	Partial Fingerprint Recognition Using Secondary Features	33
3.1	Background	34
3.2	Our Method	37
3.2.1	The Partial Fingerprint Matching System	38
3.2.2	Brute-force Matching	39
3.2.3	Secondary Feature Matching	40
3.2.4	Dynamic Tolerance Areas	44
3.2.5	Minimum Cost Flow Problem (MCF)	46
3.2.6	Similarity Score Calculation	54
3.3	Experimental Results	60
3.4	Summary	66
4	Size Specific Fingerprint Matching	69
4.1	Introduction	69
4.2	Feature Generating and Indexing	70
4.3	Feature Matching	77
4.3.1	Local Matching and Validation	77

4.3.2	Extended Matching	79
4.4	Similarity Scores	87
4.5	Experimental Results	87
4.6	Summary	94
5	Security Strength of Partial Fingerprints	96
5.1	Brute-force Attack	97
5.2	Prior Related Work	97
5.3	Bit Strength of Partial Fingerprint	99
5.4	Analysis and Summary	101
6	Conclusion	105
A	Overview of Biometrics	108
A.1	Biometrics Applications	110
A.2	Verification vs. Identification	114
A.3	Performance Evaluation	116
B	Overview of Fingerprints	122
B.1	History of Fingerprints	125
B.2	Fingerprint Acquisition	129

List of Figures

1.1	Common work flow and challenges of a partial fingerprint recognition system.	3
2.1	Comparison of using JPEG and WSQ compression techniques on fingerprint images. (a) The original fingerprint portion. (b) After being compressed by JPEG algorithm with compression ratio 12.9:1. Note the blurred details on ridges and blocking artifacts. (c) After being compressed by WSQ algorithm with compression ratio 12.9:1. Note that there is <i>no</i> blocking artifacts and ridge details are well preserved. (images obtained from www.c3.lanl.gov/~brislawn)	10
2.2	Some of the common minutiae types.	12
2.3	(a) A ridge ending minutia: (x,y) are the minutia coordinates; θ is the minutia's orientation; (b) A ridge bifurcation minutia: (x,y) are the minutia coordinates; θ is the minutia's orientation.	12
2.4	A portion of a fingerprint where sweat pores (white dots on ridges) are visible.	13

2.5	(a) A good quality fingerprint image; (b) a poor quality fingerprint caused by extremely dry skin; (c) a noisy fingerprint image.	15
2.6	(a) Local region in a fingerprint image; (b) Surface wave approximation of (a).	16
2.7	Examples of directional median filters (DMF) [105] in eight directions. Note that the shape of the filter changes along with its direction.	18
2.8	(a) The window used for analyzing surrounding pixel intensity of x; (b) the window orientated along with the local ridge direction.	22
2.9	(a) an intra-ridge pixel; (b) a ridge ending; (c) a bifurcation; (d) a crossover.	22
2.10	Pixel patterns used to detect minutiae in [28, 100].	23
2.11	Chaincode contour representation: (a) image is scanned from top-right corner counterclockwise; (b) contour elements are stored in a list. Each element contains the position and slope information of the contour pixel. Summary information of each contour is stored at the end of the array and contains the coordinates of bounding box of a contour, number of pixels on the contour, area of the closed contour, and a flag to indicate whether the contour is interior or exterior; (c) slope convention.	24
2.12	Minutiae are located in the contours by looking for <i>significant</i> turns. A ridge ending is detected when there is a sharp left turn; whereas the ridge bifurcation is detected by a sharp right turn.	26

2.13	(a) Original image; (b) the contour representation of the image; (c) detected minutiae superimposed on the contour image.	26
2.14	Minutiae-based matching.	29
3.1	Proposed fingerprint matching system. M and N are the number of minutiae on query and reference fingerprints. α is a pre-defined value.	39
3.2	The proposed secondary feature.	41
3.3	The same minutiae extracted from two different impressions, in (a) it appears as a bifurcation but a ridge ending in (b).	42
3.4	An example of two false matched secondary features. They are similar at the local structures but conflict with each other in global context (at very different locations with respect to the core and delta points).	43
3.5	Dynamic tolerance area.	45
3.6	Match two fingerprints is equivalent to find the corresponding links between feature points.	47
3.7	Minutiae of I and R are aligned with respect to the reference point r . Minutiae from I are denoted by X s, and the minutiae from R are denoted as O s. In this figure, minutia m_I^2 falls in the tolerance areas of m_R^1 and m_R^2 . If m_I^2 were matched with m_R^1 , which is the closest minutia to m_I^2 , then m_R^2 would stay unmatched.	48

3.8	An example of minimum cost flow problem. Our goal is to find a flow from s to t with a maximum flow value and a minimum cost. The numbers assigned to each edge are the capacity and unit cost shown in parentheses. .	50
3.9	Flow network representation of minutia matching problem. All the edges in the network have capacity 1. The edges between source node s and nodes from I have zero cost as well as the edges from R to sink node t . Costs of the edges between nodes from I and nodes from R are from the cost matrix c .	53
3.10	Examples of convex hulls of overlapping areas. (a) vs. (b) is a genuine test; whereas (c) vs. (d) is a impostor test. Both tests have eight matched feature points. However, the convex hulls of overlapping areas of the test (a) vs. (b) have very small areas comparing to those of test (c) vs. (d), we can probably decide whether the decision of the test of (a) vs. (b) is a genuine test but the test of (c) vs. (d) is an impostor test.	56
3.11	A heuristic rule for generating similarity scores.	58
3.12	The architecture of the neural network. The network has 2 hidden layers and 3 bias nodes link to each node. The input layer has 6 nodes. The hidden layers have 5 and 2 nodes with tangent sigmoid transfer function and logarithmic sigmoid transfer function respectively. The output layer uses logarithmic sigmoid transfer function to generate the similarity score. .	59

3.13	ROC graph of system testing result on FVC2002 DB1 database. With heuristic rules for similarity scores, the system reaches the minimum total error rate at 4.53% (with FAR at 1.24% and FRR at 3.29%), and EER at 2.39%. With NN scores, the system reaches the minimum total error rate at 3.32% (with FAR at 0.39% and FRR at 2.93%), and EER at 2.13%. . . .	62
3.14	ROC graph of system testing result on FVC2002 DB2 database. With heuristic rules for similarity scores, the system reaches the minimum total error rate at 3.17% (with FAR at 1.24% and FRR at 1.93%), and EER at 1.69%. With NN scores, the system reaches the minimum total error rate at 2.49% (with FAR at 0.85% and FRR at 1.64%), and EER at 1.57%. . . .	63
3.15	ROC graph of the brute-force matching with the neural network generated scores of FVC2002 DB1 database. The system reaches the minimum total error rate at 1.88% (with FAR at 0.31% and FRR at 1.57%), and EER at 1.01%. With heuristic rules for similarity scores, the system reaches the minimum total error rate at 5.27% (with FAR at 1.27% and FRR at 4.00%), and EER at 2.67%.	64
3.16	System performances vs. different-sized partial fingerprints at random positions.	65
3.17	The system performances vs. different-sized partial fingerprints at central positions.	67

4.1	(a) Four synthetic minutiae. The gray-colored minutia A is used as central minutia to generate secondary features. (b) A genuine secondary feature generated according to Section 3.2.3. (c) The resulting false secondary feature if there is a spurious minutia X that is close to A . (d) The resulting false secondary feature if the minutia C is missing from the minutiae set.	72
4.2	(a) Genuine secondary features generated from the closest three neighboring minutiae. (b) Under the influence of a spurious minutia, genuine secondary features remain intact. (c) Under the influence of a missing minutia, some of the genuine secondary features are still available for matching.	74
4.3	(a) The eight quadrants, Q_0 to Q_7 , of a central minutia. Note that the quadrants are aligned with the orientation of the central minutia. (b) An example of secondary feature and it can be labeled as Q_0Q_2 , Q_0Q_3 , Q_1Q_2 , and Q_1Q_3	76
4.4	s_i^{xy} is a secondary feature on the query fingerprint with index label xy . When the matching is being executing, we match the s_i^{xy} against the secondary features on the reference fingerprint with the same index label.	78
4.5	Examples of clustered minutia points (in white dashed ovals); each minutia's <i>neighborhood list</i> contains only the minutiae that are within the same oval, thus it is difficult to propagate the match from one oval to another. This simplified example will be used in illustrating the process of our extended matching later.	81

4.6	Outlines of proposed extended matching.	83
4.7	(a) Modified neighborhoods of \mathbf{A} and \mathbf{a} . (b) After all the neighboring minutiae of \mathbf{A} and \mathbf{a} have been visited.	84
4.8	(a) After all the neighboring minutiae of $\mathbf{I}[4]$ and $\mathbf{R}[4]$ have been visited. (b) After all the neighboring minutiae of $\mathbf{I}[10]$ and $\mathbf{R}[10]$ have been visited.	84
4.9	(a) Final result of the extended matching. (b) The extended matching result if the <i>seeds</i> are not put into each other's <i>neighborhood list</i>	86
4.10	A comparison of ROC curves for FVC2002 DB1 database.	89
4.11	A comparison of ROC curves for FVC2002 DB2 database.	89
4.12	A comparison of ROC curves for FVC2002 DB3 database.	90
4.13	A comparison of ROC curves for system testings on partial fingerprint (20% of original size) templates.	91
4.14	A comparison of ROC curves for system testings on partial fingerprint (30% of original size) templates.	92
4.15	A comparison of ROC curves for system testings on partial fingerprint (40% of original size) templates.	92
4.16	A comparison of ROC curves for system testings on partial fingerprint (50% of original size) templates.	93
5.1	Number of minutia extracted from different sized images.	101

5.2	Bit strength vs. various fingerprint image sizes. d is the number of quantified orientations associated with every minutia point.	103
A.1	Different types of biometrics: Fingerprints, speech, handwriting, face, hand geometry and chemical biometrics	109
A.2	Examples on biometric identification applications: (a) Automatic Facial Recognition (AFR) system is used to track down crime suspects by West Yorkshire Police, UK. (www.westyorkshire.police.uk); (b) the INSPASS uses hand geometry for passenger recognition (www.volpe.dot.gov); (c) iris scanners are used by CANPASS Air systems (www.cbsa-asfc.gc.ca). . .	113
A.3	(a) IBM ThinkPad T42 with a integrated fingerprint scanner for security identification (www.ibm.com). (b) Mouse with fingerprint scanner that provides abilities for security logon, lock/unlock computer, and file encryptions. (www.brighton-electronics.com). (c) Iris scanner is used on ATM for customers to access their accounts without using PINs, passwords, or cards. (www.jaypeetex.com).	114
A.4	General architecture of a biometric verification system	116
A.5	Examples of intraclass variation. These are eight different fingerprint impressions (biometric signals) of the same finger (individual). Note that huge differences of image contrasts, locations, rotations, sizes, and qualities, exist among them.	117

A.6	Example of genuine and impostor distributions.	119
A.7	Examples of (a) FAR and FRR curves; (b) ROC curve.	120
B.1	Example of Fingerprint Classes: (a)Tended Arch (b)Arch (c)Right Loop (d)Left Loop (e)Whorl	127
B.2	Core and delta points in a fingerprint. The circle denotes the core point and the triangle denotes the delta point.	128
B.3	Various commercial <i>live-scan</i> fingerprint scanners.	130
B.4	General schematic for an FTIR based optical sensor	132
B.5	Capacitive sensing.	133

List of Tables

3.1	Comparison of different similarity score calculations. Results are calculated on the images from FVC2002 DB1 database. Images 57_2 and 57_4 are from the same finger but different impressions. Images 23_1 and 45_1 are from different fingers.	60
3.2	System performance with difference sized partial images at random positions.	66
3.3	System performance with difference sized partial images around the center of the print.	67
4.1	Various average values of numbers of secondary features in a bin. These values are obtained from 15500 processing results.	76
4.2	A summary of the comparative results.	88
4.3	A summary of the comparative results of partial fingerprint recognition. Note that the number of testing instances is different from what we used in Section 3.3.	91
4.4	A summary of the comparative results.	93

4.5	A summary of the comparative results on partial fingerprint recognition of the proposed matching and the method that is described in Chapter 3. . . .	94
5.1	Effects on bit strength of minutiae-based fingerprint recognition system of decreasing input image size. Note that, in this table, we assume there are at least 17 matched minutiae to be considered as a successful match (i.e. $th = 17$).	104
A.1	Comparison of biometric technologies [70]. H, M, and L, denote High, Medium and Low respectively.	111

Acknowledgments

I would like to acknowledge all the people who have assisted me during my graduate study at The State University of New York at Buffalo. I am most grateful to Dr. Venu Govindaraju, my advisor, for his great encouragement, advice, and guidance professionally and personally. He has provided me the honor and opportunity to work at the Center for Excellence for Document Analysis and Recognition (CEDAR) and the Center for Unified Biometrics and Sensors (CUBS) and has also been very patient and understanding. I am very fortunate to have him as my advisor. I am indebted to my dissertation committee, Dr. Venu Govindaraju, Dr. Aidong Zhang, and Dr. Peter D. Scott for their support.

My deep appreciation goes to Dr. Wen-Jann Yang, my best friend and colleague, for his many insightful discussions, useful suggestions, personal help, and the delightful lunch meeting routine. I also want to acknowledge all my colleagues in CEDAR and CUBS, especially David Bartnik, Dr. Zhixin Shi, Dr. Xia Liu, Sergey Tulyakov, and Phil Kilinskas.

Thanks to all my fellow students, without their collaborations this dissertation could not be completed. My special thanks go to my wonderful team members, Sharat Chikkerur and Chaohong Wu. Sharat Chikkerur has provided me with numerous suggestions, discussions, and encouragements. Chaohong Wu has also provided great help in developing our fingerprint recognition systems. I deeply appreciate Sergey Tulyakov and Amit Mhatre for the discussions and suggestions. Thanks to Shamalee Deshpande for proofreading the draft of this dissertation.

My thanks extend to the staff of CEDAR and CUBS, in particular Ms. Eugenia Smith, Ms. Mary Jane Gallo, and Mr. Ed Sobczak for their administrative help.

I sincerely thank my parents for their sacrifice, understanding, patience, encouragement, love, and support and I would like to express my heartfelt thanks to my beloved wife, Chiu-Yin, for her selfless love and support.

To my beloved wife, Chiu-Yin, my parents, and family

Chapter 1

Introduction

Automatic fingerprint recognition has become a widely used technology in both forensic and biometrics applications. Despite a history of a thousand years during which fingerprints have been used as individual's proof of identity and decades of research on automated systems, reliable fully automatic fingerprint recognition is still an unsolved challenging research problem. Moreover, most of the research thus far, assumes that the two fingerprint templates being matched are approximately of the same size and cover large areas of the finger tip. However, this assumption is no longer valid. The miniaturization of fingerprint sensors has led to small sensing areas and can only capture partial fingerprints. Partial fingerprints are also common in forensic applications. Where small usable portions of latent fingerprints must be matched with large previously enrolled complete fingerprints.

In this dissertation, we present: (i) two novel minutiae based fingerprint matching methods to overcome the challenges encountered by partial fingerprint recognition and (ii) a

study of the security vulnerability of partial fingerprint identification systems.

1.1 Problem of Matching Partial fingerprints

Matching partial fingerprints presents several problems:

- the number of minutia points available in such prints is few, thus reducing its discriminating power;
- loss of singular points (core and delta) is likely and therefore, a robust algorithm that does not make use of these singularities is required;
- uncontrolled impression environments result in unspecified orientations of partial fingerprints; and
- the elasticity of human skin and humidity can cause distortions.

The challenges faced in implementation of matching systems that deal with partial or incomplete fingerprints are outlined in Figure 1.1. Since only a small number of feature points are present on a partial fingerprint, the decision making based just on the number of matched feature points is prone to failure.

1.2 Security Issues of Partial Fingerprint Matching

In general, fingerprint recognition systems are considered as being of high security strength.

Since a fingerprint data is in the order of several kilobytes, it provides the security of having

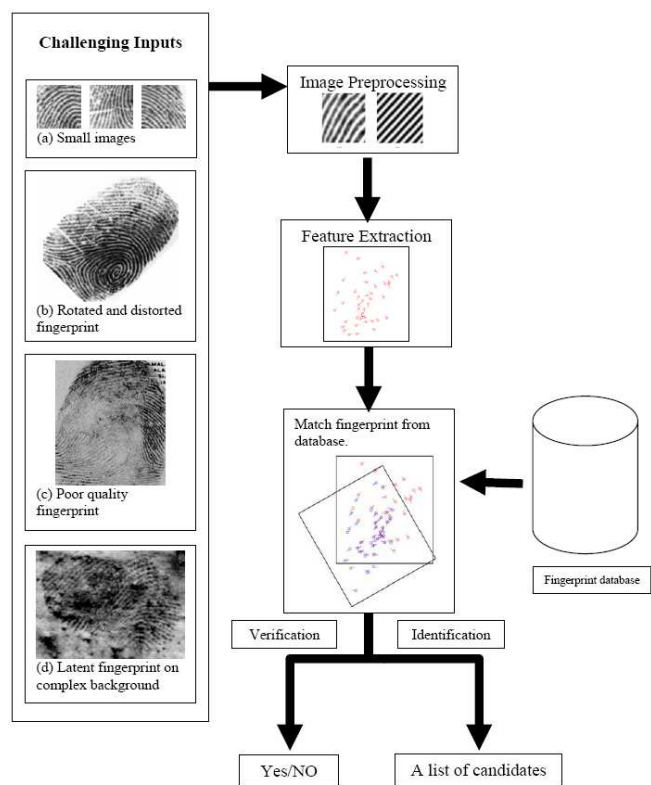


Figure 1.1: Common work flow and challenges of a partial fingerprint recognition system.

a long password without the overhead of remembering that information. However, unlike a password system, in which an exact match is expected for authentication of an individual, a fingerprint recognition system can only provide the individual's identity information with a certain confidence level. Thus, some kind of distortion tolerant mechanism is required which can reduce the security strength of the system. Moreover, with the small number of features on a partial fingerprint, the security strength of a partial fingerprint recognition is further diminished. Before we replace the password and PIN authentication systems with fingerprint recognition, we must answer the question "how secure is the fingerprint based system compared to the password or PIN based systems?" Besides, the relation between the acquired fingerprint size and its security strength plays a key role in the designing of a fingerprint recognition system. This relation between the two must be further studied before we can expect wider acceptance of fingerprint authentication systems.

1.3 Previous Work

Many automatic fingerprint matching approaches have been proposed. Among the various fingerprint representation methods, the minutiae-based fingerprint representation and matching are widely used by both machine and human experts. Minutiae representation has several advantages compared to other fingerprint representations in terms of the template size and its discriminability. In our work, we will focus on minutiae-based systems. Minutiae-based fingerprint matching involves search for the correspondence between two

lists of points in high-dimensional (usually in three-dimensional or higher) space. Minutiae matching is usually addressed as a point pattern matching problem and many approaches can be applied. However, the relaxation methods, algebraic and operational research solutions, tree-pruning approaches, and energy-minimization methods impose unrealistic requirements, such as equal number of feature points and every point has to have a match. They are also inefficient. Hough transform-based methods convert the matching problem to the problem of locating peaks in the discrete Hough space and the underlying transform parameters of participating fingerprint is recovered. Methods that depend on the pre-alignment increases the matching efficiency and accuracy. Other approaches that avoid alignment and match local features have been also proposed. However, there has been no research that explicitly address the issues of partial fingerprint matching.

The study on the security strength of a fingerprint recognition system compared to a password system has been conducted recently. They make assumptions that the two participating fingerprints have the same number of feature points and have a fixed image size. The security strength of a fingerprint system diminishes when the size of fingerprint decreases. However, the relation between fingerprint size and the system security strength and how to maintain the security level of a partial fingerprint recognition has not been addressed.

1.4 Proposed Approach

We propose to address and overcome the issues of partial fingerprint matching and the system security strength as follows:

- We will present a minutiae based multi-pass system to address the partial fingerprint matching problem. The system will utilize a set of localized features (called *secondary features*) which relies only on the relative information of minutiae. Due to the localized nature, the *secondary features* are invariant to translation, displacement, and rotation. Two different matching engines, secondary feature matching and brute-force matching, have been implemented and the matching strategy is decided based on the size of the participating fingerprints. Dynamic tolerance areas are used to handle non-linear distortions and a sophisticated scoring mechanism is used to compute the goodness of match.
- We will also present a second approach to partial fingerprint recognition using the same *secondary features* as in the first approach. However, the number of secondary features that are associated with a minutia is varied based on the fingerprint's size so that different sizes of fingerprint images have roughly the same number of features. Thus, the similarity score (goodness of match) comparison across different matches is more reliable. Indexing of secondary features and a local matching technique without global alignment are also presented.

Both approaches will be evaluated on the FVC2002 databases [70] and compared

with the popular NIST BOZORTH3 matching algorithm [100] for partial fingerprint matching as well as the regular full-sized fingerprint matching.

- We will also present a study on the vulnerability of partial fingerprint identification systems when subject to brute-force attacks. The security strength of a partial fingerprint is measured by the bit-strength. This allows us to establish the minimum size of a fingerprint image needed for a specified security level.

1.5 Thesis Outline

This thesis is organized as follows. Chapter 2 introduces various fingerprint representations and provides a general review of image enhancement, feature extraction, and matching techniques that are used in minutiae-based fingerprint recognition systems. Chapter 3 presents a novel multi-path partial fingerprint recognition system based on localized *secondary features*. The secondary features are invariant to translation and rotation and independent of the global ridge structure, therefore suitable for partial fingerprint matching. In Chapter 4, another minutiae-based partial fingerprint recognition system which completely eliminates the requirement of global alignment and generates features according to the sizes of participating images is described. We present a study of the security strength of partial fingerprints in Chapter 5. Chapter 6 summarizes the important contributions of this dissertation.

Chapter 2

Background

In this chapter, we introduce various fingerprint representations and provide a general review of image enhancement, feature extraction, and matching techniques that are used in minutiae-based fingerprint recognition systems.

2.1 Fingerprint Representation

Fingerprint representation (template) is a machine readable and understandable form of a fingertip epidermis. It influences the system's accuracy and the design of the rest of the system.

There are mainly three different kinds of fingerprint representations that are used by today's fingerprint recognition systems and each have its own advantages and drawbacks.

2.1.1 Image-based representation

In this representation, the fingerprint image itself is used as a template. There is no need for a specific feature extracting algorithm, and the raw intensity pixel values are directly used. This representation retains the most information about a fingerprint since fewer assumptions are made about the application. However, a fingerprint recognition system that uses the image-based representation requires tremendous storage space. For example, a $0.8\text{mm} \times 1.0\text{mm}$ (400×500 pixels) fingerprint is obtained by a scanner at 500 dots per inch (DPI) with 8 bits gray-scale resolution. The resulting fingerprint image is $400 \times 500 = 0.2$ Mbytes. A system with large amount of fingerprint data may have difficulty storing all the templates. For example, FBI has collected more than 200 million fingerprints since 1924 which requires more than 250 terabytes storage space [8]. Traditional compression techniques, such as JPEG tend to lose the highest frequency details, which contains discriminating information and the blocking artifacts also affect the performance of automatic fingerprint recognition systems. FBI recommends a compression method based on WSQ (Wavelet Scalar Quantization) [8], which can preserve the discriminating information without blocking artifacts while achieving a high compression ratio (around 20:1) (Figure 2.1) [8]. However, it still requires about 20 kbytes to store a compressed fingerprint image.



(a)



(b)

(c)

Figure 2.1: Comparison of using JPEG and WSQ compression techniques on fingerprint images. (a) The original fingerprint portion. (b) After being compressed by JPEG algorithm with compression ratio 12.9:1. Note the blurred details on ridges and blocking artifacts. (c) After being compressed by WSQ algorithm with compression ratio 12.9:1. Note that there is *no* blocking artifacts and ridge details are well preserved. (images obtained from www.c3.lanl.gov/~brislawn)

2.1.2 Global Ridge Pattern

This representation relies on the ridge structure, global landmarks and ridge pattern characteristics, such as the singular points, ridge orientation map, and the ridge frequency map.

This representation is sensitive to the quality of the fingerprint images [45]. However, the discriminative abilities of this representation are limited due to absence of singular points.

2.1.3 Local Ridge Detail

This is the most widely used and studied fingerprint representation. Local ridge details are the discontinuities of local ridge structure referred to as *minutiae*. Sir Francis Galton (1822-1922) was the first person who observed the structures and permanence of minutiae. Therefore, minutiae are also called “Galton details”. They are used by forensic experts to match two fingerprints.

There are about 150 different types of minutiae [45] categorized based on their configuration. Among these minutia types, “ridge ending” and “ridge bifurcation” are the most used, since all other types of minutiae can be seen as the combinations of “ridge endings” and “ridge bifurcations”. Some minutiae are illustrated in Figure 2.2.

The American National Standards Institute-National Institute of Standard and Technology (ANSI-NIST) proposed a minutiae-based fingerprint representation. It includes minutiae location and orientation[43]. The minutia orientation is defined as the direction of the underlying ridge at the minutia location (Figure 2.3). Minutiae-based fingerprint

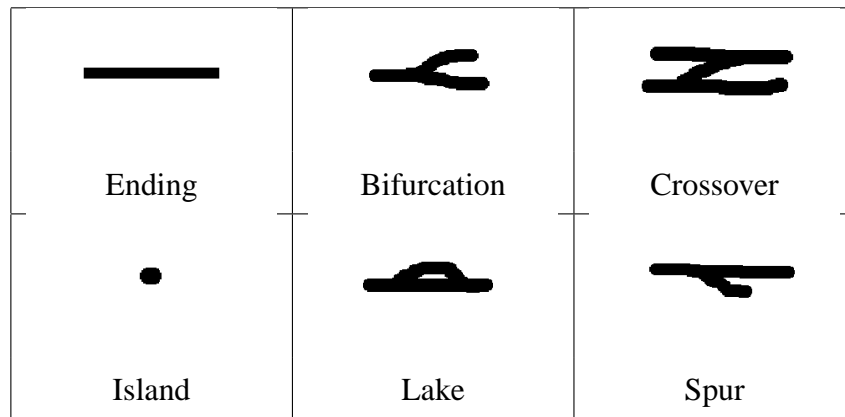


Figure 2.2: Some of the common minutiae types.

representation also has an advantage in helping privacy issues since one cannot reconstruct the original image from using only minutiae information. Minutia is relatively stable and

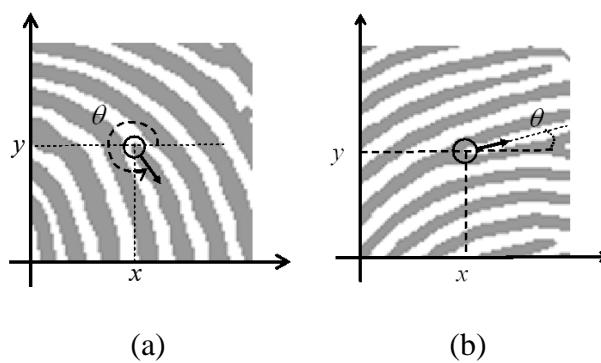


Figure 2.3: (a) A ridge ending minutia: (x,y) are the minutia coordinates; θ is the minutia's orientation; (b) A ridge bifurcation minutia: (x,y) are the minutia coordinates; θ is the minutia's orientation.

robust to contrast, image resolutions, and global distortion when compared to other representations. However, to extract the minutiae from a poor quality image is not an easy task.



Figure 2.4: A portion of a fingerprint where sweat pores (white dots on ridges) are visible.

Today, most of the automatic fingerprint recognition systems are designed to use minutiae as their fingerprint representations.

2.1.4 Intra-ridge Detail

On every ridge of the finger epidermis, there are many tiny sweat pores (Figure 2.4). Pores are considered to be highly distinctive in terms of their number, positions, and shapes. However, extracting pores is feasible only in high-resolution fingerprint images (for example 1000 DPI) and with good image quality. Therefore, this kind of representation is not practical for most applications.

2.2 Minutiae-Based Fingerprint Recognition

Our research uses the minutiae-based fingerprint representation to design the systems due to the advantages of wide accessibility and stability described in Section 2.1.3.

Minutiae-based fingerprint representation and matching are widely used by both ma-

chine and human experts. Minutiae representation has several advantages compared to other fingerprint representations (Section 2.1.3). Minutiae have been (historically) used as key features in fingerprint recognition tasks. Its configuration is highly distinctive and several theoretical models [94, 61, 79] use it to provide an approximation of the individuality of fingerprints. Minutiae-based systems are more accurate than correlation based systems [69] and the template size of minutiae-based fingerprint representation is small. Forensic experts use this representation which has now become part of several standards [43, 42] for exchange of information between different systems across the world.

2.3 Fingerprint Image Enhancement

Fingerprint image quality is an important factor in the performance of minutiae extraction and matching algorithms. A *good* quality fingerprint image (Figure 2.5(a)) has high contrast between ridges and valleys. A *poor* quality fingerprint image (Figure 2.5(b) and (c)) is low in contrast, noisy, broken, or smudgy, causing spurious and missing minutiae. Poor quality can be due to cuts, creases, or bruises on the surface of finger tip, excessively wet or dry skin condition, uncooperative attitude of subjects, damaged and unclean scanner devices, low quality fingers (elderly people, manual worker), and other factors.

The goal of an enhancement algorithm is to improve the clarity (contrast) of the ridge structures in a fingerprint. General-purpose image enhancement techniques are not very useful due to the non-stationary nature of a fingerprint image. However, techniques such as

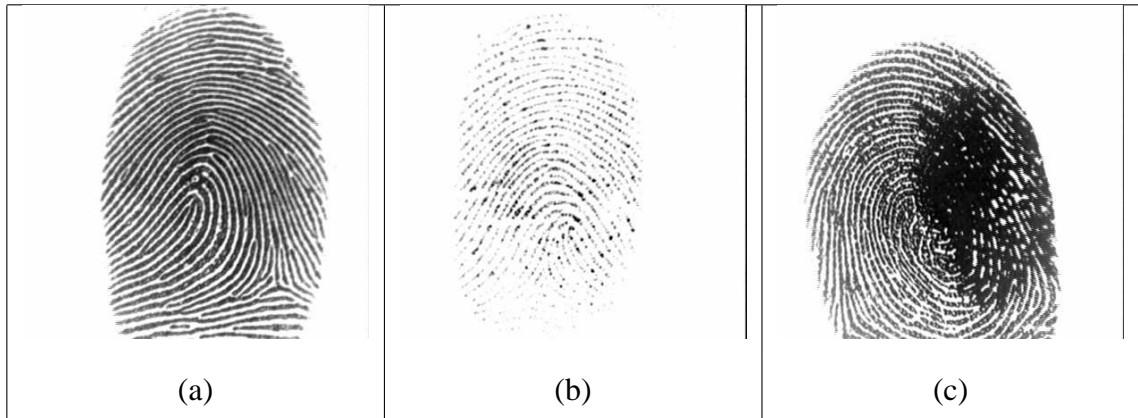


Figure 2.5: (a) A good quality fingerprint image; (b) a poor quality fingerprint caused by extremely dry skin; (c) a noisy fingerprint image.

gray-level smoothing, contrast stretching, histogram equalization, and Wiener filtering [87, 35, 12] can be used as preprocessing steps before a sophisticated fingerprint enhancement algorithm is applied.

Techniques that use single filter convolutions on the entire image are not suitable. Usually, a fingerprint image is divided into subregions and then a filter whose parameters are pre-tuned according to the region's characteristics is applied. Each local region of a fingerprint can be seen as a surface wave (Figure 2.6) of a particular wave (ridge) orientation (perpendicular to flow direction) and frequency. Several types of contextual filters in both spatial and frequency domains have been proposed in the literature. The purpose of the filters is to fill small gaps (low-pass effect) in the direction of a ridge and to increase the discrimination (band-pass effect) between ridges and valleys in the direction orthogonal to the ridge [70]. O'Gorman and Nikerson [77] were the first to propose the use of contextual

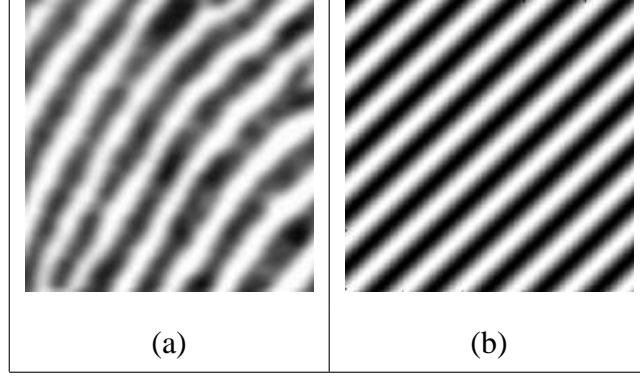


Figure 2.6: (a) Local region in a fingerprint image; (b) Surface wave approximation of (a).

filtering. By assuming that the ridge frequency remains constant across an entire fingerprint image, 16 bell-shaped filters are pre-computed. The filter whose direction best fits the subregion's orientation is selected and then convolved on every point of the subregion. Hong et al. [35] proposed a fingerprint enhancement based on Gabor filters. Gabor filters [26, 19] have both frequency-selective and orientation-selective properties which capture the periodic and non-stationary nature of a fingerprint image. For a given frequency f and orientation θ , the symmetric two-dimensional Gabor filter has the following form:

$$G(x, y) = \exp \left\{ -\frac{1}{2} \left[\frac{x_\theta^2}{\sigma_x^2} + \frac{y_\theta^2}{\sigma_y^2} \right] \right\} \cdot \cos(2\pi f x_\theta) \quad (2.1)$$

where, $x_\theta = (x \sin(\theta) + y \cos(\theta))$, $y_\theta = (-x \cos(\theta) + y \sin(\theta))$, and σ_x and σ_y are the standard deviations of the Gaussian envelope along the x - and y -axes, respectively. The values of f and θ can be estimated from the target subregions. However, the selection of σ_x and σ_y is not straight forward. Smaller values of σ_x and σ_y reduce spurious ridges and valleys and remove noise. On the other hand, larger σ_x and σ_y values make the filters ro-

bust to noise and are likely to create spurious ridges and valleys. Yang et al. [107] modified the method proposed by Hong et al. [35] by discarding the inaccurate prior assumption of sinusoidal plane wave, and making the parameter selection process independent of fingerprint images. Recently, Greenberg et al. [87] proposed the use of an anisotropic filter that adapts its parameters to the structure of the underlying subregion. Wu, Shi, and Govindaraju [105] proposed to convolve a fingerprint image with an anisotropic filter to remove Gaussian noise and then apply directional median filters (DMF) to remove *impulse noise*. On visual inspection, enhancement results of Wu et al. [105] appears to be superior to those obtained by Greenberg et al. [87]. The general form of the anisotropic filter [87, 105] is given as:

$$f(x, x_0) = S + V\rho(x - x_0)\exp\left\{-\left(\frac{((x - x_0) \cdot n)^2}{\sigma_1^2(x_0)} + \frac{((x - x_0) \cdot n_\perp)^2}{\sigma_2^2(x_0)}\right)\right\}, \quad (2.2)$$

where S and V decide the phase intensity and impact of the neighborhood, and n and n_\perp represent unit vectors parallel and perpendicular to the ridges respectively. $\sigma_1(x_0)$ and $\sigma_2(x_0)$ control the shape of the filter. $\rho(x - x_0)$ determines the support radius r of the filter and satisfies the condition that $\rho(x) = 0$ when $|x - x_0| > r$. Method of Wu et al. [105] works on the advantages of both anisotropic filters and median filters. Anisotropic filters remove Gaussian noise and smoothen the fingerprint image along the local ridge direction. The standard rectangular-shaped median filters produce artifacts in fingerprint images. Wu et al. [105] use directional median filters (Figure 2.7) whose shapes vary by their direction to remove *impulse noise* (small gaps on bridge or dots in valleys).

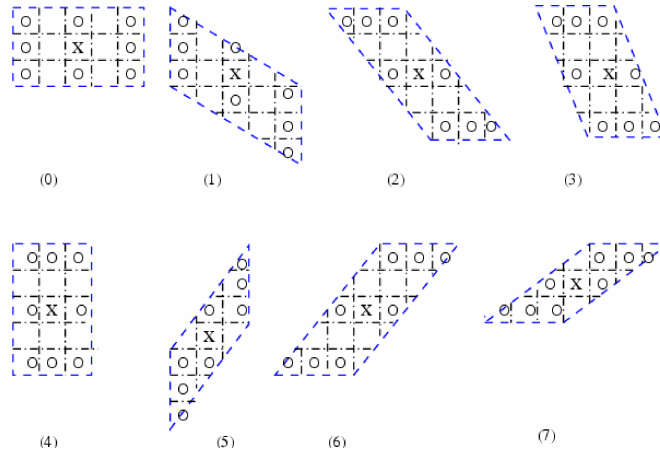


Figure 2.7: Examples of directional median filters (DMF) [105] in eight directions. Note that the shape of the filter changes along with its direction.

Sherlock, Monro, and Millard [89] proposed a fingerprint enhancement method in the Fourier domain. In this approach, a fingerprint image is convolved with pre-computed filters, that results in a set of filtered images. The enhanced fingerprint image is constructed by selecting each pixel from the filtered image whose orientation is the closest to that of the original pixel. However, their assumption of constant ridge frequency limits the performance of the approach. Willis and Myers [103] presented an FFT based fingerprint enhancement method. Instead of explicitly computing the local ridge direction and frequency, enhancement is achieved by multiplying the Fourier transform of the block by magnitude of power, k (1.4 in [103]). Chikkerur [13] proposed an algorithm based on Short Time Fourier Transform (STFT), and a probabilistic approximation of dominant ridge orientation and frequency was used instead of the maximum response of the Fourier spectrum.

The ridge orientation image, ridge frequency image, and foreground region image, are generated simultaneously while performing the STFT analysis.

A wavelet-based method is proposed by Hsieh et al. [38]. It uses both local ridge orientation and global texture information. Fingerprint image is first wavelet-decomposed into “approximation” and “detail” sub-images. A series of texture filters and a directional compensation process based on a voting technique are applied on those sub-images. The enhanced fingerprint image is then obtained by the reconstructing process of wavelet transform.

2.4 Minutia Extraction

The reliability of minutia features (see Section 2.1.3) plays a key role in automatic fingerprint recognition. Generally, the minutiae representation of a fingerprint consists of simply a list of minutia points associated with their spatial coordinates and orientation. Some methods also include the types [72, 51, 60, 80] and quality [28, 100, 80] of minutiae in the representation.

Minutiae extraction algorithms are of two types: (i) binarization-based extraction and (ii) gray-scale based extraction.

2.4.1 Binarization-based Minutiae Extraction

Most of the proposed minutiae extraction methods are binarization-based approaches. They require conversion of the gray-scale fingerprint image (8 bits per pixel, 256 gray levels) into a binary form (2 bits per pixel, black and white). Various binarization techniques have been presented in the image processing literature [96, 88]. One intuitive approach is to use a global threshold t and assign each pixel a value according to the following equation:

$$I_B(x, y) = \begin{cases} 1 & \text{if } I(x, y) > t \\ 0 & \text{if } I(x, y) \leq t \end{cases} \quad (2.3)$$

where $I(x, y)$ is the intensity value of the pixel at (x, y) in a gray-scale image. Otsu's method [78] describes a technique to obtain the global threshold t from a statistical viewpoint. Dong and Yu [21], use a data clustering approach which is equivalent to Otsu's method [78] but is more efficient. The contrast variation in a fingerprint image makes it impossible to find an optimal global threshold. Adaptive techniques are preferred in general but they fail on poor quality images.

Several methods have been proposed to utilize the flow texture of a fingerprint image in binarization tasks. Stock and Swonger [93] observed that the average local intensity of a ridge line along its flow direction is highest and used it in binarization. Ratha, Chen and Jain [84] use a 16×16 window centered and oriented along the local ridge direction on each pixel. Ridge lines are recognized as peaks of the gray-level profile of pixel intensities projected on the central segment of the window. Coetzee and Botha [15] use a local

binarization technique. The area between two edges of a local block is blob-colored and then logical **OR**ed with the result of local binarization of the same local block to produce the final binarized image. Garris et al. [28] and Watson et al. [100] propose a directional binarization technique. In this approach, each pixel is examined successively and assigned to black (0) or white (1). By consulting the intrinsic orientation map, a pixel is assigned to white if there is no detectable ridge flow for the local block. If the flow is well defined in the pixel's local block, then an orientated window (7×9) is used to analyze the neighboring pixel intensity of the pixel (Figure 2.8). The rows of the window are aligned with the local ridge and the central row sum is compared against the average row sum of the entire window. A pixel is white if the central row sum is less than the window's average row sum; otherwise, it is black. Other fingerprint binarization methods can be found in [73, 98, 90, 20, 1, 95].

Usually, the binarization-based minutiae extraction methods apply a thinning algorithm after the binarization step to obtain the *skeletons* of fingerprint ridges. Once a binary skeleton of a fingerprint is obtained, minutiae extraction becomes a trivial task. Let us assume that the foreground and background pixel values of a fingerprint skeleton are 1 and 0, respectively. Minutia can be detected by examining the 8-neighborhood (Figure 2.9) of a ridge skeleton pixel at (x, y) and classified as:

- a ridge ending if $\sum_{i,j=-1\dots 1} I(x+i, y+j) = 2$;
- an intermediate ridge point if $\sum_{i,j=-1\dots 1} I(x+i, y+j) = 3$;

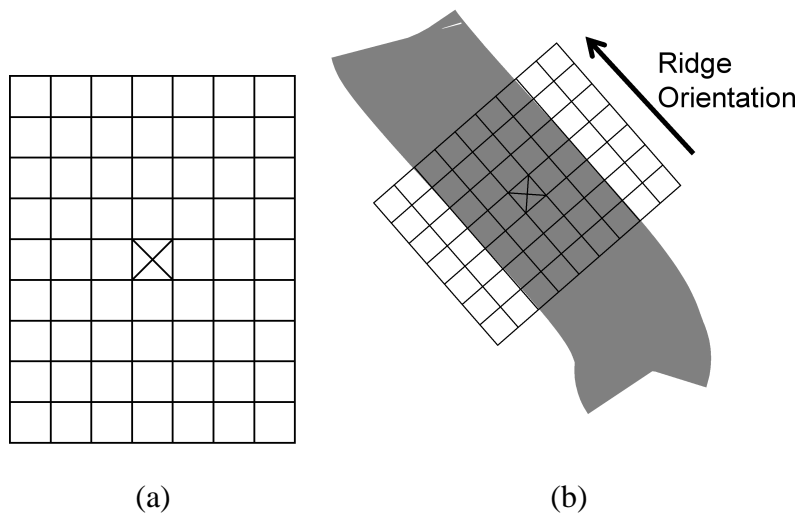


Figure 2.8: (a) The window used for analyzing surrounding pixel intensity of x ; (b) the window orientated along with the local ridge direction.

- a ridge bifurcation if $\sum_{i,j=-1\dots1} I(x+i, y+j) = 4$;
- or a crossover minugia.

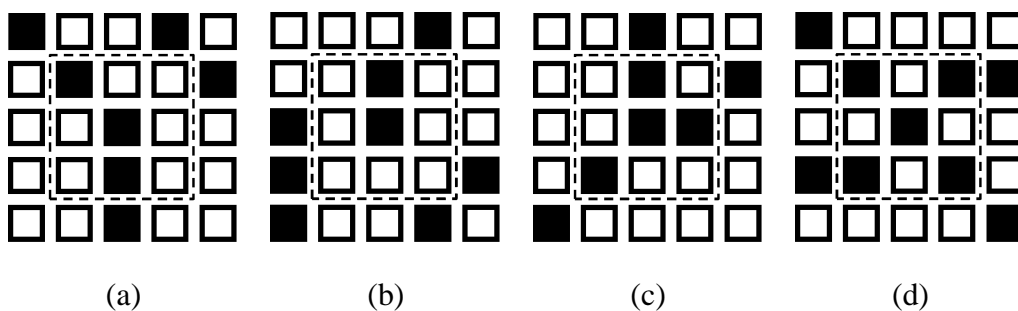


Figure 2.9: (a) an intra-ridge pixel; (b) a ridge ending; (c) a bifurcation; (d) a crossover.

Many thinning approaches [3, 59, 4, 57, 75, 18] have been proposed. However, thinning tends to introduce *hair-like* artifacts along the one-pixel wide skeleton, which leads to de-

tection of spurious minutiae. Various techniques [15, 39, 84, 24, 99, 65, 40] are introduced between the stages of binarization and thinning to improve the quality of binarized fingerprint images by filling holes, smoothing ridges, and removing small gaps and other artifacts.

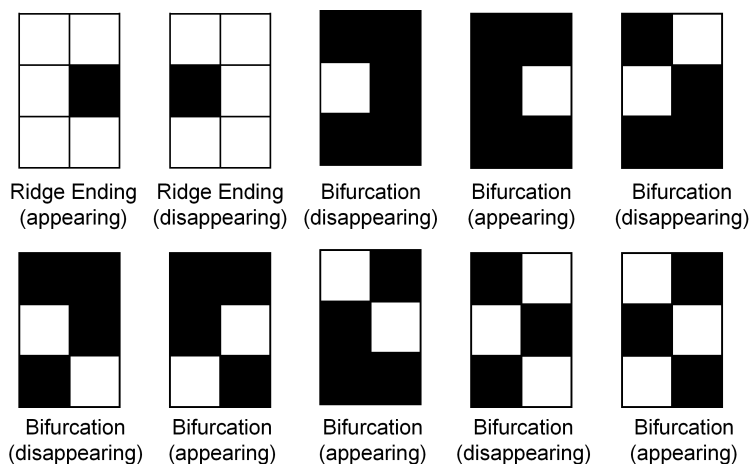


Figure 2.10: Pixel patterns used to detect minutiae in [28, 100].

Several approaches have been also proposed to extract minutiae directly from the binarized fingerprint image to avoid the computationally intensive thinning process. Weber [101] proposed a method that extracts minutiae from the thick binary ridges using a rule based ridge tracking algorithm. Garris et al. [28] (see also Watson [100]) use a series of pixel patterns (Figure 2.10) to detect minutiae on binarized fingerprint images. A method based on chaincode is proposed by Govindaraju et al. [97]. It is a lossless representation of an object contour and is widely used in document analysis and recognition research [67]. It is generated by tracing the exterior contours of a binary object counterclockwise (clock-

wise for interior contours) (Figure 2.11(a)) and stored in contour lists. In the contour list, each contour element contains the x, y coordinates of the pixel, the direction of the contour *into* the pixel, and curvature information (Figure 2.11(b)(c)). The chaincode representation of fingerprint ridge contours provides several advantages in minutia detection:

- It is a lossless representation, thus, most of fingerprint information is retained;
- It is easy to remove small objects and holes from the ridge contours. Therefore, the number of spurious minutiae is few;
- It works directly on binarized image and eliminates the need for thinning;
- Minutiae are the *significant* turns in the ridge contours (Figure 2.12).

Figure 2.13 presents an example of minutia points extracted by the chaincode based algorithm [67].

2.4.2 Direct Gray-scale Minutiae Extraction

Approaches that directly work on gray-scale images to extract minutiae are proposed to overcome some of the problems caused by fingerprint binarization and thinning. Most [68, 52, 53, 63, 9] of these algorithms are based on ridge tracing. Given a starting point (x_0, y_0) and a direction θ_0 , the method of Maio et al. [68] tracks the ridges in the gray-scale image by *sailing* according to the local orientation of the ridge pattern. The algorithm computes the next ridge point (x_t, y_t) by moving μ pixels in the direction θ_0 . Since (x_t, y_t) is only an

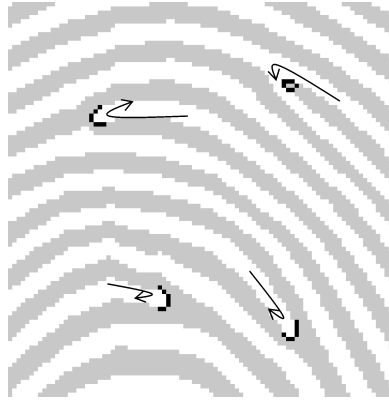


Figure 2.12: Minutiae are located in the contours by looking for *significant* turns. A ridge ending is detected when there is a sharp left turn; whereas the ridge bifurcation is detected by a sharp right turn.

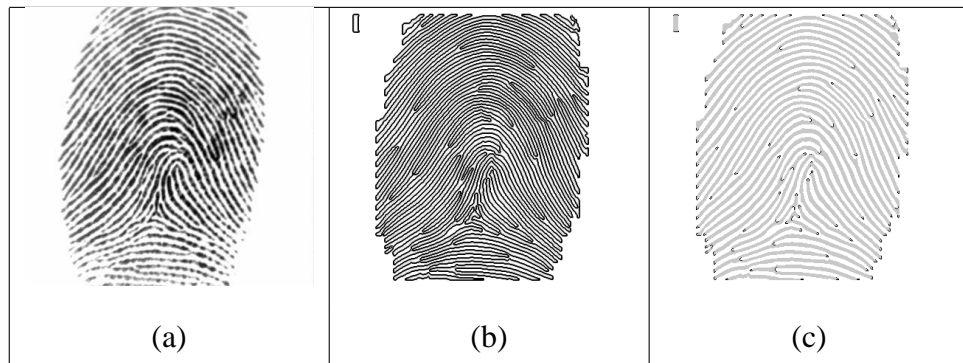


Figure 2.13: (a) Original image; (b) the contour representation of the image; (c) detected minutiae superimposed on the contour image.

approximation, the method then analyzes the gray-scale profile of the *section set* Ω (whose direction is orthogonal to θ_0 , length is $2\rho + 1$ and the median is (x_t, y_t)) and uses the local maxima on Ω as the new starting point (x_1, y_1) and the local ridge direction at (x_1, y_1) as the new start direction of the next iteration. The parameters μ and ρ are determined according to the average ridge width. The tracing is executed in the direction of a ridge and stops when a ridge comes to the end or intersects with other ridges.

Modification to Maio's method [68] was proposed by Jiang et al. [52, 53]. They utilize the ridge contrast and bending level to dynamically determine the value μ . A large μ is used when the bending level of the local ridge is low and the intensity varies along the ridge direction; otherwise, a smaller μ is used. Instead of tracing one ridge at a time, Liu, Huang, and Chang [63] simultaneously track a central ridge and its two surrounding valleys. During the tracking process, the central maximum of the ridge and two minima in each corresponding Ω are monitored, and minutiae are detected when the relation of $\langle \text{minimum, maximum, minimum} \rangle$ is changed. Chang and Fan [9] modeled the background, valleys, and ridges on Ω with Gaussian distributions. A neural network-based method is used by Leung, Engeler, and Frank [62]. The fingerprint image is first passed through a bank of oriented Gabor filters, and the outputs are fed into a three-layered back-propagation neural network to indicate the existence of minutiae.

2.5 Minutiae-Based Matching

Matching is the most important part of an automatic fingerprint recognition system. It compares two (feature) templates (\mathbf{I} and \mathbf{R}) that are extracted from the query and reference fingerprints and returns a binary decision (matched/non-matched) or a similarity score ($S(\mathbf{I}, \mathbf{R})$) to indicate how similar the two participating fingerprints are.

Minutiae-based fingerprint matching involves search for the correspondence between two lists of points in high-dimensional (usually in three-dimensional or higher) space (Figure 2.14). A triplet $m = \{x, y, \theta\}$ is the most common representation of a minutia, where (x, y) is the location and θ is the orientation of the minutia. Therefore, the templates are represented as:

$$\mathbf{I} = \{m_1, m_2, \dots, m_a\}, \quad m_i = \{x_i, y_i, \theta_i\}, \quad i = 1 \dots a$$

$$\mathbf{R} = \{m'_1, m'_2, \dots, m'_b\}, \quad m'_j = \{x'_j, y'_j, \theta'_j\}, \quad j = 1 \dots b,$$

where a and b are the number of minutiae in \mathbf{I} and \mathbf{R} , respectively. A minutia m'_j in \mathbf{R} matches the minutia m_i in \mathbf{I} , if they are *sufficiently close* in terms of spatial distance and orientation difference. Given two tolerance distances r_0 and θ_0 , minutia m_i matches minutia m'_j if and only if:

$$\sqrt{(x_i - x'_j)^2 + (y_i - y'_j)^2} \leq r_0 \quad (2.4)$$

and

$$\min(|\theta_i - \theta'_j|, 360 - |\theta_i - \theta'_j|) < \theta_0. \quad (2.5)$$

Usually, minutia m_i in \mathbf{I} relates to the minutia m'_j in \mathbf{R} through some geometric transforma-

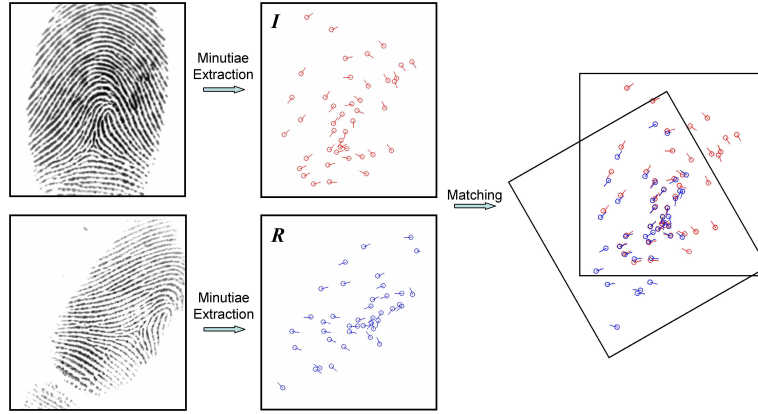


Figure 2.14: Minutiae-based matching.

tion $T(\cdot)$ due to the intraclass variance of fingerprint impressions. Let $m_i^T = \{x_i^T, y_i^T, \theta_i^T\} = T(m_i)$. Equation (2.4) and (2.5) can be written as:

$$\sqrt{(x_i^T - x_j^T)^2 + (y_i^T - y_j^T)^2} \leq r_0 \quad (2.6)$$

and

$$\min(|\theta_i^T - \theta_j^T|, 360 - |\theta_i^T - \theta_j^T|) < \theta_0. \quad (2.7)$$

The transformation parameters of $T(\cdot)$ are not known in advance. One must recover the transformation function $T(\cdot)$ that maps the point set from I to I^T . The underlying assumptions of the geometric transformation (such as rigid transformation, affine transformation, complex non-linear transformation, etc.) are important to the design of a matching algorithm.

The Hough transform [36] is a standard tool used in image processing that allows the recognition of global patterns. In the context of minutiae matching, Hough transform-based

methods convert the matching problem to the problem of locating peaks in the discrete Hough space. Ratha et al. [85] proposed a method that searches the geometric transformation parameters in the four-dimensional $(\Delta x, \Delta y, \theta, s)$; where s is the scale parameter) Hough space. To eliminate the infinite combination of transformation parameters, the parameter space is discretized into small cells. A four-dimensional array A is maintained for accumulating the evidence of transformation parameters. The parameter values with the highest evidence are used for computing the geometric transformation $T(\cdot)$. The correspondences of minutia points are determined by Equation (2.6) and (2.7). The algorithm for finding the optimal transformation parameters $(\Delta x^*, \Delta y^*, \theta^*, s^*)$ is as follows:

for each $m_i \in \mathbf{I}, i = 1, \dots, a$

for each $m'_j \in \mathbf{R}, j = 1, \dots, b$

for each $\theta \in \{\theta_1, \theta_2, \dots, \theta_c\}$

if $\min(|\theta_i + \theta - \theta'_j|, 360 - |\theta_i + \theta - \theta'_j|) < \theta_0$

for each $s \in \{s_1, s_2, \dots, s_d\}$

$$\begin{bmatrix} \Delta \bar{x} \\ \Delta \bar{y} \end{bmatrix} = \begin{bmatrix} x_i \\ y_i \end{bmatrix} - s \begin{bmatrix} \cos(\theta) & -\sin(\theta) \\ \sin(\theta) & \cos(\theta) \end{bmatrix} \begin{bmatrix} x'_j \\ y'_j \end{bmatrix}$$

Let $(\Delta x, \Delta y)$ be the quantized versions of $(\Delta \bar{x}, \Delta \bar{y})$, respectively.

$$A(\Delta x, \Delta y, \theta, s) = A(\Delta \bar{x}, \Delta \bar{y}, \theta, s) + 1$$

Chang et al. [10] proposed an alternative Hough transform-based approach. Instead of

pairing minutiae, line segments between two minutiae are used to estimate transformation parameters and accumulate the evidence.

Wegstein [102] describes a method which pre-aligns two fingerprints with respect to the core positions and the average orientation of two regions reside on the two sides of the core. Every fingerprint template is translated before storing in the database. Thus, the minutiae matching task is simply a pairing process and the speed of $(1 : N)$ identification is significantly improved. Bazen and Gerez [6] proposed a different pre-alignment strategy that is based on the orientation of singularities. However, the reliable and precise detection of singular points in a fingerprint is difficult, especially in poor quality images. The pre-alignment error results in unavoidable matching error. The relative pre-alignment method requires N alignment steps in the $(1 : N)$ identification task although it is more effective in terms of both system accuracy and speed [70]. Jian, Hong, and Bolle [45, 44] align ridge curves. In addition to the standard information of a minutia, they also record a segment (represented as a planar curve) of ridge curve that associates with the minutia. Curve matching is performed on all possible pairs of curves on query and reference fingerprint templates (I and R) until a match within a certain criterion is reached. Then, the minutiae associated with the two matched curves are used as reference points and the remaining minutiae are converted to polar coordinates. The converted minutiae are translated into symbolic strings and the correspondence between minutiae is then obtained by a dynamic programming algorithm that finds the minimum *edit distance* between the strings. A variant of Jian, Hong, and Bolle's [45, 44] method was proposed by Luo, Tian and Wu [66]. The

curves are matched by the distances and relative angles of the curve sample points.

In two-staged *local-global* matching, the first matching stage is at the local level to derive a list of candidate matches of local features. Various local features have been described in the literature [37, 11, 72, 99, 83, 51, 60] which are invariant to global transformations, such as translation, rotation, etc. Although the local features have high distortion tolerance, their global configurations (such as fingerprint types, global orientations, etc.) are not ensured. In the validation step, the candidate matches are checked to see whether their global relations are valid. Our proposed fingerprint matching algorithms belongs to this category. Details will be presented in Section 3.1.

Bazen and Gerez [5] proposed a method to overcome the problems of alignment. They introduced an *intrinsic coordinate system* (ICS) of a fingerprint. The ICS partitions the fingerprint image into regions and minutiae locations are defined by the orientation field. Therefore, the intrinsic coordinates of a minutia are invariant to translation, displacement, and rotation. However, the reliable partitioning of a fingerprint into regions, estimating orientation field, and defining the intrinsic coordinates in poor quality images become major research challenges.

Chapter 3

Partial Fingerprint Recognition Using Secondary Features

Despite advances in fingerprint identification techniques, matching incomplete or partial fingerprints still poses a difficult challenge. While the introduction of compact silicon chip-based sensors that capture only a part of the fingerprint area have made this problem important from a commercial perspective, there is also considerable interest on the topic for processing partial and latent fingerprints obtained at crime scenes. Attempts to match partial fingerprints using singular ridge structures based alignment techniques fail when the partial print does not include such structures (e.g., core or delta). Moreover, when the fingerprint size gets smaller, the security of the system against brute-force attacks reduces (see section 5.3). Therefore, more details associated with the fingerprint representation are needed to maintain the security level of the system. We present an approach that uses localized secondary features derived *only* from relative minutiae information. A flow network-

based matching technique is introduced to obtain one-to-one correspondence of secondary features. Our method balances the tradeoffs between maximizing the number of matches and minimizing the total feature distance between query and reference fingerprints. A two-hidden-layer fully connected neural network is trained to generate the final similarity score based on minutiae matched in the overlapping areas. Since the minutia-based fingerprint representation is an ANSI-NIST standard [43], our approach has the advantage of being directly applicable to existing fingerprint template databases.

3.1 Background

During the last four decades, various algorithms have been proposed to match minutia templates of fingerprints. Most of these algorithms assume that the templates are approximately the same size. The matching of partial fingerprint templates against full fingerprint templates is rarely addressed. Because of the nature of a partial fingerprint, matching techniques [102], [46] that utilize only global information, or rely on the existence of some global landmarks are not suitable for partial fingerprint matching.

Minutia-based fingerprint representation is the best choice for an automatic partial fingerprint recognition system because it is formed by the local discontinuity and the direction of ridges. No global information, which may be missed in partial fingerprints, is involved. Furthermore, the wide use of this representation makes our proposed algorithm compatible with various feature extraction methods and any existing minutia-based fingerprint template

databases without additional processing.

To eliminate the need for prior global alignment, a feature that is invariant with respect to global transformation (for example, translation, rotation, etc.) is essential. Hrechak and McHugh [37] proposed an eight-element vector $[v_{i1}, v_{i2}, \dots, v_{i8}]$ associated with each minutia m_i where every element represents the number of occurrences of one of the eight types of minutiae. The considered minutiae types are dots, ridge endings, bifurcation, island, spurs, crossovers, bridges, and short ridges. However, to accurately distinguish between minutiae types is a difficult task, thus this method is not practical. Variations [11, 99] have been made to include more relative information, such as the distance, ridge count, relative orientation of the central minutia and its neighbor, and the angle between central minutia orientation and the segment formed by the central minutia and its neighbor.

Jiang and Yau [51] describe an eleven dimensional feature vector, v_i , constructed by considering the two nearest neighbors (m_j, m_k) of each minutiae m_i . The feature vector v_i is represented as:

$$[d_{ij}, d_{ik}, \theta_{ij}, \theta_{ik}, \phi_{ij}, \phi_{ik}, n_{ij}, n_{ik}, t_i, t_j, t_k],$$

where d_{ab} is the Euclidean distance between minutiae m_a and m_b ; θ_{ab} is the relative orientation of minutia m_b with respect to minutia m_a ; ϕ_{ab} represents the relative angle of the edge connecting m_a to m_b with respect to the orientation of m_a ; n_{ab} represents the ridge count between the minutiae m_a and m_b ; and t_a identifies the minutia type of m_a . The matching is performed in two stages: (i) the local structure match and (ii) the global structure match.

In the local matching stage, for each pair of m_i and m'_j , the weighted distance between v_i and v'_j is calculated. The best matched minutiae pair is then used as reference points to align the two fingerprints. In the global matching stage, every minutia on both fingerprints is converted into the polar coordinate system with respect to the reference points obtained in the local matching stage, and then the remaining minutiae are matched within a fixed bounding box. The final similarity score is calculated by combining the similarity levels that are obtained from both stages. A variant to this approach is described by Lee, Choi, and Kim [60]. The distance is normalized by using the local ridge frequency, thus reducing the distortion. Since the best matched minutiae pair is not always correct, they use additional minutiae pairs in the global matching stage.

Mital and Teoh [72] proposed a local feature structure constructed by a central minutia, m_i , along with its five nearest neighboring minutiae, n_1, \dots, n_5 , within a fixed radius of m_i . The match is achieved in two stages. In the first stage, correspondences between the local features of query and reference fingerprints are obtained by a heuristic rule that compares the correlation between local features. The best matching pair of the first stage is chosen as reference. The central minutiae of the matched features of the first stage are used to construct a global feature with respect to the chosen reference and their correlation is calculated. Mital and Teoh [72] consider only the minutia types of central minutia, the distances between neighboring and central minutiae, the types of neighboring minutiae, and the angles between the vectors $\vec{Om_i}$ and $\vec{m_in_j}$, where O is the origin and $j = 1, \dots, 5$. Ratha et al. [83] represent the local structure using a “Minutiae Adjacency Graph (MAG)”.

For each minutia m_i , the associated graph is defined as $G_i = (V_i, E_i)$, where

- V_i is the set of vertices containing all the minutiae m_j such that the distance between m_i and m_j is less than or equal to a predefined value d_{max} ;
- E_i is the set of edges (e_{ij}); each $e_{ij} \in E_i$ connects the minutiae m_i and m_j , and is labeled with a five-element tuple $(i, j, d_{ij}, rc_{ij}, \phi_{ij})$, where d_{ij} , rc_{ij} , and ϕ_{ij} are the Euclidean distance, ridge count between m_i and m_j , and the angle subtended by the edge with x -axis, respectively.

During the first local matching stage, each *MAG* from the query fingerprint is matched against each *MAG* from the reference fingerprint. The local matching process results in a set of candidate *MAG* pairs. In the consolidation stage, each candidate *MAG* pair is checked for consistency. A *MAG* pair is said to be consistent if the spatial relationships with a certain fraction of the remaining *MAG*s in the candidate list are consistent.

3.2 Our Method

We present a multi-pass matching algorithm that utilizes the localized secondary features. The matching pass (brute-force matching or secondary feature matching) is decided by the algorithm based on the size of the input (query) and template (reference) fingerprints. Both the matching schemes use the minimum cost maximum flow (MCF) algorithm to obtain the optimal pairing of features. Localized features along with dynamic tolerance areas reduce the effects of non-linear distortion. Similarity score calculation is not only based on the

number of matched minutiae but also takes the overlapped areas on both prints and the average distance between all the matched minutiae into consideration.

3.2.1 The Partial Fingerprint Matching System

The matching scheme is based on the number of minutiae on the query (I) and the reference (R) fingerprints (Figure 3.1). A *full* fingerprint is about $1.0'' \times 1.0''$ and usually leads to greater than α (a pre-defined threshold) minutiae. There are three matching scenarios:

1. both the numbers of minutiae on I and R are less than α ;
2. either I or R has number of minutiae less than α ;
3. both I and R contain more than α minutiae.

In the first two cases, we have fewer minutiae on at least one of the fingerprints. In such cases, we match (by brute-force) all the feature points directly by examining all the possible solutions and finding the most matches as our final result. A brute-force matching technique tries all possible correspondences between the minutiae on query and reference fingerprints. This technique is usually very time-consuming. To make it practical, we use brute-force matching only when there are a small number of minutiae. When, we have more than α minutiae, we use a secondary feature-based matching method [49, 50] instead of the brute-force method, to improve speed and accuracy.

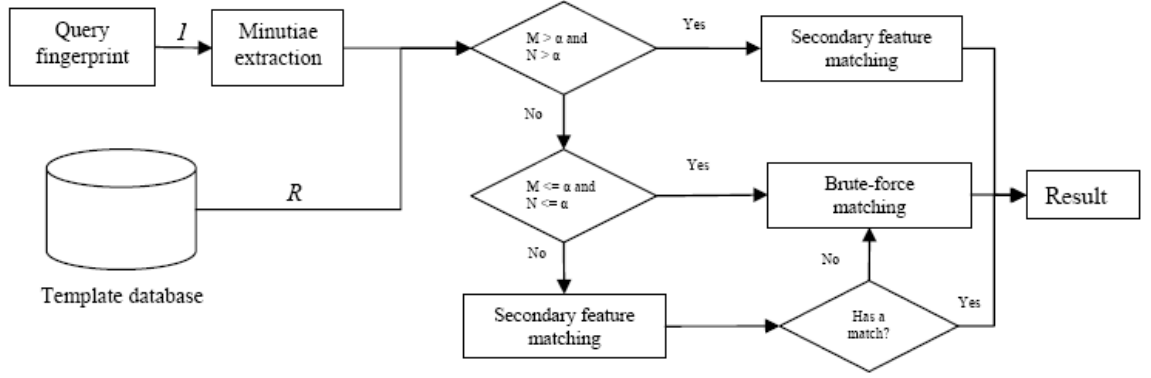


Figure 3.1: Proposed fingerprint matching system. M and N are the number of minutiae on query and reference fingerprints. α is a pre-defined value.

3.2.2 Brute-force Matching

The brute-force matching method works directly on the minutiae information. For each minutia $p_i(x_i, y_i, \theta_i)$ on I and $q_j(x_j, y_j, \theta_j)$ on R , we take p_i and q_j as the matched reference points and find all the other matched minutiae in the polar coordinate system by converting the matching into a Minimum Cost Flow (section 3.2.5) problem to obtain the optimal pairing. In polar coordinates, a minutia $m_i(x_i, y_i, \theta_i)$ is represented as $(r_{ik}, \Phi_{ik}, \Theta_{ik})$, with respect to the reference point $m_k(x_k, y_k, \theta_k)$. (r_{ik}, Φ_{ik}) is the polar coordinates and Θ_{ik} is the orientation difference between θ_i and θ_k . Given a matched minutiae pair $p_{i'}$ and $q_{j'}$ as reference points, a minutia, $p_i(r_{ii'}, \Phi_{ii'}, \Theta_{ii'})$ matches $q_j(r_{jj'}, \Phi_{jj'}, \Theta_{jj'})$, if and only if q_j is within the dynamic tolerance area (section 3.2.4) of p_i .

3.2.3 Secondary Feature Matching

When both I and R have large numbers of minutiae (larger than α), brute-force matching is computationally expensive for real applications. In such cases, we perform the match by using secondary features. Three stages are executed sequentially: (i) local matching stage, (ii) validation stage, and (iii) similarity score calculation stage.

Secondary Feature

In order to overcome the challenges that a fingerprint verification system based on partial fingerprints would face, we carefully select the features that we want to use for partial fingerprints. A secondary feature is derived only from minutia information so that it is invariant under translation and orientation. As proposed by Jiang and Yau [51], for each minutia $m_i(x_i, y_i, \theta_i)$ and its two nearest neighboring minutiae $n_0(x_{n_0}, y_{n_0}, \theta_{n_0})$ and $n_1(x_{n_1}, y_{n_1}, \theta_{n_1})$, we construct a secondary feature $s_i = (r_{i0}, r_{i1}, \theta_{i0}, \theta_{i1}, \phi_{i0}, \phi_{i1})$ (Figure 3.2), in which, r_{i0} and r_{i1} are the Euclidean distances between the central minutia m_i and its neighbors, n_0 and n_1 , respectively. θ_{i0} and θ_{i1} are the relative orientations of neighboring minutiae with respect to θ_i , and ϕ_{i0} and ϕ_{i1} are the relative angles of the line segments $\overline{m_i n_0}$ and $\overline{m_i n_1}$ with respect to θ_i , respectively. Note that the two nearest neighbors of the central minutia m_i are ordered not by their Euclidean distances but by satisfying the equation:

$$\overrightarrow{m_i n_0} \times \overrightarrow{m_i n_1} \leq 0.$$

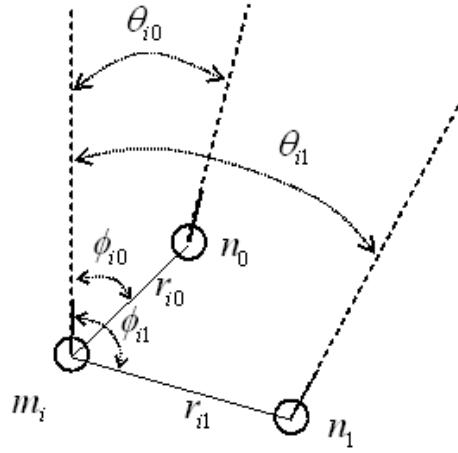


Figure 3.2: The proposed secondary feature.

Thus, n_0 is the first and n_1 is the second minutia we would encounter when we traverse the angle $\angle n_0 m_i n_1$ in counter-clockwise. If we order the neighboring minutiae according to their Euclidean distances instead of the angles, there is a high chance that the order of the neighboring minutiae will be flipped due to elastic deformation. Moreover, we do not include ridge counts and minutiae types in our secondary features, like other local features [37, 11, 99, 51, 72]. Not all the minutiae-based fingerprint representations have the ridge count information. If we want to apply our matching scheme on other existing fingerprint databases or if we wish to use other ready-to-use minutiae extraction libraries, then we cannot use the ridge count information. We do not use minutiae type as features because they are not very reliable. There may be a change between impressions due to the different vertical forces on different applications. Figure 3.3 illustrates how a minutia is categorized as two different types in two different impressions.

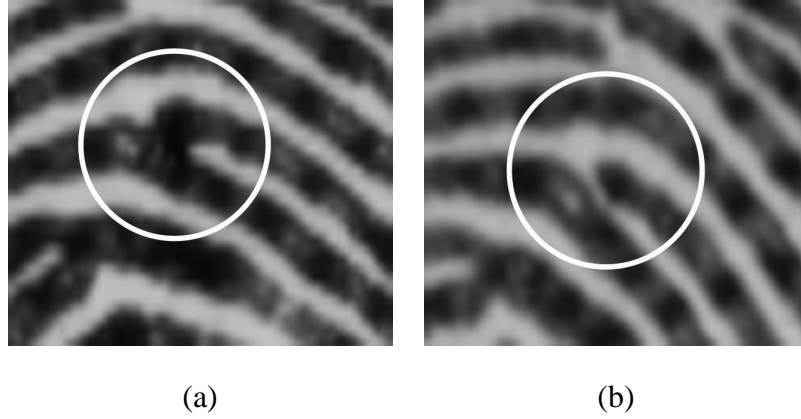


Figure 3.3: The same minutiae extracted from two different impressions, in (a) it appears as a bifurcation but a ridge ending in (b).

Local Matching Stage

The secondary features are localized and invariant to rotation, hence we do not need the pre-alignment stage. Moreover, Kovács-Vajna [55] has demonstrated that small local deformations can result in a large global distortion. Therefore, matching based on localized features has the advantage of better handling of non-linear global distortion. Let $s_i^q = (r_{i0}, r_{i1}, \theta_{i0}, \theta_{i1}, \phi_{i0}, \phi_{i1})$ and $s_j^r = (r_{j0}, r_{j1}, \theta_{j0}, \theta_{j1}, \phi_{j0}, \phi_{j1})$ be the secondary features on the query and reference fingerprints respectively. s_i^q is matched to s_j^r if and only if both the neighbors, n_{i0}^q and n_{i1}^q of s_i^q , fall in the corresponding dynamic tolerance areas (section 3.2.4) of n_{j0}^r and n_{j1}^r of s_j^r respectively. The goal of this phase is to obtain the possible initial correspondence relationships between secondary features on both \mathbf{I} and \mathbf{T} , and to create a candidate list that represents the correspondences of secondary features. At first, we construct a cost matrix that indicates all the matched (with respect to dynamic tolerance

areas) secondary features and their feature distances. The cost matrix is used to convert the secondary feature matching problem into an equivalent Minimum Cost Flow problem. By solving the equivalent MCF problem, the candidate list is obtained (Section 3.2.5).

Validation Stage

Since matching is performed within the local areas around minutia points, the global structural relationships between feature points are not captured. Certain secondary features in the candidate list are in conflict with each other in the global context (Figure 3.4).



Figure 3.4: An example of two false matched secondary features. They are similar at the local structures but conflict with each other in global context (at very different locations with respect to the core and delta points).

To resolve the conflicts, a validation step checks that all the matched feature pairs have similar orientation differences if they come from the same finger. We approximate the orientation difference between fingerprints by plotting a histogram, where each bin is about

10°. The dominating bin and its neighbors are identified. The matched feature pairs in the other bins (not in the dominating bin and its neighbors) are removed from the candidate list.

Jiang and Yau [51] estimate the orientation difference between features pairs using the best fit method. They make the best fit local feature structure pairs as reference points between two fingerprints. However, this may not always work since the best-matched feature is not necessarily correct. We use the top C best matched secondary feature pairs as reference points. For each reference point pair, we convert the minutiae on both I and R into polar coordinates with respect to the chosen reference points. Therefore, we can get the number of matched minutiae by once again applying MCF with the dynamic tolerance area. The largest number of matched minutiae is chosen as the final result and used to calculate the similarity score.

3.2.4 Dynamic Tolerance Areas

Distortions are inevitable when mapping a 3-dimensional fingertip onto a 2-dimensional plane. These can be caused by varying vertical pressures, shear forces and impression conditions. We observe that within a localized secondary feature $s_i(r_{i0}, r_{i1}, \theta_{i0}, \theta_{i1}, \phi_{i0}, \phi_{i1})$, we should expect larger angular distortion but smaller distance variation when r_{i0} and r_{i1} are small. On the other hand, as r_{i0} and r_{i1} increase, the distance distortion gets larger when the angular distortion reduces. Therefore, it is reasonable to adjust the tolerance areas according to the values of r_{i0} and r_{i1} .

Since the thresholds should change with the length of the line segment of central minugia and its neighbors, we use threshold functions of the length instead of fixed values. The tolerance area is decided by three threshold functions $Thld_r(\cdot)$, $Thld_\theta(\cdot)$, and $Thld_\phi(\cdot)$. The distance thresholds function ($Thld_r(\cdot)$) should be more restrictive (smaller) when r_{i0} and r_{i1} are smaller and more flexible when r_{i0} and r_{i1} are larger. On the other hand, the thresholds on angles ($Thld_\theta(\cdot)$ and $Thld_\phi(\cdot)$) should be larger in order to allow large distortions when r_{i0} and r_{i1} are small, but smaller when r_{i0} and r_{i1} are large (Figure 3.5).

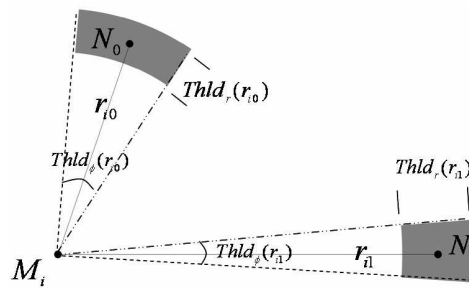


Figure 3.5: Dynamic tolerance area.

In our study, the threshold functions are defined as:

$$Thld_r(r) = D_{max} \cdot \max\{5, r \cdot D_{ratio}\} \quad (3.1)$$

$$Thld_\theta(r) = \begin{cases} A1_{max} \cdot C_{lb} & \text{if } r \geq R_{max} \\ A1_{max} \cdot C_{ub} & \text{if } r \leq R_{min} \\ A1_{max} \cdot \left(C_{ub} - \frac{(r-R_{min})(C_{ub}-C_{lb})}{(R_{max}-R_{min})}\right) & \text{otherwise} \end{cases} \quad (3.2)$$

$$Thld_\phi(r) = \begin{cases} A2_{max} \cdot C_{lb} & \text{if } r \geq R_{max} \\ A2_{max} \cdot C_{ub} & \text{if } r \leq R_{min} \\ A2_{max} \cdot \left(C_{ub} - \frac{(r-R_{min})(C_{ub}-C_{lb})}{(R_{max}-R_{min})}\right) & \text{otherwise} \end{cases} \quad (3.3)$$

where D_{max} , D_{ratio} , $A1_{max}$, $A2_{max}$, C_{lb} , C_{ub} , R_{max} , and R_{min} are predefined constants. We set these values differently in local matching stage and validation stage, since stricter constraints are desired in the latter case. For the local matching stage, we set these constants to: $D_{max} = 1.5$, $D_{ratio} = 0.1$, $A1_{max} = 1.5$, $A2_{max} = 1.5$, $C_{lb} = 5$, $C_{ub} = 20$, $R_{max} = 210$, and $R_{min} = 10$. For the validation stage, we set these constants to: $D_{max} = 1.0$, $D_{ratio} = 0.1$, $A1_{max} = 1.5$, $A2_{max} = 1.2$, $C_{lb} = 10$, $C_{ub} = 20$, $R_{max} = 100$, and $R_{min} = 5$.

3.2.5 Minimum Cost Flow Problem (MCF)

The matching of the minutiae feature points in fingerprints presents several unique challenges. The matching of feature points on two fingerprints is equivalent to finding the correspondences between the feature points (Figure 3.6). The numbers of feature points on the query and reference fingerprints are rarely equal and therefore not every feature point finds a matched feature point. Thus, obtaining an optimal pairing is not trivial even when

two fingerprints are aligned.



Figure 3.6: Match two fingerprints is equivalent to find the corresponding links between feature points.

The most important rule to matching feature points is to guarantee a one-to-one correspondence between the feature points; that is, one feature point on the query fingerprint I can have at most one corresponding feature point in the reference fingerprint R . To comply with this constraint, one can mark the minutiae that have already been matched to avoid them being matched again. But it is hard to find the optimal pairing of the feature points. Given that the feature point (m_I^2 in Figure 3.7) of a query fingerprint, I , can fall within the tolerance area of more than one feature point of the template fingerprint, R , the best pairing is defined as the configuration that maximizes the final number of matched minutia pairs. A more sophisticated method is needed to obtain the optimum pairing [70].

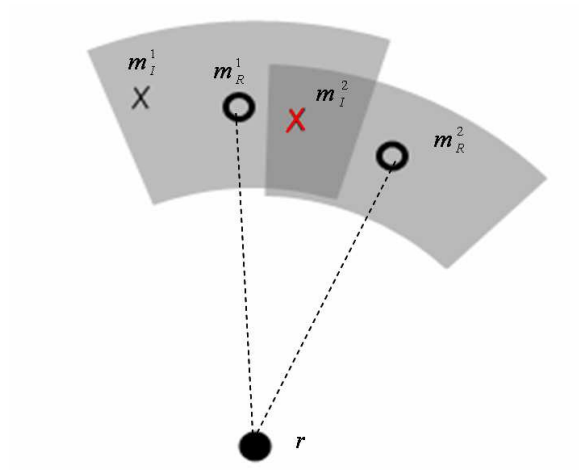


Figure 3.7: Minutiae of I and R are aligned with respect to the reference point r . Minutiae from I are denoted by X s, and the minutiae from R are denoted as O s. In this figure, minutia m_I^2 falls in the tolerance areas of m_R^1 and m_R^2 . If m_I^2 were matched with m_R^1 , which is the closest minutia to m_I^2 , then m_R^2 would stay unmatched.

Families of point pattern matching methods have been studied in many pattern recognition and computer vision tasks. Relaxation methods [81] iteratively adjust the confidence level of the pairing until a certain acceptance criterion is satisfied. Energy minimization methods, such as genetic algorithms, find the optimal solutions by minimizing the energy functions associated with each solution. These methods are slow and unsuitable for real-time matching. Tree pruning approaches usually require an equal number of points in both the matching templates, which is difficult to satisfy in real applications. Hough transform-based methods are also used [85].

We obtain alignment parameters by secondary feature matching and apply operational research techniques to find the one-to-one correspondence between the feature points. We use Minimum Cost Maximum Flow (in short, Minimum Cost Flow or MCF) technique (Figure 3.8), to find the optimal pairing. The translation from fingerprint feature points matching to a equivalent MCF problem is intuitive. *Minimum Cost Maximum Flow* problem is the generalization of many network problems, such as the shortest path problem, maximum flow problem, transportation problem, transshipment problem and maximum bipartite matching problem [16]. In this thesis, we explore its use for fingerprint matching. Figure 3.8 gives a simple example of an MCF problem. Imagine a small portion of routes with 7 cities. We want to transport as many supplies as possible from city s to city t . There are 5 cities on different toll-routes between s and t with varying road widths (capacities) and tolls (costs). To solve the MCF problem, we must find the amount of supplies that t can receive with a minimum cost. The MCF problem is formally defined as:

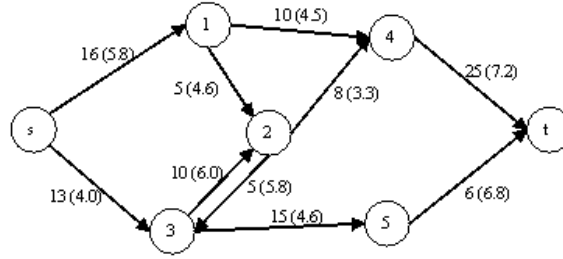


Figure 3.8: An example of minimum cost flow problem. Our goal is to find a flow from s to t with a maximum flow value and a minimum cost. The numbers assigned to each edge are the capacity and unit cost shown in parentheses.

Given a directed graph $G = (V, E)$, where V and E are the sets of nodes and edges in G , with the source node s , sink node t , a real-valued capacity function $w(u, v)$ and a real-valued cost function $c(u, v)$ for all $u, v \in V$, a flow f in G is a real-valued function $f : V \times V \rightarrow R$ such that

$$\forall u, v \in V, f(u, v) \leq w(u, v) \quad [\text{Capacity constraint}]$$

$$\forall u, v \in V, f(u, v) = -f(v, u) \quad [\text{Skew symmetry}]$$

$$\forall u \in V - \{s, t\}, \sum_{v \in V} f(u, v) = 0 \quad [\text{Flow conservation}]$$

The value of the flow is $|f| = \sum_{v \in V} f(s, v)$, and the cost of the flow is $C(f) = \sum_{u, v \in V} (c(u, v)f(u, v))$.

The capacity constraint simply implies that the net flow from one node to another must not exceed the given capacity. Skew symmetry states that the net flow from one node to another is the negative of the net flow in the reverse direction. The property of flow conservation states that any node, which is not

the source or sink, must have outgoing flow equal to the incoming flow [16].

Different approaches are available to effectively solve the MCF problem [64].

The objective is to find the maximum flow $|f|$ with the minimum cost $C(f)$.

MCF and its applications are extensively discussed by Ford and Fulkerson [25], and Edmonds and Karp [23]. Other methods such as network simplex, cost-scaling, relaxation, and push-relabel are also available [64, 30]. The *Scaling & Canceling* algorithm proposed by Orlin et al. [92] can solve the problem in polynomial-time ($O(m(m+n \log n) \log(nU))$), where n is the number of nodes in the network, m is the number of edges and U is the upper bound of the value of capacity (which would be 1 in our case).

In the context of fingerprint recognition, we are not only interested in the maximum number of matches but also the minimum cost. We translate our feature point matching problem into an MCF problem. Matching the feature points on two fingerprints is equivalent to finding the correspondences between the feature points (Figure 3.6). Suppose we have two sets of feature points from different fingerprint images (\mathbf{I} and \mathbf{R}) which are already aligned with respect to a pair of reference points in each image. To construct a flow network, we add one extra point (node), say the source s , into the set of \mathbf{I} and add a point (node), say sink t , into the set of \mathbf{R} . We also set up the links (edges) between nodes by adhering the following rules:

- There is one and only one link that connects s to every point in the first set.
- There is one and only one link that connects t to every point in the second set.

- There is no link between the points within the same set.
- There is exactly one link between every point in the first set and every point in the second set.
- Every link is associated with a capacity and a cost.

The cost matrix $c(i, j) = \text{dist}(m_i, m'_j)$, where $1 \leq i \leq N_I$ and $1 \leq j \leq N_R$, represents the costs of the edges between \mathbf{I} and \mathbf{R} . N_I and N_R are the number of feature points on \mathbf{I} and \mathbf{R} , respectively. The function, $\text{dist}(a, b)$, is the distance measure of two feature points, a and b , on \mathbf{I} and \mathbf{T} , respectively. For efficiency purposes, we remove the edge between m_i and m'_j if m_i is not in the tolerance area of m'_j . There are a total of $N_I + N_R + 2$ (with the source s and sink t nodes) nodes in the network. In our application, the capacity on every edge is set to 1. The costs associated with the edges that come from s and going to t are set to 0. The costs associated with the edges connecting \mathbf{I} and \mathbf{R} are set to $\text{dist}(a, b)$ in which $a \in \mathbf{I}$ and $b \in \mathbf{R}$. The configuration of the fingerprint matching problem is shown in Figure 3.9. The optimal flow value in this network is the number of matched feature points. Because the capacity of every edge is set to 1, there will be no two feature points in \mathbf{I} that would match with the same feature point of \mathbf{R} and vice versa. Thus, the one-to-one matching of feature points is guaranteed. Solving the minimum cost flow problem of the generated flow network is equivalent to finding the maximum number of matched feature points (maximum flow) with the minimum total feature distance (minimum cost).

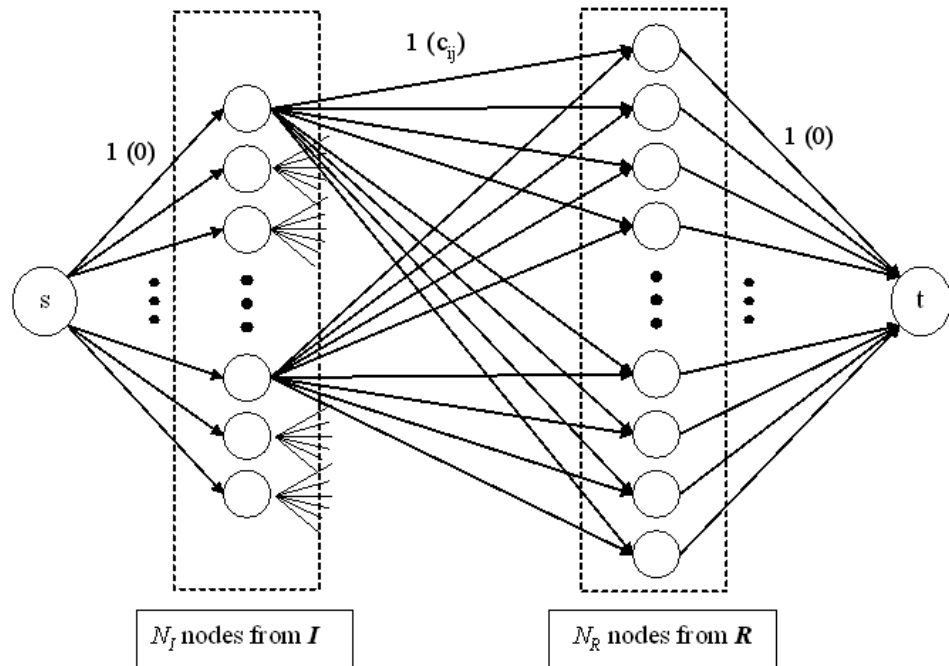


Figure 3.9: Flow network representation of minutia matching problem. All the edges in the network have capacity 1. The edges between source node s and nodes from I have zero cost as well as the edges from R to sink node t . Costs of the edges between nodes from I and nodes from R are from the cost matrix c .

3.2.6 Similarity Score Calculation

Similarity score is the value that measures how similar the two fingerprints are when compared to each other, and its generation is important to an automatic fingerprint recognition system. It is used to make the final decision of verification in the identification process and is usually the last stage of the system. Human experts make the final decision according to forensic guidelines which suggests that a minimum of 12 matched minutiae is sufficient to conclude that the two fingerprints are from the same finger [70]. However, a minutiae-based automatic fingerprint recognition system can not make a decision using an absolute value alone, as a human expert can. Unlike human experts who have access to all the information that a fingerprint image contains, such as overall ridge flow pattern, location and configuration of singular points (core and delta), location of pores, and ridge counts between pairs of minutiae, the minutiae-based automatic systems have access to only the information from the minutiae representation of fingerprints.

A traditional way of calculating the similarity scores for a minutiae-based system is $\frac{n^2}{(size_I \times size_R)}$, where $size_I$ and $size_R$ represent the numbers of minutiae on query and reference fingerprints, and n is the number of matched minutiae on both prints. Bazen and Gerez [7] claim that using $\frac{2n}{(size_I + size_R)}$ provides more consistent similarity scores. In our study, we found both methods are unreliable, especially when matching fingerprints of different sizes. We use the number of matched minutiae, the number of minutiae points on overlapping areas, and the average feature distances to calculate reliable similarity scores.

Overlapping Areas

We estimate the overlapping areas of both prints using a convex hull based technique. After the matching, the two fingerprints are aligned and converted into the same coordinate system. We create the convex hull of each fingerprint so that it contains all the feature points (minutiae). Let us denote the convex hull constructed from feature points on query fingerprint (\mathbf{I}) as C_I , and the convex hull constructed from feature points on reference fingerprint (\mathbf{R}) as C_R . For every feature point on the reference fingerprint (\mathbf{R}), if it falls inside C_I , we say it is in the overlapping area of \mathbf{I} . Similarly, there is a set of feature points in \mathbf{I} that fall in the overlapping area of \mathbf{R} . The feature points in the overlapping areas of both fingerprints are obtained, and denoted as O_I and O_R . The convex hulls of the overlapping areas give us the coarse boundaries of the overlapping areas and provide useful information to calculate the similarity scores. Figure 3.10 shows examples of the convex hulls of overlapping areas, a genuine match (Figure 3.10.(a) vs. Figure 3.10.(b)) and an impostor match (Figure 3.10.(c) vs. Figure 3.10.(d)). Both the genuine and impostor matches return a result of eight matched feature points, thus we cannot decide whether the test is genuine just based on the number of matched feature points. However, by comparing the convex hulls of the overlapping areas, we can make the distinction.

Similarity Score Generation

We consider the following information to compute the similarity scores.

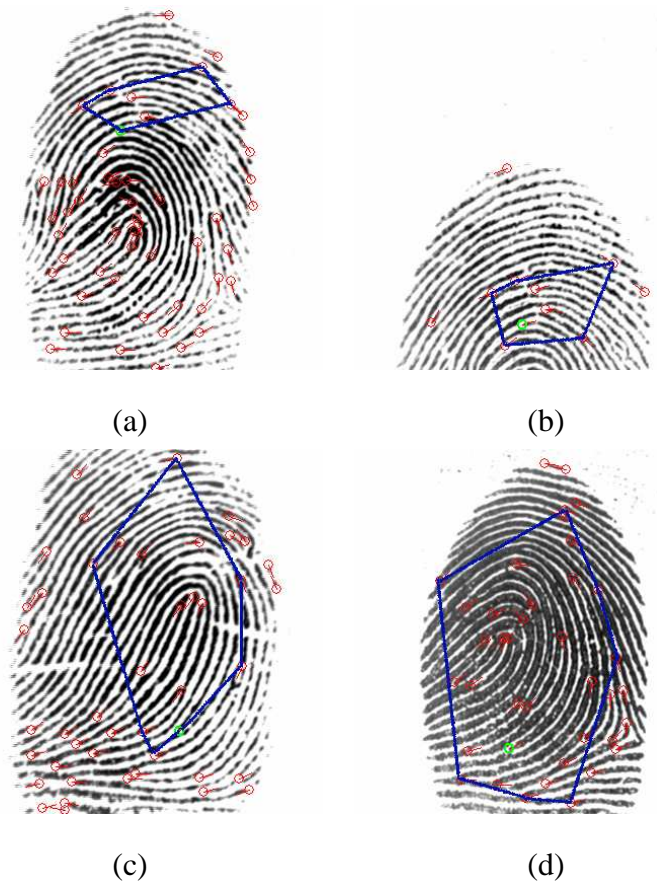


Figure 3.10: Examples of convex hulls of overlapping areas. (a) vs. (b) is a genuine test; whereas (c) vs. (d) is a impostor test. Both tests have eight matched feature points. However, the convex hulls of overlapping areas of the test (a) vs. (b) have very small areas comparing to those of test (c) vs. (d), we can probably decide whether the decision of the test of (a) vs. (b) is a genuine test but the test of (c) vs. (d) is an impostor test.

- n : The number of matched feature points;
- $size_I$: The number of feature points on the query fingerprint (I);
- $size_R$: The number of feature points on the reference fingerprint (R);
- O_I : The number of feature points in the overlapping area of query fingerprint (I);
- O_R : The number of feature points in the overlapping area of reference fingerprint (R);
- S_{avg} : The average feature distance of all the matched features.

We describe two methods, one based on a heuristic rule and the other based on a neural network, to calculate the similarity scores.

1. **Heuristic rule:** Following conditions should be met.

- The dimensions of the *combined fingerprint* should not exceed certain ranges. A *combined fingerprint* is a fingerprint constructed from the query and reference fingerprints with respect to the overlapping areas. If the two fingerprints are correctly matched, then the dimensions of the *combined fingerprint* should not be too big, for example, it is expected to be smaller than twice the size of an average fingerprint.
- The overlapping areas of the matched fingerprints should not be too small. We assume that there are at least a certain number (five, in our experiments) of

minutiae points in the overlapping areas.

- The average feature similarity, S_{avg} , of every paired minutiae gives an indication of the goodness of match.
- The number of matched minutiae plays an important role.

The details of the heuristic rule are illustrated in Figure 3.11.

```
Let  $S$  as the similarity score; Let  $height_c$  as the height of combined fingerprint;  
Let  $width_c$  as the width of combined fingerprint;  
Let  $max_h$  as the maximum possible height;  
Let  $max_w$  as the maximum possible width;  
Let  $T_m$  as a integer-valued threshold;  
If ( $N < 7$  And ( $height_c > max_h$  Or  $width_c > max_w$ )) then  
     $S = 0$ ;  
Else  
    If ( $O_a < 5$ ) then  
         $O_a = 5$ ;  
    Endif  
    If ( $O_b < 5$ ) then  
         $O_b = 5$ ;  
    Endif  
    If ( $N > T_m$  And  $N > \frac{3}{5}O_a$  And  $N > \frac{3}{5}O_b$ ) then  
         $S = S_{avg}$ ;  
    Else  
         $S = \frac{N^2 S_{avg}}{O_a O_b}$ ;  
        If  $S > 1.0$  then  
             $S = 1.0$ ;  
        Endif  
    Endif  
Endif
```

Figure 3.11: A heuristic rule for generating similarity scores.

2. **Neural Network:** Neural network techniques have been used for a long time to find solutions to problems that have too many variables. In addition to finding a linear separating boundary, multi-layer neural networks, given an adequate number of hidden neurons, can implement arbitrary decision boundaries [22]. A two-hidden-layer fully connected neural network (Figure 3.12) is trained to take the six values as input and return a similarity score between 0 and 1. Our experiments show a 1.21% and 0.68% improvement on the minimum total error rate on the FVC2002 [69] DB1 and DB2 databases by simply using this similarity score calculation method.

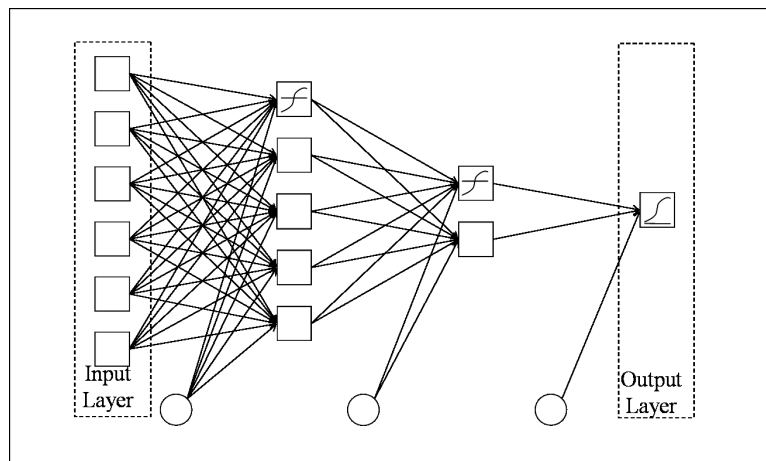


Figure 3.12: The architecture of the neural network. The network has 2 hidden layers and 3 bias nodes link to each node. The input layer has 6 nodes. The hidden layers have 5 and 2 nodes with tangent sigmoid transfer function and logarithmic sigmoid transfer function respectively. The output layer uses logarithmic sigmoid transfer function to generate the similarity score.

	n	$size_I$	$size_R$	$\frac{n^2}{size_I \times size_R}$	$\frac{2n}{size_I + size_R}$	Heuristic	NN
57_2 vs. 57_4	10	41	21	0.12	0.32	0.55	0.999996
23_1 vs. 45_1	14	39	45	0.13	0.35	0.18	0.005490

Table 3.1: Comparison of different similarity score calculations. Results are calculated on the images from FVC2002 DB1 database. Images 57_2 and 57_4 are from the same finger but different impressions. Images 23_1 and 45_1 are from different fingers.

A comparison of different similarity score calculations is shown in Table 3.1. The comparison shows our method gives higher scores on genuine tests (the first case in Table 3.1) than on impostor tests (the second case in Table 3.1).

3.3 Experimental Results

Our system has been tested on fingerprint databases of FVC2002 [69]. The DB1 database contains 110 different fingers and 8 impressions of each finger yielding a total of 880 fingerprints ($388 \text{ pixels} \times 374 \text{ pixels}$) at 500 dots-per-inch (dpi). The DB2 database has the same number of fingerprint images as DB1 but at different size and resolution ($296 \text{ pixels} \times 560 \text{ pixels}$ at 569 dpi). Each database has two different sets: A and B. Set A contains the fingerprint images from the first 100 fingers, while Set B has the images from the other 10 fingers. We use Set B of each database as our training set for matching parameters and then we perform the experiment on the fingerprints of Set A.

We followed the protocols [69] of FVC2002 to evaluate the FAR (False Accept Rate)

and FRR (False Reject Rate) of our system. For FRR, the total number of genuine tests (with no rejection) is $(8 \times 7)/2 \times 100 = 2800$. For FAR, the total number of false acceptance tests (with no rejection) is $(100 \times 99)/2 = 4950$. On an Intel Pentium 4, 1.4 GHz machine, the average matching time for a genuine test is about 179 ms and 8 ms for a false acceptance test. The reasons for faster matching time in cases of false acceptance tests are the following: (i) the matching decision of impostor pairs is made earlier, right after the secondary feature matching, thus there is no need to match the corresponding minutiae, and (ii) there are fewer overlapping minutiae. To evaluate the performance of the neural network generated scores, we use the first 1400 results of FRR and FAR testing for neural network training. The experimental results are shown in Figure 3.13 and Figure 3.14. For DB1, our system reaches the equal error rate (EER) at 2.13%. For DB2, the EER is 1.57%

We have analyzed the failures and found that they are caused by spurious minutiae or small overlapped areas. Problems like these make the secondary feature matching difficult but can probably be solved by applying brute-force matching techniques. However, knowing when to apply the brute-force matching still remains a challenge.

Figure 3.15 demonstrates the performance of brute-force matching. We improve the system performance from 2.13% EER to 1.01% EER for DB1. Thus, without improving the accuracy of minutiae extraction, the ceiling of performance is about 1.01% equal error rate.

In order to test the influence of the size of partial fingerprints, we generated two series of partial fingerprint databases with different sizes (in percentage) from the FVC2002 DB1

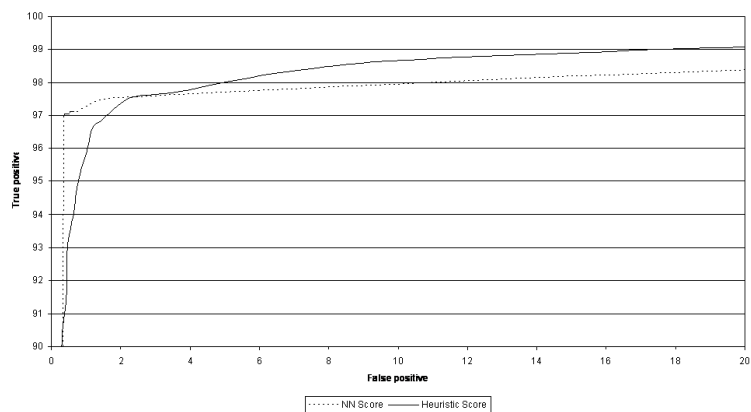


Figure 3.13: ROC graph of system testing result on FVC2002 DB1 database. With heuristic rules for similarity scores, the system reaches the minimum total error rate at 4.53% (with FAR at 1.24% and FRR at 3.29%), and EER at 2.39%. With NN scores, the system reaches the minimum total error rate at 3.32% (with FAR at 0.39% and FRR at 2.93%), and EER at 2.13%.

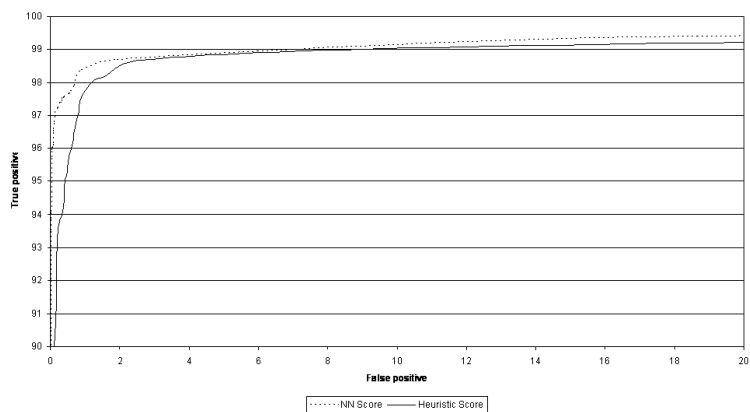


Figure 3.14: ROC graph of system testing result on FVC2002 DB2 database. With heuristic rules for similarity scores, the system reaches the minimum total error rate at 3.17% (with FAR at 1.24% and FRR at 1.93%), and EER at 1.69%. With NN scores, the system reaches the minimum total error rate at 2.49% (with FAR at 0.85% and FRR at 1.64%), and EER at 1.57%.

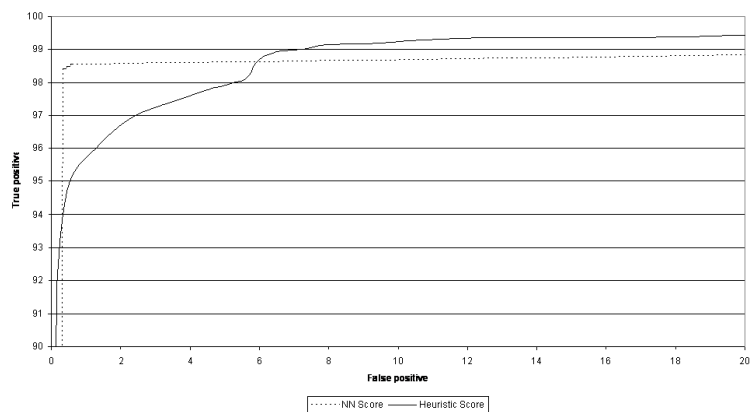


Figure 3.15: ROC graph of the brute-force matching with the neural network generated scores of FVC2002 DB1 database. The system reaches the minimum total error rate at 1.88% (with FAR at 0.31% and FRR at 1.57%), and EER at 1.01%. With heuristic rules for similarity scores, the system reaches the minimum total error rate at 5.27% (with FAR at 1.27% and FRR at 4.00%), and EER at 2.67%.

data set. (i) The first data set was generated by considering the minutiae at random regions within the fingerprint. The region sizes considered were 10%, 15%, 20%, 25%, 30%, 35%, 40%, 45%, 50%, 55%, 60%, 65%, 70%, 75%, 80%, 85%, and 90% of the fingerprint foreground area. (ii) The second data set was generated by considering the central region of the fingerprint only. This is done to simulate conditions where physical guides are used to ensure that the finger is placed centrally on the sensor. We tested the system by matching the partial fingerprint templates of the second impressions against the first impression of every finger in DB1. The system test results for the first case are shown in Figure 3.16 and Table 3.2. The results for the second condition are shown in Figure 3.17 and Table 3.3.

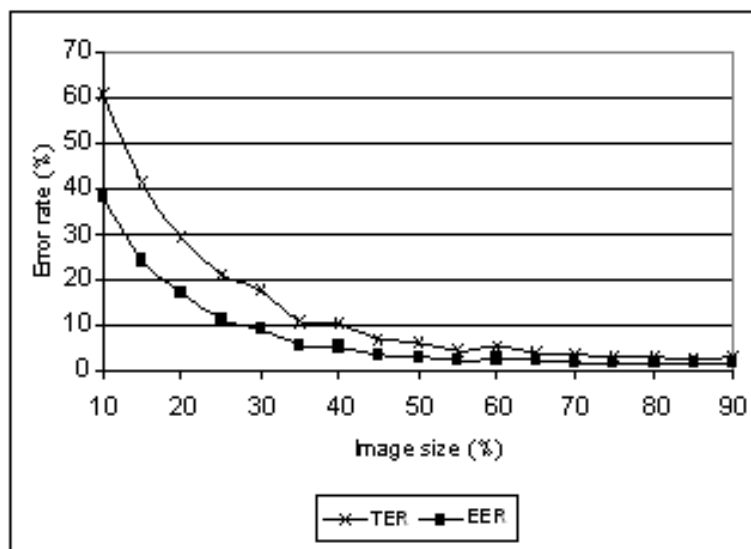


Figure 3.16: System performances vs. different-sized partial fingerprints at random positions.

As expected, the performance of the partial fingerprints on the second data set is slightly

Size(%)	avg. width (pixels)	avg. height (pixels)	avg. minu. num.	Min. Total Error Rate (%)			EER (%)
				FAR	FRR	TER	
90	196.61	283.30	34.89	1.844871	1.090909	2.93578	1.71
80	185.32	267.07	32.00	1.988324	0.909091	2.897415	1.74
70	173.35	249.78	28.74	1.721435	1.818182	3.412844	1.77
60	160.42	231.22	25.28	2.675563	2.363636	5.039199	2.52
50	146.41	211.03	21.56	2.378649	3.636364	5.981651	3.17
40	130.90	188.70	17.49	2.905755	7.454545	10.3603	5.25
30	113.31	163.36	13.36	4.647206	13.09091	17.738115	9.12
20	92.42	133.30	8.84	9.611343	19.63636	29.247707	17.11
10	65.20	94.11	4.23	15.23937	45.63636	60.87573	38.21

Table 3.2: System performance with difference sized partial images at random positions.

better than on the first data set. However, the system performance drops significantly even on the second data set when the image sizes are smaller than 60% (about $0.32'' \times 0.46''$) of the full prints.

3.4 Summary

Automated partial fingerprint identification is a problem that has not yet been adequately addressed by researchers. Our matching algorithm overcomes the drawbacks of conventional approaches to partial fingerprint matching by using localized *secondary features* and a flow network based brute-force matching. The *secondary features* and matching algorithm have the following advantages: (i) *secondary features* are generated from minutiae information alone and hence can be adapted to existing applications; (ii) *secondary features*

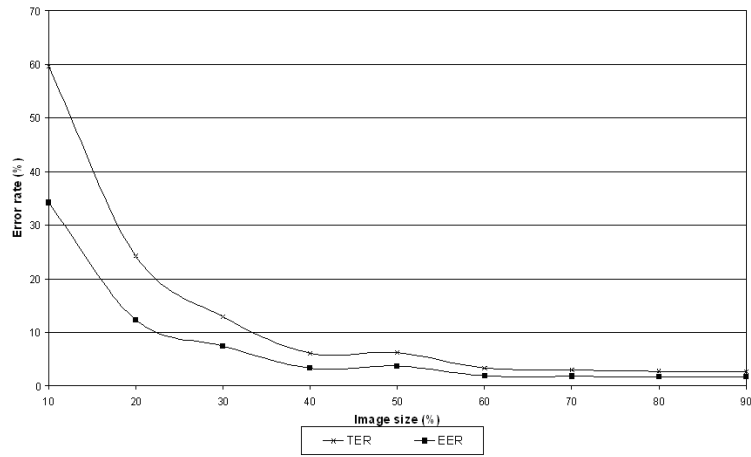


Figure 3.17: The system performances vs. different-sized partial fingerprints at central positions.

Size(%)	avg. minu. num.	Min. Total Error Rate (%)			EER (%)
		FAR	FRR	TER	
90	36.24	1.784821	0.909091	2.693912	1.67
80	33.40	1.834862	0.909091	2.743953	1.68
70	30.33	0.266889	2.727273	2.994162	1.78
60	26.65	2.435363	0.909091	3.344454	1.88
50	22.90	2.552127	3.636364	6.188491	3.69
40	18.56	2.468724	3.636364	6.105088	3.32
30	14.47	3.761284	9.090909	12.852193	7.43
20	9.95	9.681188	14.545455	24.226643	12.31
10	5.02	16.948302	42.727273	59.675575	34.20

Table 3.3: System performance with difference sized partial images around the center of the print.

are invariant to orientation, thus overcoming one of the biggest challenges in partial fingerprint matching; (iii) localized features and dynamic tolerance areas provide the ability to handle spatial distortions; and (iv) solving the minutia matching problem by converting it into a minimum cost flow problem gives us an efficient way of finding the optimal one-to-one correspondence of minutiae between query and reference fingerprints. A convex hull based method of estimating the overlapping areas of query and reference fingerprints has also been presented in this chapter. Our experiments show that using a neural network for generating similarity scores improves accuracy. By changing the similarity score generation scheme alone, we obtained 1.21% and 0.68% improvements on minimum total error rates on the FVC2002 [69] DB1 and DB2 databases respectively.

Chapter 4

Size Specific Fingerprint Matching

4.1 Introduction

The matching algorithm that is proposed in Chapter 3 has the advantage of being able to handle problems in fingerprint matching, such as non-linear distortion, unknown alignment, and score generation, by using localized secondary features (see Section 3.2.3), dynamic tolerance areas (see Section 3.2.4), MCF algorithms (see Section 3.2.5), and intelligent score generation methods (see Section 3.2.6). Matching of small partial fingerprints is performed by brute-force matching (see Section 3.2.2) when the number of feature points present on the fingerprints is less than a certain threshold (α). The selection of α is important to the system's performance in terms of speed and accuracy. If α is set too low, only those fingerprints which have few feature points would benefit from brute-force matching. This may result in a high false reject rate (FRR), since most of the participating fingerprints contain more feature points than α , and some of them do not have enough

feature points to obtain a successful match in the first stage of secondary feature matching. On the other hand, if α is set too high, most matches would be performed by the brute-force matching lowering the speed of the system and causing a higher false accept rate (FAR).

In this chapter, we overcome the issues of selecting an α by proposing a new matching algorithm that uses the same localized secondary features. The number of secondary features associated with each minutia point is decided by the size of the fingerprint. An indexing technique is used to speed up the process of secondary feature matching in the local matching stage, without compromising the system accuracy. After validating the matchings in the first stage, a novel matching technique that accumulates matching evidence on local areas without a global alignment is applied to achieve the final minutiae pairing between the query and reference fingerprints.

4.2 Feature Generating and Indexing

The features that we use in this algorithm are the same secondary features as described in Section 3.2.3. Each secondary feature is composed of a central minutia and its two neighboring minutiae. A secondary feature is represented as $s_i = (r_{i0}, r_{i1}, \theta_{i0}, \theta_{i1}, \phi_{i0}, \phi_{i1})$ where r_{i0} and r_{i1} are the Euclidean distances between the central minutia m_i and its neighbors, n_0 and n_1 , respectively. θ_{i0} and θ_{i1} are the relative orientations of the neighboring minutiae with respect to θ_i , and ϕ_{i0} and ϕ_{i1} are the relative angles of the line segments $\overline{m_i n_0}$ and $\overline{m_i n_1}$ with respect to θ_i (see Figure 3.2).

In Chapter 3, each minutia is associated with only one secondary feature. However, the structure of a secondary feature changes significantly due to the presence of spurious or missing minutiae that are close to the central minutia (Figure 4.1). A spurious or missing minutia causes the disappearance of a genuine secondary feature, while at the same time introduces a false secondary feature (Figure 4.1(c) or Figure 4.1(d)). Structure variation of the secondary features is the main contributor to error cases of the matching algorithm described in Section 3.2.3 especially when there are few feature points on the fingerprints.

To address this problem, we propose to associate more secondary features with a central minutia by generating secondary features from the k nearest neighboring minutiae instead of just the closest two. Bazen and Gerez [7] have proposed a similar approach. However, they used a fixed value of k , whereas we propose to adjust k according to the size of the fingerprint image to maintain similar numbers of features among the images of various sizes. Therefore, for every minutia on the fingerprint we can have

$$h = \binom{k}{2} = \frac{k!}{2! \times (k-2)!} \quad (4.1)$$

secondary features assigned to it. A *neighborhood list* is assigned to each minutia. It contains the following information on:

1. The distance between the central and neighboring minutiae,
2. The relative angle between the neighboring minutia with respect to the orientation of the central minutia,

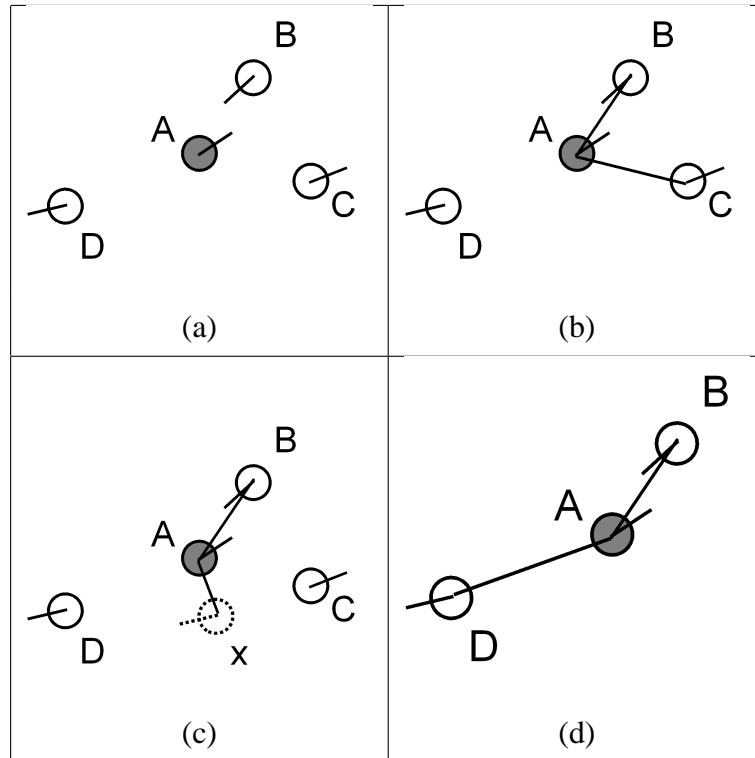


Figure 4.1: (a) Four synthetic minutiae. The gray-colored minutia *A* is used as central minutia to generate secondary features. (b) A genuine secondary feature generated according to Section 3.2.3. (c) The resulting false secondary feature if there is a spurious minutia *X* that is close to *A*. (d) The resulting false secondary feature if the minutia *C* is missing from the minutiae set.

3. The relative orientation of the neighboring minutia with respect to the orientation of the central minutia, and
4. A pointer to the neighboring minutia.

The elements in the *neighborhood list* are sorted by the incremental distances.

Supposing there are $size_{fp}$ minutiae on the fingerprint, the resulting number of secondary features is $size_{fp} \times h$. By associating more secondary features to a central minutia, we reduce the influence of spurious and missing minutiae. Because we create secondary features from the nearest k neighboring minutiae, the majority of genuine secondary features remain intact despite the influence of noisy minutiae. We name a secondary feature using the labels of the central minutia and its two neighboring minutiae. For example, the three genuine secondary features that are illustrated in Figure 4.2(a) are labeled as ABC , ACD , and, ADB . Because of the presence of spurious minutia, X , in Figure 4.2(b), we have six secondary features: ABC , ACX , AXD , ADB , ABX , and ACD . All the *genuine secondary features* exist and can be matched against. In the case of missing genuine minutia (Figure 4.2(c)), portion of the genuine secondary features remain existing and can be matched.

Depending on the size of the fingerprint and the value of k we choose, the range of the number of secondary features varies from less than one hundred to nearly a thousand. It is desirable to have the number of features on all fingerprints participating in the matching process to be within a tight range, so that the matchings are comparable to each other. We

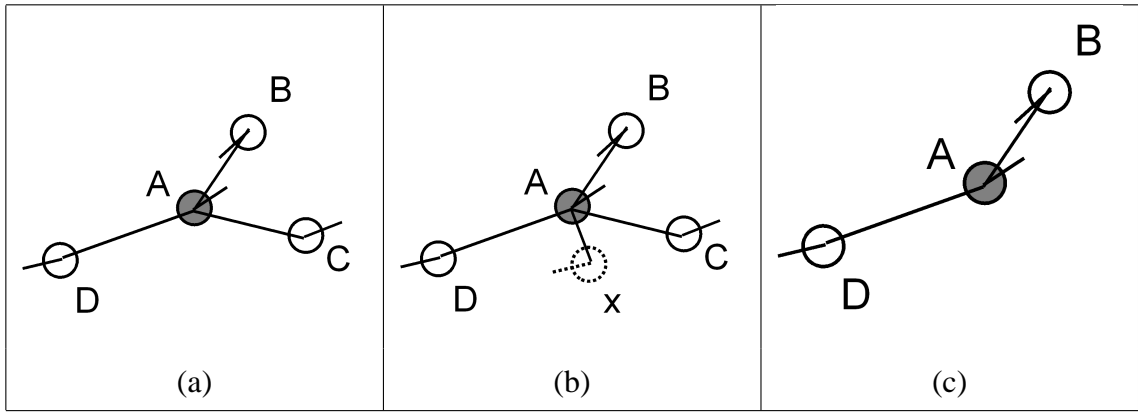


Figure 4.2: (a) Genuine secondary features generated from the closest three neighboring minutiae. (b) Under the influence of a spurious minutia, genuine secondary features remain intact. (c) Under the influence of a missing minutia, some of the genuine secondary features are still available for matching.

do not need to associate many secondary features to a central minutia when the fingerprint is large enough and contains sufficient information for matching. On the contrary, we need a larger k to generate more secondary features for a small fingerprint to increase the confidence and the chance of a successful match. The value of k controls the amount of secondary features within a fingerprint. If k is too small, a false reject may result for a small fingerprint which contains few minutia points. On the other hand, a large k increases the effect of distortion and slows down the matching speed. Hence, balancing sufficient number of secondary features with the value of k is important. We heuristically determine the value of k according to the number of minutia points on the fingerprint. When the number of minutiae is larger than 30, we set k as 6; when the number of minutiae is less than 20, then k is set to 10; otherwise, k is set to 7. Using this rule, we have about 600

secondary features for every fingerprint.

Because of the large number of secondary features, the matching process becomes time consuming. For example, if both the query (\mathbf{I}) and reference (\mathbf{R}) have 600 secondary features, we need to perform 600 matches for every secondary feature on \mathbf{I} to obtain a possible match. In total, there are $600 \times 600 = 360000$ feature matchings executed. We propose to alleviate this problem by indexing (classifying) the secondary features on a fingerprint. Many indexing techniques are applicable. We put each secondary feature into a bin according to the configuration (shape) of the secondary feature. Our method is based on an idea of clustering the secondary features by their geometric characteristics, such as *geometric hashing* [58, 104, 29]. To classify the configuration of a secondary feature, we first divide the plane around the central minutia into several (eight, in our experiment) non-overlapping quadrants (Figure 4.3(a)). The quadrants are aligned with respect to the orientation of the central minutia. Due to the presence of distortion, one cannot precisely determine in which quadrant the neighboring minutia actually lies. Thus, each neighboring minutia in the secondary feature is labeled with the names (numbers, signs, etc.) of the quadrants which the neighboring minutia resides in and is close to (Figure 4.3(b)). In this scheme, the binning is invariant to rotation, translation, and scaling, and every secondary feature is present in a minimum of 2 and maximum 4 bins. When matching is performed, we only need to measure the feature distances of the secondary features that are in the same bin. We remove the *poor* secondary features that introduce ambiguities when performing secondary matching. A secondary feature is *poor* if the angle formed by the central and neighboring minutiae is

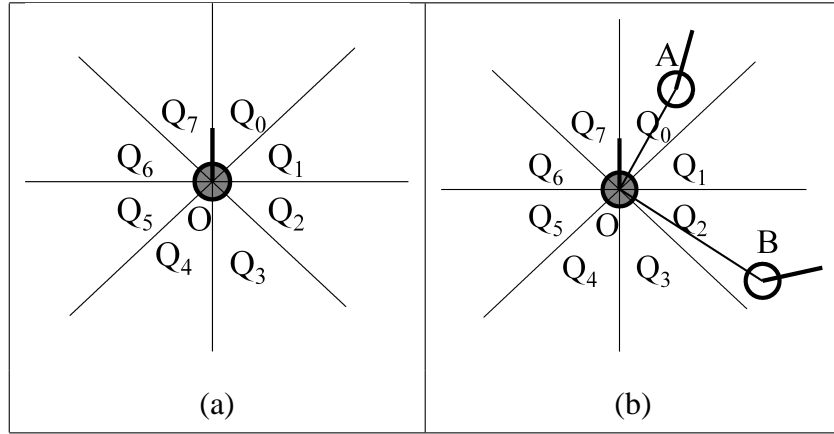


Figure 4.3: (a) The eight quadrants, Q_0 to Q_7 , of a central minutia. Note that the quadrants are aligned with the orientation of the central minutia. (b) An example of secondary feature and it can be labeled as Q_0Q_2 , Q_0Q_3 , Q_1Q_2 , and Q_1Q_3 .

extremely large (close to 180°), or extremely small (close to 0°). On average, each bin contains about 47 secondary features. Following our previous assumption, the total number of feature matches will reduce from 360000 to (600×46.89) 28134 which is a 92% reduction.

The average values of numbers of secondary features in a bin are listed in table 4.1.

Avg. SFV on a fingerprint	580.32
Avg. SFV in a bin	46.89
Min. SFV in a bin	3.69
Max. SFV in a bin	101.91

Table 4.1: Various average values of numbers of secondary features in a bin. These values are obtained from 15500 processing results.

4.3 Feature Matching

Similar to other fingerprint matching algorithms [37, 11, 72, 99, 51, 83] that are based on local structures (secondary features), our feature matching process includes local structure matching and validation stages. However, we have an additional stage after the validation of local structures called *extended matching*. In the *extended matching* stage, we obtain the correspondence of the minutiae between the query fingerprint (\mathbf{I}) and reference fingerprint (\mathbf{R}).

4.3.1 Local Matching and Validation

In the local structure matching stages of other studies [72, 83] that use multiple neighboring minutiae to form a local structure, the matching of the central minutia is determined by the correspondence of the neighboring minutiae. Our algorithm treats each secondary feature individually. For example, if a central minutia and its four neighboring minutiae generate six secondary features (no poor secondary features), then these six secondary features are seen as separate features and not as a central minutia with six feature elements. Every secondary feature is matched independently. The matching based on localized features has the advantage of superior handling of non-linear global distortion.

The matching of secondary features is similar to what we described in Section 3.2.3. Let $s_i^q = (r_{i0}, r_{i1}, \theta_{i0}, \theta_{i1}, \phi_{i0}, \phi_{i1})$ and $s_j^r = (r_{j0}, r_{j1}, \theta_{j0}, \theta_{j1}, \phi_{j0}, \phi_{j1})$ be the secondary features on the query and reference fingerprints respectively. s_i^q is matched to s_j^r if and

only if both the neighbors, n_{i0}^q and n_{i1}^q of s_i^q , fall in the corresponding dynamic tolerance areas (Section 3.2.4) of n_{j0}^r and n_{j1}^r of s_j^r respectively. The dynamic tolerance area changes its shape with the distance between the central and neighboring minutiae to accommodate different levels of distortion in terms of angle and distance. Since the secondary features are indexed according to their spatial configurations (shapes), the search of possible matches for a given secondary feature with a certain index label, xy , need only be performed among those secondary features in the bin which have the same index label xy (Figure 4.3.1).

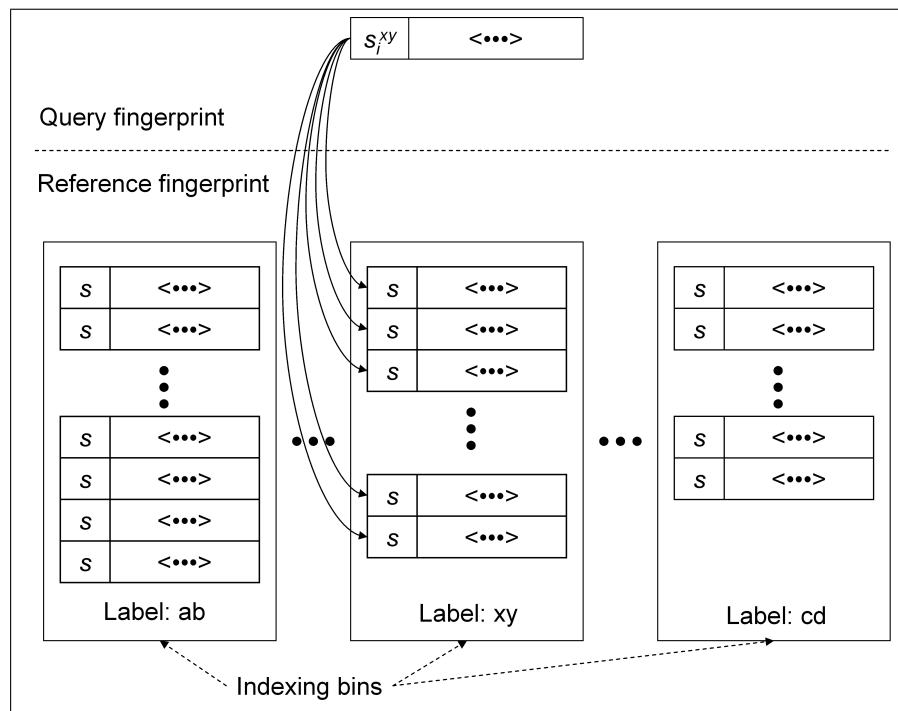


Figure 4.4: s_i^{xy} is a secondary feature on the query fingerprint with index label xy . When the matching is being executing, we match the s_i^{xy} against the secondary features on the reference fingerprint with the same index label.

The matching of secondary features is performed by comparing the similarity of local

structures. While the local feature matching reduces the effect of global distortion and unknown alignments, the information of the fingerprint's global structural relationship is lost. Thus, to reinforce and recover the global relationship between secondary features, a validation stage is needed to remove the falsely matched secondary feature pairs which are in conflict with the global context. We create a histogram of the global rotation parameter from those candidate secondary feature pairs, and then prune the candidate pairs that are far from the histogram peak (detail in 3.2.3). After the validation, a set of possible matched secondary feature pairs is created, and the secondary features that belong to the set are referred to as *seeds*. The *seeds* produced after the validation stage may not be correct, and the correspondence between minutia points (not secondary features) is not fully recovered.

4.3.2 Extended Matching

We improve the matching accuracy by extending the match based on the set of candidate *seeds*, collected from the local structure matching. In [72, 83, 51, 49, 50], minutia points on both query and reference fingerprints are transferred to a new space with respect to a pair of matched local features from the local structure matching stage. This process is referred to as global alignment.

We propose a different approach that does not involve any global alignment to obtain the extended matching of minutia points, and all the matchings are performed locally. Since local distortion is easier to handle [55], our approach has a better chance of dealing with the effect of fingerprint deformation. Moreover, the *neighborhood list* of a secondary feature

(Section 4.2) contains all the information needed for the extended match without a need for re-calculation. The information is generated only once during the feature extraction process. The extended match is to search the possible matches from the immediate neighborhood around the previously matched minutiae. However, there are some issues that need to be dealt with:

1. If the minutiae are clustered, the extended match would be restricted to a small portion of the fingerprint, and may not propagate the match globally (Figure 4.5);
2. Since the extended match can start from any pair of matched feature points, the selection of the best result is challenging. One solution is to use every pair of *seeds* that are returned from the validation stage as starting points, and chose the extended matching result with the largest number of matched feature points as the final outcome. Another approach would be to combine the extended matching results with different starting points, since each extended matching result represents the correspondence of a local portion of a fingerprint.

We address these two issues by adding the *seeds* into each other's *neighborhood list*. This gives a better chance of propagating the match throughout the fingerprint. The combination problem is automatically solved because each pair of matched *seeds* represents a different region of the participating fingerprints. The results have no conflicts if the matching extends from one pair of *seeds* to another pair. Many methods can be applied to find the optimal matching between the minutiae in the *neighborhood list* of two matched *seeds*. For

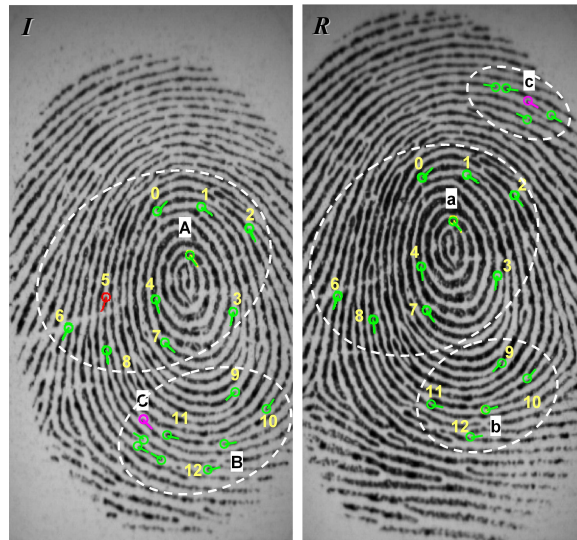


Figure 4.5: Examples of clustered minutia points (in white dashed ovals); each minutia's *neighborhood list* contains only the minutiae that are within the same oval, thus it is difficult to propagate the match from one oval to another. This simplified example will be used in illustrating the process of our extended matching later.

example, the MCF method (Section 3.2.5), dynamic programming [13, 45], or even the exhaustive brute-force approach can be used since the number of elements in a *neighborhood list* is a small constant (6 to 10).

Different from Chikkerur’s approach [13], which exhaustively uses all possible correspondence pairs as starting points, our extended matching chooses the starting points from the set of *seeds* that are returned from the validation stage which makes our approach more efficient. Given a pair of starting *seeds* on the query (I) and the reference (R) fingerprints, a breadth first search is simultaneously executed on both fingerprints. The algorithm is outlined in Figure 4.6. This algorithm is best understood by an example. In Figure 4.7(a), a few minutiae are shown on the query (I , on the left side) and reference (right) fingerprints. The labeled minutiae belong to the set of *seeds*, where minutia **A** matches minutia **a**, minutia **B** matches minutia **b**, and minutia **C** matches minutia **c**. Minutiae **C** and **c** are falsely matched seeds due to the similarity in local configurations. The neighbors of minutiae **A** and **a** are also linked by solid lines, and the added *seeds* are shown by dashed lines in the figure.

1. We select minutiae **A** in I and **a** in R as our starting points, and add the pair $\langle \mathbf{A}, \mathbf{a} \rangle$ into the list M , that keeps all the matched feature points. After every neighboring minutiae (including the added *seeds*) of the starting points have been visited (match is performed), all the matched (link with an arrow) neighboring minutia pairs are added into M . Since there is no unvisited neighboring minutiae of **A** and **a**, they are marked

```

Algorithm: ExtendedMatch
Inputs :  $NL_q$ , the array of neighborhood lists of query fingerprint ( $I$ )
            $NL_r$ , the array of neighborhood lists of reference fingerprint ( $R$ )
            $SL$ , the array of seed pairs  $\langle s_q, s_r \rangle$ 
Outputs :  $M$ , the array of matched minutiae

Let  $M_{local}$  be an array for matched minutia pairs;
Let  $SL_{flag}$  be a boolean array to indicate if a pair of seeds has been used;
Let  $Mask_q$  be a boolean array to indicate if a minutia on  $I$  has found a match;
Let  $Mask_r$  be a boolean array to indicate if a minutia on  $R$  has found a match;
Let  $Q_q$  be a queue of minutiae on  $I$  that has found matched minutiae on  $R$ ;
Let  $Q_r$  be a queue of minutiae on  $R$  that has found matched minutiae on  $I$ ;
Initialize all elements in  $SL_{flag}$ ,  $Mask_q$ , and  $Mask_r$  to false;
FOR each seed pair,  $\langle s_q, s_r \rangle$ , in  $SL$ 
    Insert  $s_q$  into  $NL_q[s_{q'}]$ ,  $\forall s_{q'} \in SL$ , and  $s_{q'} \neq s_q$ ;
    Insert  $s_r$  into  $NL_r[s_{r'}]$ ,  $\forall s_{r'} \in SL$ , and  $s_{r'} \neq s_r$ ;
ENDFOR
FOR  $\langle s_q, s_r \rangle$  in  $SL$ 
    IF ( $SL_{flag}[\langle s_q, s_r \rangle] == \text{true}$ )
        CONTINUE;
    ENDIF
     $SL_{flag}[\langle s_q, s_r \rangle] = \text{true}$ ;
     $Q_q = \{s_q\}$ ;
     $Q_r = \{s_r\}$ ;
     $Mask_q[s_q] = \text{true}$ ;
     $Mask_r[s_r] = \text{true}$ ;
     $M_{local} = \{\}$ ;
    WHILE ( $Q_q$  is not empty and  $Q_r$  is not empty)
         $m_q = \text{DEQUEUE}(Q_q)$ ;
         $m_r = \text{DEQUEUE}(Q_r)$ ;
        Find matched neighbors in  $NL_q[m_q]$  and  $NL_r[m_r]$ ;
        FOR each matched neighbor pair  $\langle m_{q_i}, m_{r_j} \rangle$ 
            IF ( $Mask_q[m_{q_i}] == \text{false}$  and  $Mask_r[m_{r_j}] == \text{false}$ )
                ENQUEUE( $m_{q_i}$ );
                ENQUEUE( $m_{r_j}$ );
                 $Mask_q[m_{q_i}] = \text{true}$ ;
                 $Mask_r[m_{r_j}] = \text{true}$ ;
                Add  $\langle m_{q_i}, m_{r_j} \rangle$  into  $M_{local}$ ;
            ENDIF
        ENDFOR
    ENDWHILE
    IF ( $\text{SIZEOF}(M_{local}) > \text{SIZEOF}(M)$ )
         $M = M_{local}$ ;
    ENDIF
ENDFOR
RETURN  $M$ ;

```

Figure 4.6: Outlines of proposed extended matching.

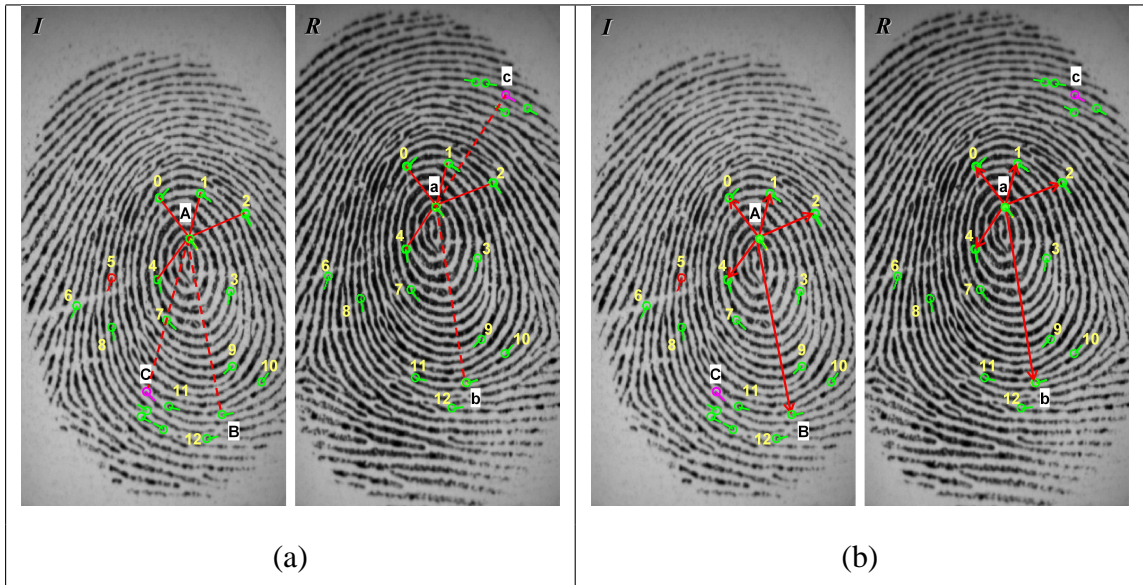


Figure 4.7: (a) Modified neighborhoods of **A** and **a**. (b) After all the neighboring minutiae of **A** and **a** have been visited.

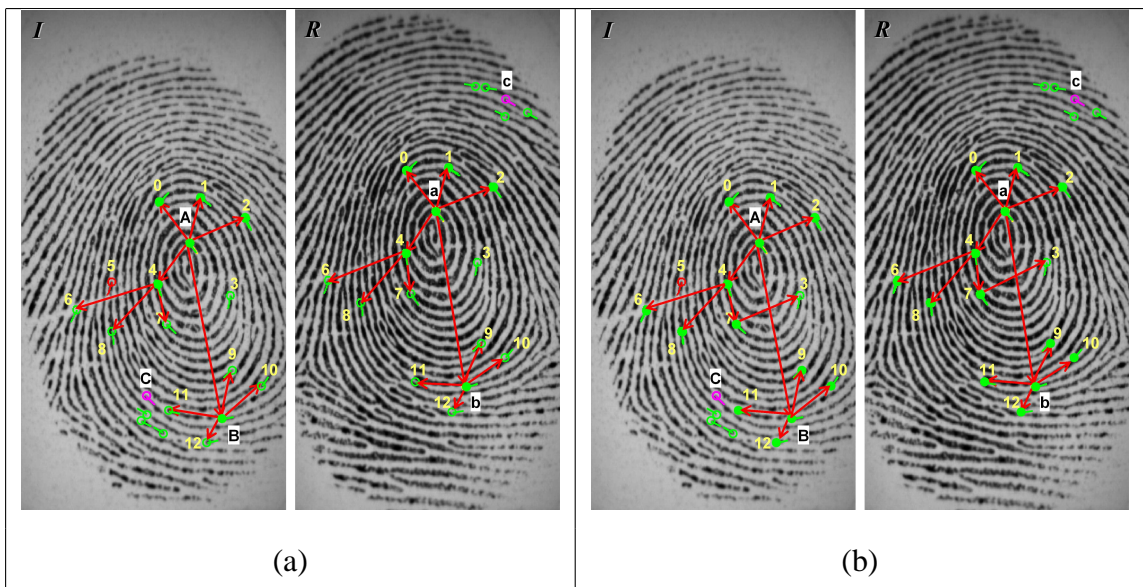


Figure 4.8: (a) After all the neighboring minutiae of **I[4]** and **R[4]** have been visited. (b) After all the neighboring minutiae of **I[10]** and **R[10]** have been visited.

by solid circles which indicate that the extended matching has been completed for them (Figure 4.7(b)). The falsely matched **C** and **c** are excluded and not appended to M . Now, M contains the pairs: $\langle \mathbf{A}, \mathbf{a} \rangle$, $\langle \mathbf{I}[1], \mathbf{R}[1] \rangle$, $\langle \mathbf{I}[0], \mathbf{R}[0] \rangle$, $\langle \mathbf{I}[2], \mathbf{R}[2] \rangle$, $\langle \mathbf{I}[4], \mathbf{R}[4] \rangle$, and $\langle \mathbf{B}, \mathbf{b} \rangle$.

2. Minutia $\mathbf{I}[1]$, $\mathbf{I}[0]$, $\mathbf{I}[2]$, $\mathbf{R}[1]$, $\mathbf{R}[0]$, and $\mathbf{R}[2]$ have no valid neighboring minutia for matching, therefore they are marked as finished. However, minutiae $\mathbf{I}[4]$, \mathbf{B} , $\mathbf{R}[4]$, and \mathbf{b} have valid neighboring minutiae to match, and the temporary results of the extended matching are shown in Figure 4.8(a). Note that the spurious minutia $\mathbf{I}[5]$ is not added to M . At this stage, the list M contains the pairs: $\langle \mathbf{A}, \mathbf{a} \rangle$, $\langle \mathbf{I}[1], \mathbf{R}[1] \rangle$, $\langle \mathbf{I}[0], \mathbf{R}[0] \rangle$, $\langle \mathbf{I}[2], \mathbf{R}[2] \rangle$, $\langle \mathbf{I}[4], \mathbf{R}[4] \rangle$, $\langle \mathbf{B}, \mathbf{b} \rangle$, $\langle \mathbf{I}[7], \mathbf{R}[7] \rangle$, $\langle \mathbf{I}[8], \mathbf{R}[8] \rangle$, $\langle \mathbf{I}[6], \mathbf{R}[6] \rangle$, $\langle \mathbf{I}[12], \mathbf{R}[12] \rangle$, $\langle \mathbf{I}[9], \mathbf{R}[9] \rangle$, $\langle \mathbf{I}[11], \mathbf{R}[11] \rangle$, and $\langle \mathbf{I}[10], \mathbf{R}[10] \rangle$.

3. Minutiae $\mathbf{I}[7]$ and $\mathbf{R}[7]$ have the only neighbors, $\mathbf{I}[3]$ and $\mathbf{R}[3]$, to match against, and are appended to M . Minutiae $\mathbf{I}[8]$, $\mathbf{I}[6]$, $\mathbf{I}[12]$, $\mathbf{I}[9]$, $\mathbf{I}[11]$, $\mathbf{I}[10]$, $\mathbf{R}[8]$, $\mathbf{R}[6]$, $\mathbf{R}[12]$, $\mathbf{R}[9]$, $\mathbf{R}[11]$, and $\mathbf{R}[10]$ have no valid neighbors to match, therefore they are marked as completed. At this stage, the list M contains the pairs: $\langle \mathbf{A}, \mathbf{a} \rangle$, $\langle \mathbf{I}[1], \mathbf{R}[1] \rangle$, $\langle \mathbf{I}[0], \mathbf{R}[0] \rangle$, $\langle \mathbf{I}[2], \mathbf{R}[2] \rangle$, $\langle \mathbf{I}[4], \mathbf{R}[4] \rangle$, $\langle \mathbf{B}, \mathbf{b} \rangle$, $\langle \mathbf{I}[7], \mathbf{R}[7] \rangle$, $\langle \mathbf{I}[8], \mathbf{R}[8] \rangle$, $\langle \mathbf{I}[6], \mathbf{R}[6] \rangle$, $\langle \mathbf{I}[12], \mathbf{R}[12] \rangle$, $\langle \mathbf{I}[9], \mathbf{R}[9] \rangle$, $\langle \mathbf{I}[11], \mathbf{R}[11] \rangle$, $\langle \mathbf{I}[10], \mathbf{R}[10] \rangle$, and $\langle \mathbf{I}[3], \mathbf{R}[3] \rangle$ (Figure 4.8(b)).

4. After $\mathbf{I}[3]$ and $\mathbf{R}[3]$ have been marked as completed, all the connected minutiae

have been visited (matched) by the algorithm. Thus, the list M contains the final correspondence between minutiae, and the result of extended matching is as shown in Figure 4.9(a). The final result successfully combines the extended matching results of different starting points, such as $\langle \mathbf{A}, \mathbf{a} \rangle$ and $\langle \mathbf{B}, \mathbf{b} \rangle$, and excludes the falsely matched *seed* ($\langle \mathbf{C}, \mathbf{c} \rangle$).

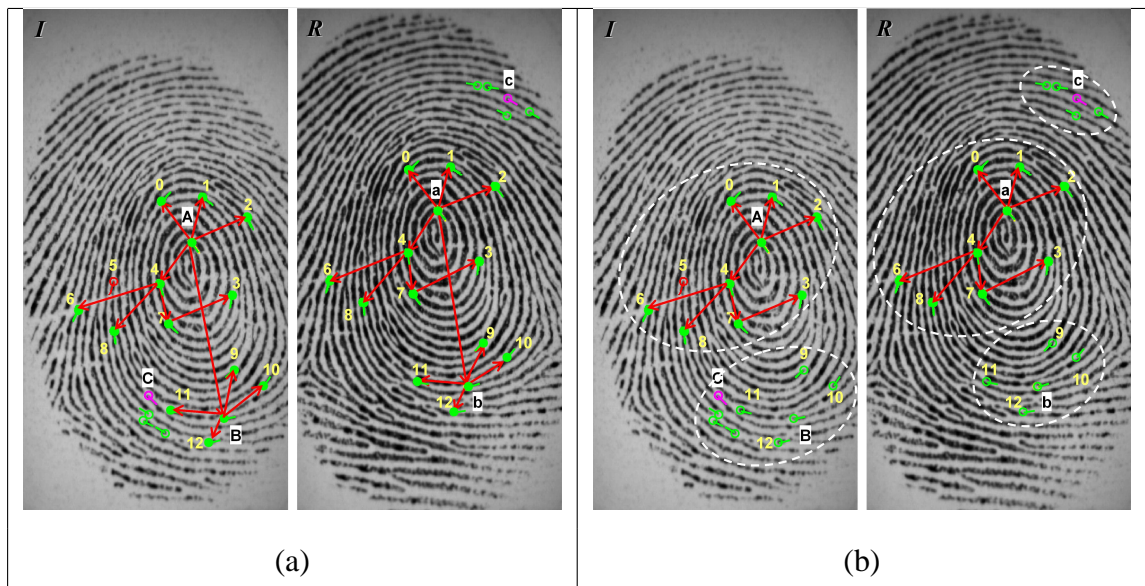


Figure 4.9: (a) Final result of the extended matching. (b) The extended matching result if the *seeds* are not put into each other's *neighborhood list*.

Comparing the extended matching results (Figure 4.9(a)) with that shown in Figure 4.9(b), we observe that we get better results when we link the *seeds* together to avoid the problems of clustered minutia points and then combining results of different starting points.

4.4 Similarity Scores

After the extended matching, we gather all the available information, such as the number of matched feature points (n), the number of feature points on the query and the reference fingerprints ($size_I$ and $size_R$), the number of feature points on the overlapping areas of the query and reference fingerprints (O_I and O_R), and the average feature distance of all the matched features (S_{avg}), to calculate the similarity scores. The convex hull technique (Section 3.2.6) is applied to obtain the overlapping areas on both fingerprints and then the previously introduced heuristic rule (Figure 3.11) is used to generate similarity scores.

4.5 Experimental Results

To measure the performance of the above described matching algorithm, we have tested the system on FVC2002 DB1, DB2, and DB3 databases [69]. Each database consists of 800 images (100 distinct fingers, 8 impressions each). We also compare the performance of our matching algorithm with a publicly available fingerprint matcher (Bozorth3) [100]. The Bozorth3 and our matching algorithm are both minutiae-based systems. The same feature extraction algorithm described in [28] is used in both systems. The experiments can be divided into two parts: (i) experiment on original live scanned images, and (ii) experiment on the partial fingerprint templates described in Section 3.3.

In the case of experiment part (i), a total of 2800 genuine tests (with no rejection) were performed (each impression of a finger is compared against the remaining impressions)

Database	Bozorth3		Proposed Matching	
	EER	Min. TER	EER	Min. TER
FVC2002 DB1	4.67%	6.55%	1.06%	1.58%
FVC2002 DB2	3.37%	5.46%	1.16%	1.96%
FVC2002 DB3	11.11%	19.96%	9.28%	15.88%

Table 4.2: A summary of the comparative results.

and a total of 4950 false acceptance tests (with no rejection) were performed. The first impression of each finger is compared against the first impression of all other fingers in the database. On an Intel Pentium 4, 1.4 GHz machine, the average matching time for a genuine test is about 138 ms and 136 ms for a false acceptance test. The experimental results are presented in Table 4.2. The ROC curves of both algorithms testing on FVC2002 DB1, DB2, and DB3 databases are presented in Figures 4.10 – 4.12.

In experiment part (ii), we use the partial fingerprint templates that are generated from the FVC2002 DB1 database. Datasets of various sizes (20%, 30%, 40%, and 50% of the original fingerprint size) are constructed. Each dataset contains five partial fingerprint templates of the target size that are created at random positions from every second impression of each finger in the FVC2002 DB1 database. To evaluate the false rejection rate of a system, we match every partial fingerprint template against the original full templates of the remaining 7 impressions (excluding the second impression) of the same finger. As a result, there are $100 \times (5 \times 7) = 3500$ genuine matching tests. To evaluate the false acceptance rate of a system, the first partial fingerprint template is matched against the first impressions of

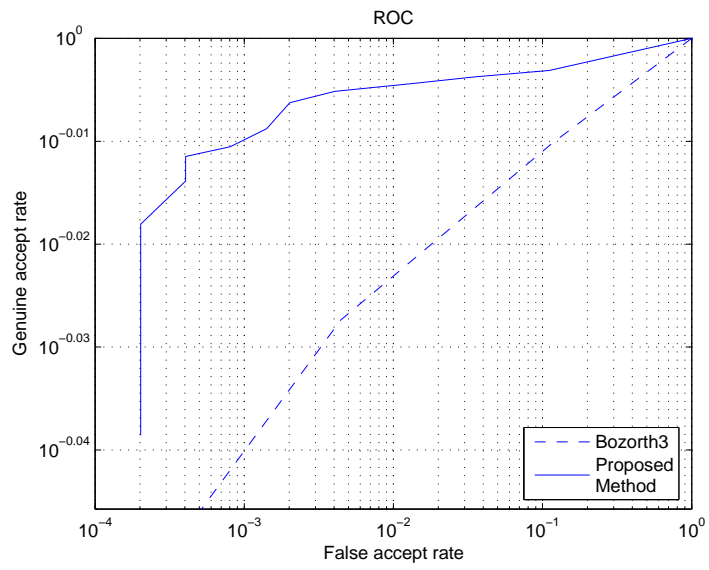


Figure 4.10: A comparison of ROC curves for FVC2002 DB1 database.

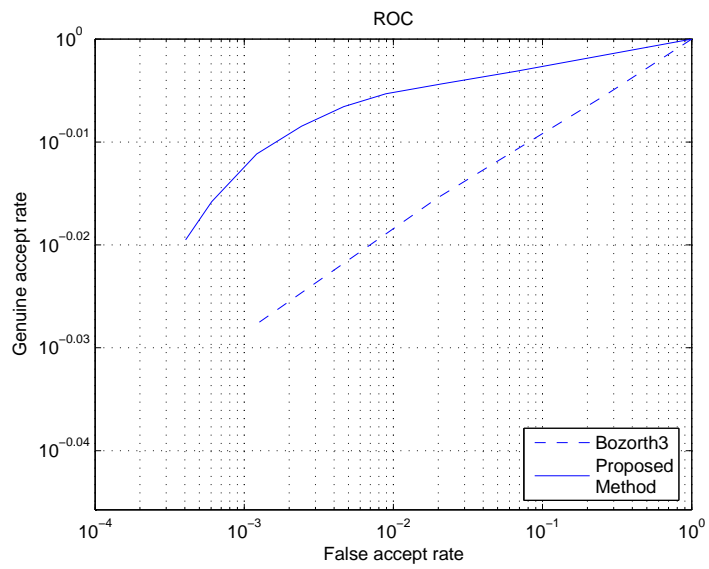


Figure 4.11: A comparison of ROC curves for FVC2002 DB2 database.

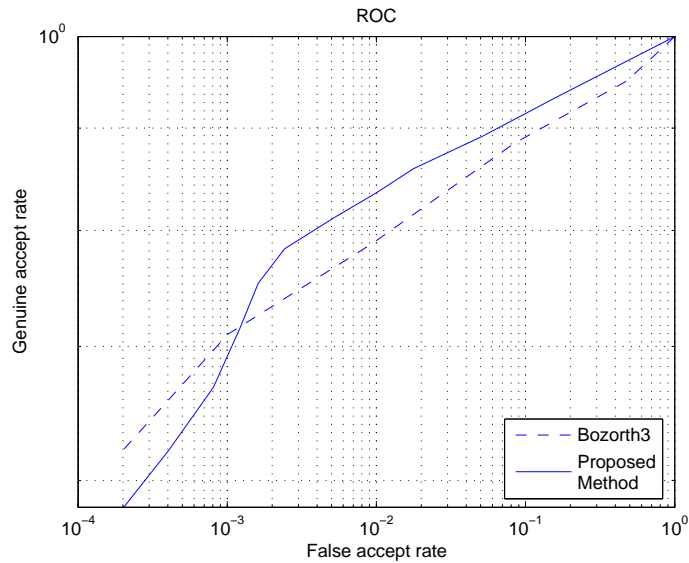


Figure 4.12: A comparison of ROC curves for FVC2002 DB3 database.

the remaining fingerprints in the database and $100 \times 99 = 9900$ imposter tests are generated. A summary of experimental results of both the Bozorth3 and our algorithm is presented in Table 4.3. The ROC curves of both algorithms testing on different sizes of partial fingerprint templates are presented in Figures 4.13 – 4.16. Our algorithm outperforms the Bozorth3 method in all categories of partial fingerprint matching.

The performance comparison between this method and the method described in Section 3.2 is summarized in Table 4.4 and Table 4.5. This method improves the system's performance with respect to both EER (Equal Error Rate) and Min. TER (Minimum Total Error Rate) in almost every test. In the tests of very small partial fingerprints (20% and 30%), Chapter 3's method produces slightly better results due to the use of brute-force matching that finds the global optimal result by examining all possible solutions.

Fingerprint Size	Avg. Width (pixels)	Avg. Height (pixels)	Bozorth3		Proposed Matching	
			EER	Min. TER	EER	Min. TER
20%	92.42	133.30	43.90%	68.40%	20.97%	30.92%
30%	113.31	163.36	25.63%	33.18%	9.79%	16.20%
40%	130.90	188.70	12.35%	19.69%	6.16%	10.17%
50%	146.41	211.03	8.28%	11.77%	3.16%	5.16%

Table 4.3: A summary of the comparative results of partial fingerprint recognition. Note that the number of testing instances is different from what we used in Section 3.3.

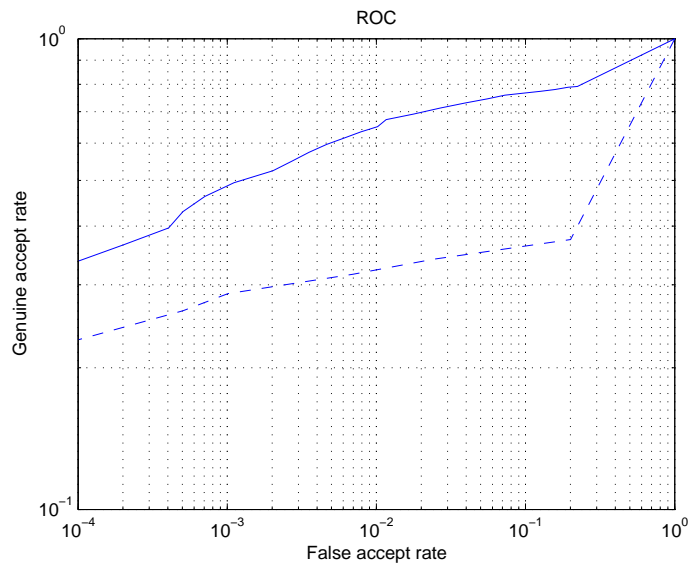


Figure 4.13: A comparison of ROC curves for system testings on partial fingerprint (20% of original size) templates.

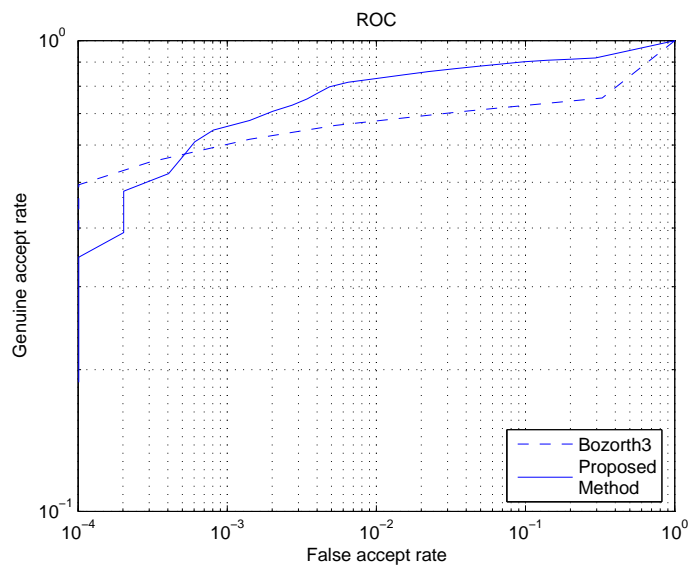


Figure 4.14: A comparison of ROC curves for system testings on partial fingerprint (30% of original size) templates.

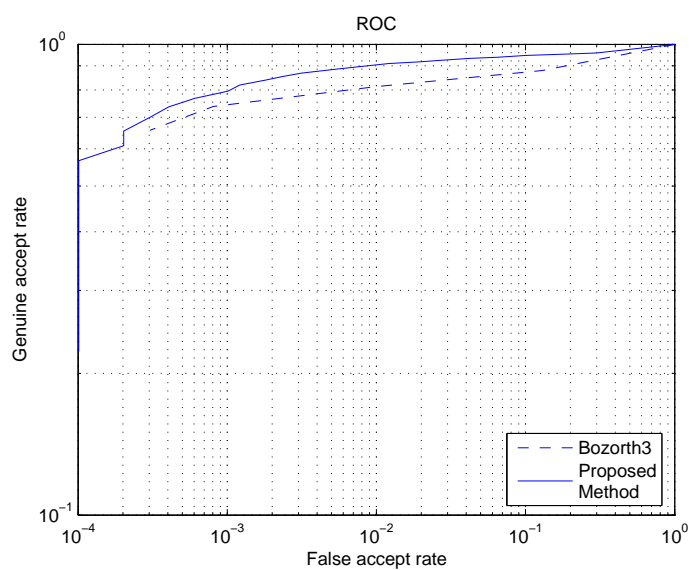


Figure 4.15: A comparison of ROC curves for system testings on partial fingerprint (40% of original size) templates.

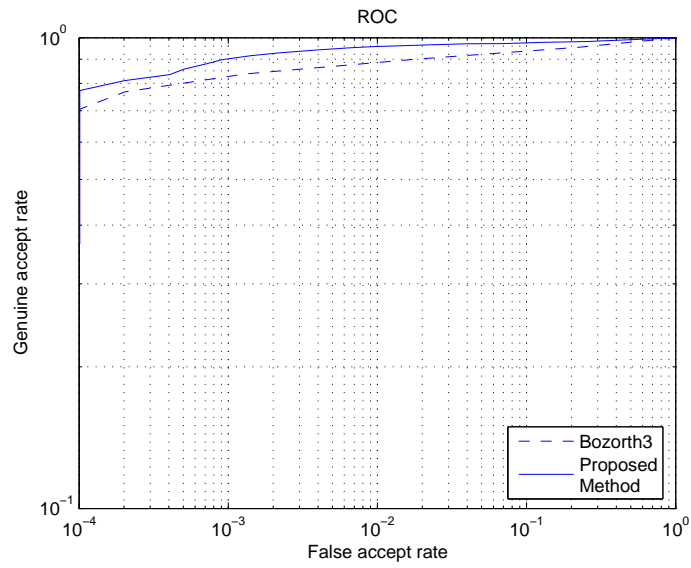


Figure 4.16: A comparison of ROC curves for system testings on partial fingerprint (50% of original size) templates.

Database	Chapter 3's Matching		Proposed Matching	
	EER	Min. TER	EER	Min. TER
FVC2002 DB1	2.13%	3.32%	1.06%	1.58%
FVC2002 DB2	1.57%	2.49%	1.16%	1.96%

Table 4.4: A summary of the comparative results.

Fingerprint Size	Avg. Width (pixels)	Avg. Height (pixels)	Chapter 3's Matching		Proposed Matching	
			EER	Min. TER	EER	Min. TER
20%	92.42	133.30	16.12%	28.02%	20.97%	30.92%
30%	113.31	163.36	9.55%	17.19%	9.79%	16.20%
40%	130.90	188.70	6.26%	11.17%	6.16%	10.17%
50%	146.41	211.03	4.72%	7.93%	3.16%	5.16%

Table 4.5: A summary of the comparative results on partial fingerprint recognition of the proposed matching and the method that is described in Chapter 3.

4.6 Summary

Our algorithm overcomes the difficulties of matching partial fingerprints in which the number of minutia points is small. Pure localized secondary feature which relies on relative information between minutiae and the matching process which involves no global alignment give the system the ability to handle distortions in fingerprints. By using multiple neighbors and generating different number of secondary features according to the size of a fingerprint, the chance of false rejection is reduced. At the same time, the rate of false acceptance also decreases due to the increased number of features. An indexing technique based on the shape of a secondary feature is also presented to ease the time requirements for matching hundreds of secondary features. Linking the matched *seeds* with each other makes the match propagate throughout the entire fingerprint, and provides a way to combine extended matching results using different starting points. The system performance is

compared to a publicly available system (Bozorth3 [100]). Using the same feature extraction algorithm described in [28], (that is same feature templates are used in both systems), we have shown that our method is superior to the method described in Chapter 3 and the Bozorth3 algorithms.

Chapter 5

Security Strength of Partial Fingerprints

Partial fingerprints represent only a small portion of the original fingerprint. In case of scanners that can cover only a small region of the entire fingerprint, a small number of minutiae are obtained, which then have to be matched with a reference template obtained during enrollment which has substantially more number of minutiae. For example, a fingerprint scanner on a PDA or cell phone would acquire a small section of the fingerprint and match it with a previously stored template on a chip. Automatic fingerprint systems are increasingly being used for access control in both the physical world and in cyberspace. Before we replace the password and PIN authentication systems with fingerprint recognition, we must answer the question “how secure is the fingerprint based system compared to the password or PIN based systems?”

We determine whether minutiae-based fingerprint matching systems have advantage over password or PIN based systems. We consider brute-force attack against both systems

and measure their security strength against the attack. The security strength is measured by *bit strength*, which is the information content given by the \log_2 value of the cumulative probability that a randomly generated template has more than a certain number of minutiae matched against the reference template.

5.1 Brute-force Attack

In a brute force-attack, the attacker attempts to circumvent the system by offering a large number of different biometric features to the authentication system, anticipating a coincidence with the stored reference features. Unlike a password based system which is vulnerable to brute-force attacks, attacking a fingerprint system requires more effort. However, in e-commerce applications or login process of a file system, the authenticating process is at remote unattended sites, hackers may gain enough time to make considerable attack attempts.

5.2 Prior Related Work

Ratha et. al [82] presented a mathematical model that defines the equivalence between a fingerprint matching system and a password based system. The analysis aims to identify the factors that influence the probability of a false match. They assumed the following.

- The fingerprint matcher tolerates the displacements of minutia points at most by the width of ridge and valley (in pixels)

- The angles at every minutiae are not constrained
- The number of matched minutiae reflects the degree of match
- Fixed image size $S = 300 \times 300$
- The width of a ridge and valley $f = 15$ pixels
- Total number of possible locations $l = \frac{300 \times 300}{15 \times 15} = 400$
- Number of allowed minutia orientation $d = 4, 8, 16$
- Numbers of minutiae on query fingerprint (N_q) and reference fingerprint (N_r) are the same ($N_q = N_r = N$)

Then, the probability that a randomly generated minutia will match one of the minutiae in the reference fingerprint is

$$p_{est} = \frac{N_r}{ld}. \quad (5.1)$$

Since it is not desirable to generate two minutiae at the same location, the probability that the j th generated minutia will match one of the minutia in the reference fingerprint becomes

$$\frac{N_r}{(l - j + 1)d}. \quad (5.2)$$

Conservatively, the matching probability of each of the N_q generated minutia can be assumed to be

$$p = \frac{N_r}{(l - N_q + 1)d}, \quad (5.3)$$

and the total probability of exactly t minutiae matched is

$$p_{exact} = \binom{N_r}{t} p^t (1-p)^{N_q-t}. \quad (5.4)$$

However, matching equal or more than th minutiae is considered to be a positive match.

Thus, the probability of a randomly generated template with N_q minutiae being considered as a positive match is:

$$p_{ver} = \sum_{t=th}^N \binom{N}{t} p^t (1-p)^{N-t}. \quad (5.5)$$

Equation (5.5) is further approximated and simplified by using the Poisson approximation and Stirling's approximation. Finally, we have

$$p_{ver} \approx \frac{(Np)^{th} e^{-Np}}{\sqrt{(2\pi th) e^{-th} m^{th}}}, \quad (5.6)$$

and the bit strength is given as

$$Strength_{bits} = -\log_2 p_{ver}. \quad (5.7)$$

In [82], the authors claimed a minutiae based fingerprint recognition system can roughly have 82 bits of information content in the representation when $N = 40$, $d = 4$, $l = 400$, and $th = 25$.

5.3 Bit Strength of Partial Fingerprint

To study the effect of decreasing size of query fingerprints on the bit strength of the system, we keep most of the assumptions in Ratha's work [82] unchanged but we consider different

values of N_q and N_r instead of a fixed number N . N_r denotes the number of minutia in the reference fingerprint (complete), and N_q denotes the number of minutia in the query fingerprint, which varies from 100% to 40% of the original fingerprint image size.

We observe that images whose size is less than 40% of the original contains less than 17 minutiae. In contrast to the analysis performed by Ratha et. al [82], instead of a fixed image size, we use x and y to represent the average dimensions of the fingerprint images. We assume the inter-ridge distance (f) to be 15 pixels in the analysis. Thus, the maximum possible minutia locations (l) is given by:

$$\frac{x \times y}{f^2} \quad (5.8)$$

As in Section 5.2, we can have the cumulative probability of matched minutia points from a fixed threshold value th to be the maximum number of available minutia points in the query fingerprint N_q . That is

$$p'_{ver} = \sum_{t=th}^{N_q} \binom{N_r}{t} p^t (1-p)^{N_r-t}, \text{ where } p = \frac{N_r}{(l - N_q + 1)d}. \quad (5.9)$$

Then the bit strength ($Strength'_{bits}$) of a minutiae-based partial fingerprint recognition system can be given as

$$Strength'_{bits} = -\log_2 p'_{ver}. \quad (5.10)$$

5.4 Analysis and Summary

We studied the effect of the size of fingerprint on the actual number of minutiae retrieved from the FVC2002 DB1 database [70]. Unfortunately, there is no partial fingerprint database available for this study. We have generated a series of partial fingerprint databases with different sizes (in percentage) at random positions from the FVC2002 DB1 data set. For every fingerprint we have 5 partial fingerprint templates of each target size. The target sizes are 10%, 15%, 20%, 25%, 30%, 35%, 40%, 45%, 50%, 55%, 60%, 65%, 70%, 75%, 80%, 85%, and 90% of the fingerprint foreground areas.

We observed that there was a substantial decrease in the number of minutia that could be extracted as the size of the fingerprint was reduced (Figure 5.1). Bit strength is plotted

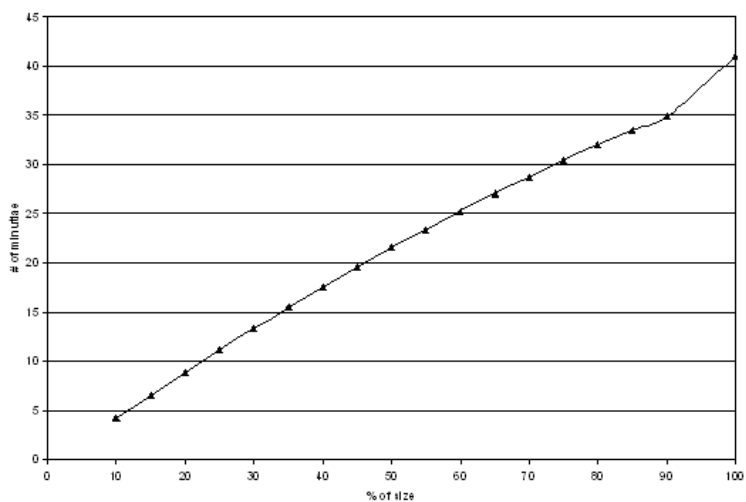


Figure 5.1: Number of minutia extracted from different sized images.

in Figure 5.2 against the image size decreasing from 100% to 40% of the original size

with $N_r = 41$ and N_q values ranging from 17 to a maximum of 41. The image sizes and the values of N_r and N_q used for the mathematical analysis are the actual image sizes and the number of minutia in the reference and the query fingerprints respectively. We fix the threshold for match as 17. It is assumed that the matcher will tolerate shifts between the query and reference minutiae up to the width of a ridge and valley in pixels, and an angular difference of up to half a quantization bin (± 45 degrees for $d = 4$) [82]. The bit strength is evaluated at $d = 4, 8, 16$ and 36 . We make several important observations. Fewer number of minutia points available leads to a natural degradation of the bit strength and makes the system vulnerable to brute-force attacks. The bit strength of the fingerprint matching system as calculated from Equation (5.10) indicates that it is directly dependent on the number of minutia points matched. However, if the query fingerprint contains less number of minutiae to be matched, the bit strength would be substantially lower as shown by results in Table 5.4. For $d = 16$, bit strength is about 68 bits (or approximately 8.5 characters) at 100% image size and diminishes to 44 bits (or 5.5 characters) at 40% of the image size. (Note that we assume there are at least 17 matched minutiae to be considered for a successful match (i.e. $th = 17$)). If we consider bit strength of 45 as adequate for the model with $d = 8$ we would require a fingerprint scanner with a sensing area of at least $0.32'' \times 0.53''$. We need to associate more information with the representation in a minutia-based approach to decrease the threat of a brute force attack. In our matching algorithm we supplement the original minutia information, with a secondary feature vector that captures localized detail containing six additional elements.

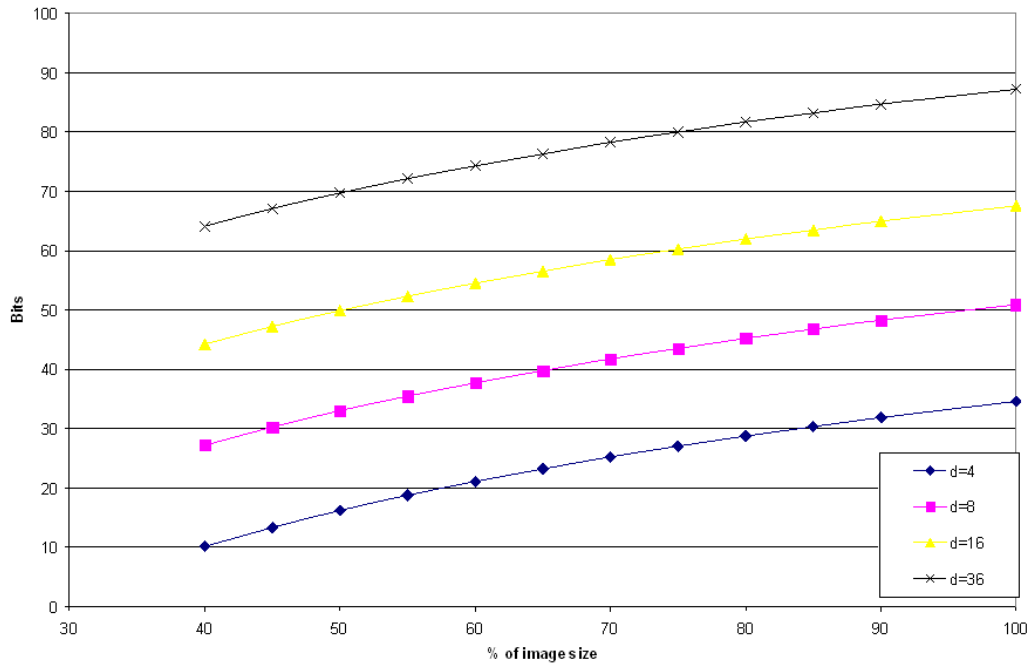


Figure 5.2: Bit strength vs. various fingerprint image sizes. d is the number of quantified orientations associated with every minutia point.

% of Image Size	Average Image Size (pixels)		N	$d=4$	$d=8$	$d=16$	$d=36$
	Width	Height					
100	207.7	299.1	41	34.6117	50.9020	67.5516	87.2469
90	196.6	283.3	35	31.8619	48.2902	65.0078	84.7406
85	191.0	275.2	33.5	30.3455	46.7747	63.4929	83.2261
80	185.3	267.0	32	28.7721	45.2463	61.9866	81.7319
75	179.4	258.5	30.5	27.0431	43.5221	60.2647	80.0114
70	173.3	249.7	29	25.2415	41.7767	58.5467	78.3085
65	167	240.6	27	23.2335	39.7801	56.5555	76.3202
60	160	231.2	25	21.1049	37.7245	54.5351	74.3190
55	153	221.3	23.4	18.7792	35.4865	52.3392	72.1459
50	146	211.0	21.6	16.2080	33.0226	49.9261	69.7605
45	138	200.2	19.5	13.3419	30.2893	47.2557	67.1240
40	130	188.7	17.5	10.1480	27.2140	44.2482	64.1562
35	122.4	176.4	15.5	N/A	N/A	N/A	N/A
30	113.3	163.3	13.3	N/A	N/A	N/A	N/A
25	103.6	149.3	11	N/A	N/A	N/A	N/A
20	92.4	133.2	8.4	N/A	N/A	N/A	N/A
15	79.9	115.3	6.5	N/A	N/A	N/A	N/A
10	65.1	94.1	4	N/A	N/A	N/A	N/A

Table 5.1: Effects on bit strength of minutiae-based fingerprint recognition system of decreasing input image size. Note that, in this table, we assume there are at least 17 matched minutiae to be considered as a successful match (i.e. $th = 17$).

Chapter 6

Conclusion

The goal of this thesis is to study the security impact of partial fingerprints on automatic fingerprint recognition systems and to develop an automatic system that can overcome the challenges presented by partial fingerprint matching. The contributions of our research are as follows:

- The security strength of a partial fingerprint matching algorithm was measured in terms of *bit-strength* and compared with password-based authentication systems. It had been shown that the *bit-strength* of a system that matches a partial fingerprint against a full fingerprint decreases along with the reduction in size of partial fingerprints. To maintain the security level of a partial fingerprint recognition system, features that contain more information must be considered.
- We use localized secondary features for partial fingerprint matching. The limited foreground area offered by a partial fingerprint has a high chance of missing global

singular points, such as core and delta points, which are essential for any pre-alignment based matching algorithm. Secondary features rely only on relative information between minutiae and handle fingerprint distortion more effectively.

- Our proposed dynamic tolerance areas give systems the ability to manage the global deformation locally.
- We use the Minimum Cost Maximum Flow (MCF) method to solve the ambiguity of pairing feature points and to obtain optimal matching solutions.
- Instead of using rectangular boxes to define overlapping areas, the proposed convex hull based approach can generate more accurate and reliable overlapping areas and is a better approximation of the shape of the overlapping regions of fingerprints.
- We proposed an indexing technique based on the geometric characteristics of secondary features to increase the speed of matching secondary features.
- We presented implementations of two partial fingerprint recognition systems.
 1. A multi-path matching system is presented which can operate in three modes: (i) secondary feature matching only, (ii) brute-force matching only or (iii) secondary feature matching followed by a conditional brute-force matching. The matching mode is decided by the size of the participating fingerprints. Balance between the processing speed and system performance for both full and partial fingerprint recognition is analyzed.

2. A system that obtains the global correspondence between minutiae of two fingerprints by evolving the matching from local neighborhoods of each minutia is presented. The number of secondary features is determined by its size, thus each fingerprint has approximately the same number of feature points.

Both methods perform well in terms of EER and Min. TER compared to NIST's Bozorth3 [100] matcher.

Appendix A

Overview of Biometrics

Positive identification of individuals is a crucial societal requirement. Until recently, automatic personal identification technologies followed two approaches: (i) a token-based approach and (ii) a knowledge-based approach. Token-based approaches are based on identification using tokens such as a magnetic swipe card, drivers license, etc. Knowledge-based approaches use passwords and personal identification numbers (PINs) to identify or validate a person's identity. Both these forms of identification are not secure, because these credentials can be lost, stolen or duplicated. On the other hand, biometrics is a science of verifying and establishing the identity of an individual through physiological features or behavioral characteristics that are unique to that individual and hence cannot be stolen, lost or misused.

Biometric authentication refers to establishing the identity of a person using certain physiological and/or behavioral characteristics that are associated with the person [47, 86].

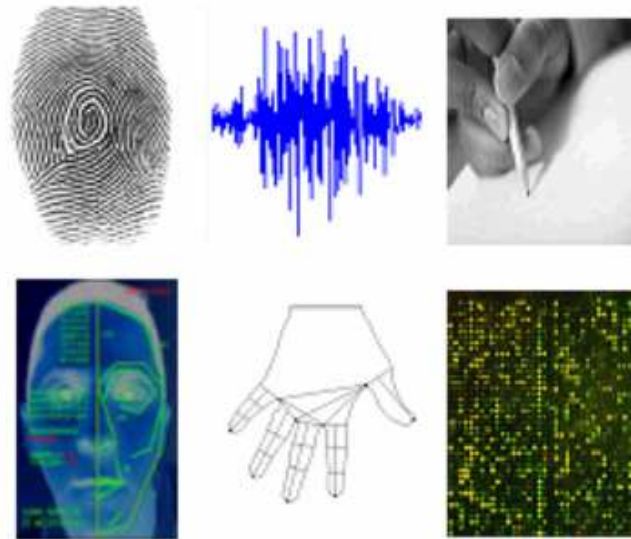


Figure A.1: Different types of biometrics: Fingerprints, speech, handwriting, face, hand geometry and chemical biometrics

It relies on “something that you are or you do”. Biometrics requires that the person to be identified is physically present near the biometric capturing equipment for the biometric sample to be obtained. Thus it is possible to distinguish between authorized users and unauthorized users with passwords/ID cards. Biometrics can be classified into three categories: physiological, behavioral, and chemical. Physical biometrics rely on physiological features such as fingerprints, hand geometry, iris pattern, facial features etc., for identity verification while behavioral biometrics depends on behavioral features such as speech patterns, handwriting, signature, and gait. DNA and odor lie within the category of chemical biometrics (Figure A.1). Biometrics satisfies, in various degrees, several properties that are desirable for successful human identification [14, 45]. These properties are:

- **Universality:** The features used for recognition should be available to or within every individual.
- **Uniqueness:** The features should contain enough information that can be used to distinguish between separate individuals.
- **Permanence:** The features should remain unchanged with time.
- **Indispensability:** The features should be available at all times.
- **Collectability:** The features should be extracted efficiently and accurately and measured quantitatively.
- **Storability:** The features should be storable in manual or automated systems.

Table A.1 shows a comparison of various biometric techniques.

A.1 Biometrics Applications

Biometrics is a quickly evolving technology. Its scope ranges from the government to fields of civilian (commercial) applications. In the government, biometrics has been used for criminal identification (Figure A.2 (a)) and prison security. Examples of biometrics being used in government projects are:

- **Immigration and Naturalization Service's (INS) Passenger Accelerated Service System (INSPASS):** It utilizes hand geometry to verify the identity of the traveler at

Biometrics	<i>Universality</i>	<i>Uniqueness</i>	<i>Permanence</i>	<i>Collectability</i>	<i>Performance</i>	<i>Acceptability</i>	<i>Circumvention</i>
DNA	H	H	H	L	H	L	L
Ear	M	M	H	M	M	H	M
Face	H	L	M	H	L	H	H
Facial thermogram	H	H	L	H	M	H	L
Fingerprint	M	H	H	M	H	M	M
Gait	M	L	L	H	L	H	M
Hand geometry	M	M	M	H	M	M	M
Hand vein	M	M	M	M	M	M	L
Iris	H	H	H	M	H	L	L
Keystroke	L	L	L	M	L	M	M
Odor	H	H	H	L	L	M	L
Retina	H	H	M	L	H	L	L
Signature	L	L	L	H	L	H	H
Voice	M	L	L	M	L	H	H

Table A.1: Comparison of biometric technologies [70]. H, M, and L, denote High, Medium and Low respectively.

an automated inspection station, thus allowing the passenger to bypass the personal interview/inspection part of the entry process [32]. Since 1993, INSPASS is being used in airports such as John F. Kennedy International Airport and Newark International Airport, and at Pearson International Airport in Toronto, Canada (Figure A.2 (b)) (www.volpe.dot.gov).

- **CANPASS:** CANPASS is the Canadian version of INSPASS. The goal is to ease the transfer of people and goods between US and Canada. There are several different types of CANPASS that have been implemented for various groups of people, such as CANPASS Air (Figure A.2 (c)), CANPASS Corporate Aircraft, CANPASS Private Aircraft, CANPASS Private Boats, and CANPASS Remote Area Border Crossing [32, 2].
- **Federal Bureau of Prisons:** It uses hand geometry to monitor the activity of prisons, staff, and visitors. Once people are enrolled in the system, their hand geometry features are placed in a database and each person is issued a magnetic swipe card that must be carried at all times. By the end of 1995, around 30 Federal prisons were scheduled to have the hand geometry monitoring system installed [76].
- **Automated Fingerprint Image Reporting and Match (AFIRM):** It uses fingerprint biometric to reduce fraudulent and duplicate welfare benefits. Within the first six months of operation, Los Angeles County in California saved \$5.4 million dollars, and the savings have been growing ever since [76].

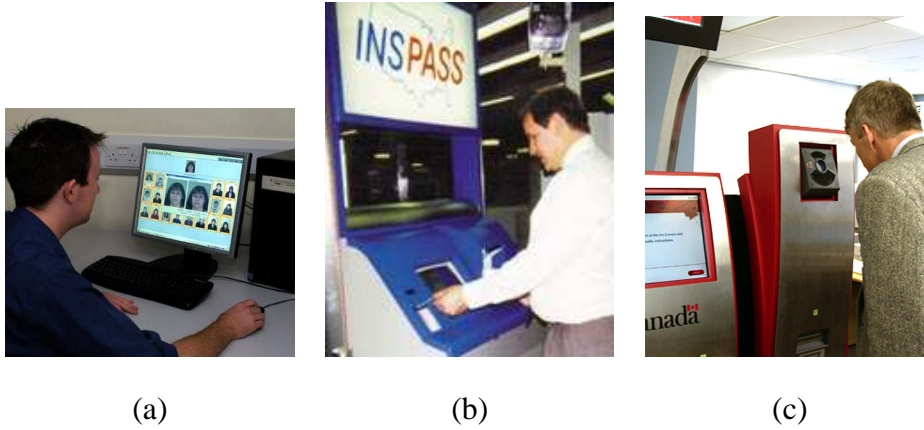


Figure A.2: Examples on biometric identification applications: (a) Automatic Facial Recognition (AFR) system is used to track down crime suspects by West Yorkshire Police, UK. (www.westyorkshire.police.uk); (b) the INSPASS uses hand geometry for passenger recognition (www.volpe.dot.gov); (c) iris scanners are used by CANPASS Air systems (www.cbsa-asfc.gc.ca).

In civilian domains, electronic commerce and electronic banking are emerging application areas due to the increasing amounts of electronic transactions. These applications include ATM security, bank security, credit card transactions, check cashing, and electronic fund transfer, etc [45]. The other sector of this domain is focused on replacing the old token-based/knowledge-based systems with new biometric systems to increase their security level. Such applications include physical access control, network/pc/workstation login security, employee attendance system, and so on. With the advances in today's technology, biometric recognition systems are also used for personal digital devices such as laptop computers, mobile phones, and personal digital assistants (PDAs) for data and information protection (Figure A.3).

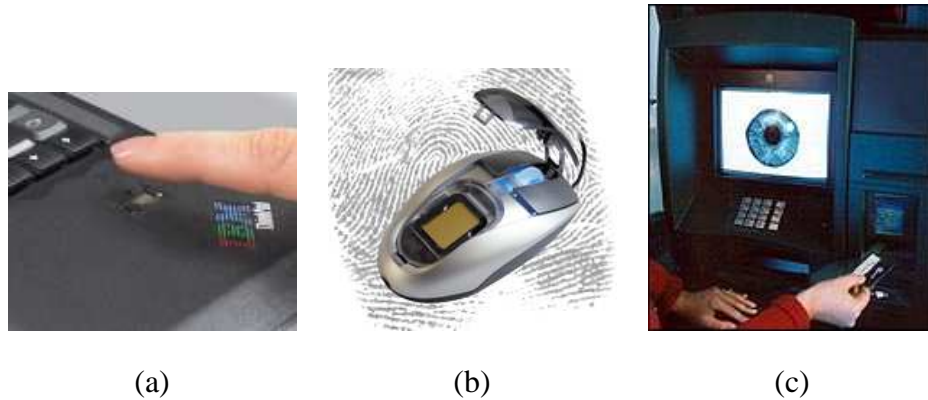


Figure A.3: (a) IBM ThinkPad T42 with a integrated fingerprint scanner for security identification (www.ibm.com). (b) Mouse with fingerprint scanner that provides abilities for security logon, lock/unlock computer, and file encryptions. (www.brighton-electronics.com). (c) Iris scanner is used on ATM for customers to access their accounts without using PINs, passwords, or cards. (www.jaypeetex.com).

A.2 Verification vs. Identification

Biometric recognition can be classified into two categories: *verification* (1 : 1 matching) and *identification* (1 : N matching) systems. In both verification and identification systems, the enrollment process takes the user's identity, i , and biometric feature(s), B_i , to construct a machine readable/understandable template, \hat{B}_i^T , then stores \hat{B}_i^T into a database D_B . The process of converting a biometric signal into a template is usually referred to as feature extraction. Note that, B_i could be the union of more than one biometric signal in a multimodal biometrics system [47, 91], for example, a system may use both face and fingerprint to perform recognition.

In a verification system, a user presents his/her biometric signal(s), B_i , and claims an

identity, i . The system tries to answer the user's question "Am I who I claim to be?"[45]. As with the enrollment process, the feature extraction module converts the biometric signal(s) B_i into a machine readable/understandable representation, \hat{B}_i . Then the system retrieves the biometric template, \hat{B}_i^T , of the claimed identity from its database and computes the similarity measurement (similarity score) $S(\hat{B}_i, \hat{B}_i^T)$. For a given threshold, th , the system either rejects ($S(\hat{B}_i, \hat{B}_i^T) < th$) or accepts ($S(\hat{B}_i, \hat{B}_i^T) \geq th$) the submitted claim of identity.

In an identification system, the user does not claim any identity. The goal of the system is to answer the question "Who am I?" for the presented biometric signal(s) B_i with an unknown identity i . The system calculates similarity measurements $S_j(\hat{B}_i, \hat{B}_j^T)$ for all biometric templates \hat{B}_j^T in the database, D_B . The output of the system is a list of possible identities (candidates), $j_1 \dots j_n$, for the unknown identity i , where n is the number of possible identities, j_k , of i that satisfies $S_{j_k}(\hat{B}_i, \hat{B}_{j_k}^T) \geq th$ for a given threshold th . Because of the large amount of instances in the database, identification systems also have research problems associated with scalability and efficiency which has been dealt with in depth here [71].

In this research, we will be dealing solely with the problem of verification using fingerprints. In general, biometric verification system consists of two stages: (i) Enrollment and (ii) Authentication (Figure A.4). In the enrollment stage, the biometric signal(s) of the user is captured by biometric sensors. The feature extraction module converts the biometric signal(s) into a machine readable/understandable representation (we also call this represen-

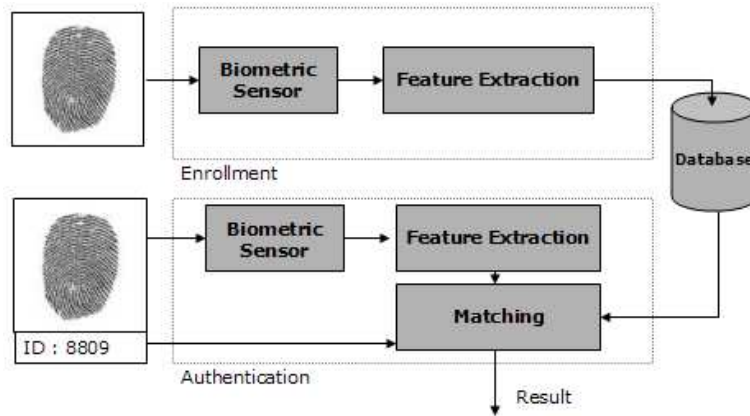


Figure A.4: General architecture of a biometric verification system

tation as *feature template* or simply *template* in our research) and stored in the database. During authentication stage, the biometric signal(s) of the user is captured again and the extracted feature template is compared with the ones already existent in the database to determine a match. The specific record to be retrieved from the database is determined by the claimed identity of the user that is submitted to the system, usually via a magnetic stripe card, login name, or smart card [45].

A.3 Performance Evaluation

Due to the variations existing within any biometric signal, a biometric authentication or recognition system cannot give an absolute answer about the individual's identity; instead it provides the individual's identity information with a certain *confidence level*. This is contrary to traditional authentication systems (for example, a password system) where the



Figure A.5: Examples of intraclass variation. These are eight different fingerprint impressions (biometric signals) of the same finger (individual). Note that huge differences of image contrasts, locations, rotations, sizes, and qualities, exist among them.

match has to be exact and an absolute “yes” or “no” answer is returned. The biometric signal variations of an individual are usually referred to as *intra*class variations (Figure A.5); whereas variations between different individuals are called *inter*class variations.

A biometric matcher takes two biometric signals, B_I and B_J , and returns a similarity measurement $S(B_I^T, B_T^T)$ (without loss of generality, $0 \leq S(B_I^T, B_T^T) \leq 1$) as the result. As $S(B_I^T, B_T^T)$ becomes closer to 1, the matcher recognizes more confidently that both biometric signals come from the same individual; as $S(B_I^T, B_T^T)$ becomes closer to 0, the matcher recognizes that both biometric signals come from the same individual with lesser confidence. Generally, the identity of a submitted biometric signal is either a *genuine type* or an *impostor type*; hence, there are two statistical distributions of similarity scores, which

are called genuine distribution and impostor distribution (Figure A.6). Each type of input identity has one of the two possible results, “accept” or “reject”, from a biometric matcher. Consequently, there are four possible outcomes:

1. a genuine individual is accepted;
2. a genuine individual is rejected;
3. an impostor individual is accepted;
4. an impostor individual is rejected.

The first and fourth outcomes are correct while the second and third outcomes represent the error situations. The second outcome is referred to as “false reject” and the corresponding error rate is called false reject rate (FAR); the third outcome is referred to as “false accept” and the corresponding error rate is called false reject rate (FRR). They are the most widely used measurements in today’s commercial environment. Given a genuine distribution, p_g , and impostor distribution, p_i , the FAR and FRR at threshold th is given by

$$FAR(T) = \int_{th}^1 p_i(x)dx \quad (A.1)$$

$$FRR(T) = \int_0^{th} p_g(x)dx \quad (A.2)$$

Strict tradeoff exists between FAR and FRR in every biometric system [31]. Both FAR and FRR are actually functions of threshold th . When th decreases, the system would have more tolerance to intraclass variations and noise, however the FAR will increase. Similarly, if the value of th is lower, the system would be more secure and the FRR decreases.

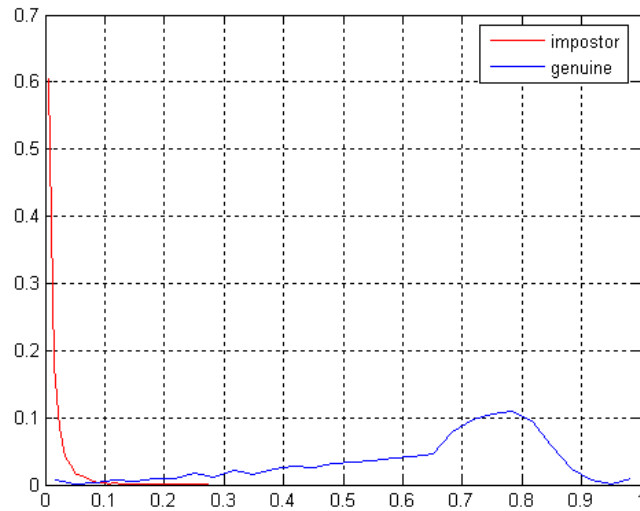
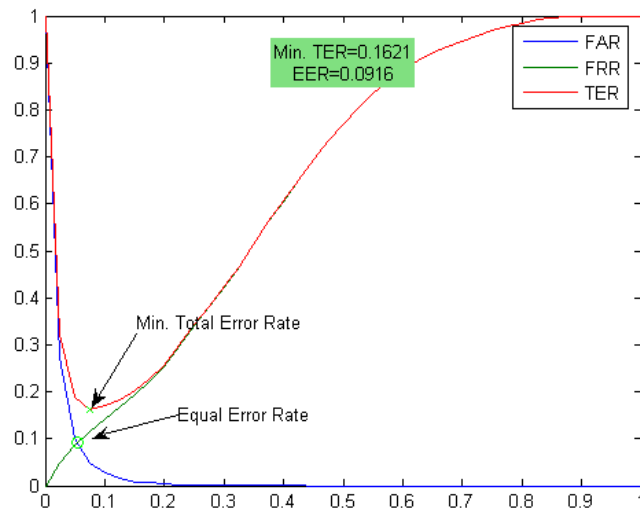


Figure A.6: Example of genuine and impostor distributions.

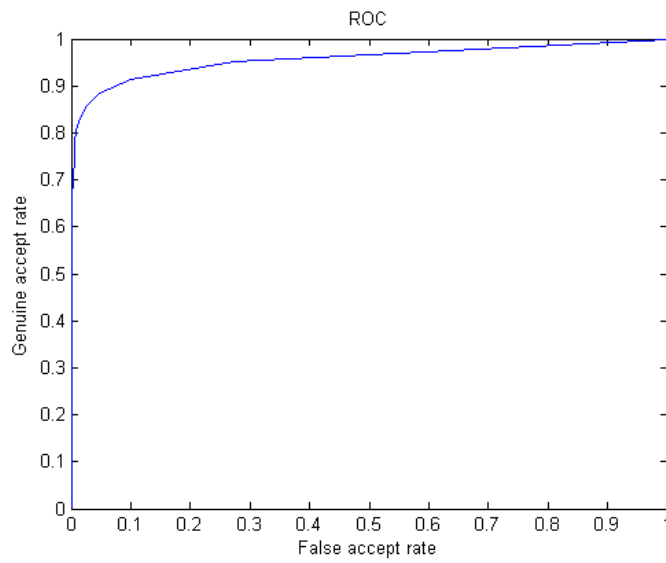
Depending on the nature of an application, the biometric system may be chosen to operate at low FAR configuration (for example, login process in ATMs), or to operate at low FRR configuration (for example, the access control system for a library). A system designer may have no prior knowledge about the nature of the application in which the biometric system is to be applied, thus it is helpful to report the system performance at all possible operating points (thresholds). A *Receiver Operating Characteristic* (ROC) curve is obtained by plotting FAR(x-axis) versus 1-FRR(y-axis) at all thresholds. Figure A.7 displays the typical curves of FAR, FRR, and ROC.

Other useful performance measurements are:

- **Equal Error Rate (EER)**: the error rate where FAR equals to FRR.



(a)



(b)

Figure A.7: Examples of (a) FAR and FRR curves; (b) ROC curve.

- **ZeroFNMR:** the lowest FAR at which no false reject occurs.
- **ZeroFMR:** the lowest FRR at which no false accept occurs.
- **Failure To Capture Rate:** the rate at which the biometric acquisition device fails to automatically capture the biometric signals. A high failure to capture rate makes the biometric system hard to use.
- **Failure To Enroll Rate:** the rate at which users are not able to enroll in the system. This error mainly occurs when the biometric signal is rejected due to its poor quality.
- **Failure To Match Rate:** occurs when the biometric system fails to convert the input biometric signal into a machine readable/understandable biometric template. Unlike FRR, a failure to match the error occurs at a stage prior to the decision making stage in a biometric system.

Appendix B

Overview of Fingerprints

Among all the biometrics, fingerprint is the most established and well studied. Archaeological evidence has shown that our forefathers noticed the individuality of fingerprints about five thousand years ago (3000 B.C.) [61]. From the early twentieth century, fingerprint recognition has been officially accepted as a valid personal identification method and has become a standard forensic routine. In the 1960s, the invention of *live-scan devices* became an important turning point in modern fingerprint technology. When the FBI announced its plan to stop using paper fingerprint cards in their integrated automatic fingerprint identification system (IAFIS) sites, automatic fingerprint recognition technologies developed beyond the forensic domain and stepped into civilian applications.

For the purpose of personal identification, fingerprint has several advantages in terms of the required properties for human recognition that are described in Section A. Moreover, fingerprints are better than other biometrics in some ways. The advantages of fingerprint-

based human recognition are:

- **High universality:** Every individual within the human population has fingerprints, thus can be used for easy authentication.
- **High uniqueness:** Even identical twins who share the same DNA structures have been shown to have different fingerprints. Study has shown that identical twins tend to have fingerprints that are similar globally, i.e. have the same fingerprint classes (e.g. loop, whorl, tent, etc.), but the ridge structures are very different in the detail (minutia) level [48].
- **High permanence:** The ridge patterns on the surface of the finger are formed in the foetal stage and remain structurally unchanged throughout a person's life time except in the case of severe burns or deep physical injuries [70, 56]. Some biometrics like face, voice or gait may change with time, and the template databases need to be update accordingly. This also shows that fingerprint is perhaps more suitable than DNA as a human recognition method.
- **High Indispensability:** Using fingerprints for human identification does not lead to problems of being lost or stolen, as in token-based authentications. Moreover, fingerprints would never be forgotten like PINs, passwords, or other knowledge-based systems. In most cases, fingerprints would accompany the individual throughout his/her life time unless there is some serious injury to their fingers.

- **High collectability:** Fingerprints are easily collected compared to other biometric signals, such as retina, iris, DNA, etc. which require complete cooperation and high-cost special equipment to obtain the biometric signals. With today's "live-scan" technologies in fingerprint sensors, high resolution images of the finger surface can be captured within seconds [70]. Furthermore, this process requires minimal or no user training and can be collected easily from cooperative or non cooperative users.
- **Good storability:** Fingerprints can be easily stored in a database. The required storage space depends on the representation of fingerprints that is chosen for the system. Usually, the fingerprint template size is less than 500 bytes, however, depending on the application and fingerprint representation, sizes of fingerprint data can range from 52 bytes (www.tssi.co.uk) to several megabytes (high resolution gray scale image).
- **Difficult to circumvent:** Combined with techniques of cryptographic and vitality detection, fingerprint systems become quite difficult to circumvent [70].

In practice, there are other important properties:

- **High performance:** Although iris recognition is the most accurate biometric technology, it has a higher false reject rate (FRR) due to the requirements of users to be fully cooperative and well trained. Fingerprints remain one of the most accurate biometric modalities available to date while considering both false accept rate (FAR) and false reject rate (FRR).

- **Wide acceptability:** Since the beginning of the twentieth century, fingerprints have been formally accepted as a valid personal identification trait and have become a standard routine in forensics.

B.1 History of Fingerprints

Archaeologists have discovered many historical items and artifacts that have human fingerprints on them. The earliest instances of purposely impressed fingerprints were made about 5000 years ago (in Mesopotamia, about 3000 B.C.) [61]. In addition, a prehistoric picture writing of a hand with ridge patterns was discovered in Nova Scotia, and fingerprint impressions were found on a standing stone on Goat Island. Although these impressions, drawings, and carvings might not be used to indicate identity, they provide evidence to show that ancient people were aware of the individuality of fingerprints[61]. It was common practice for the Chinese to use inked fingerprints on official documents, land sales, contracts, loans and acknowledgments of debts. The oldest existing documents is dated as far back as 300 BC[61], and it was still an effective practice until recent times. The first scientific paper on fingerprints was published in 1684 by an English plant morphologist Dr. Nehemiah Grew, that mainly reported his systematic study of the ridge, furrow, and pore structure in fingerprints. Since then, many researchers have invested efforts in the study of fingerprints. In 1788, Mayer made a study on detailed description of the anatomical formations of the fingerprint, in which many fingerprint ridge characteris-

tics were identified[74]. In 1823, Professor Johannes Evangelist Purkinje published the most detailed description of fingerprints to have appeared anywhere up to that time. Professor Purkinje's thesis entitled "*A Commentary on the Physiological Examination of the Organs of Vision and the Cutaneous System*" describes, with illustrations, nine fingerprint patterns classified in Latin[17]. Some of his classifications refer to the same classes which Henry would later name arches, tented arches, loops, wholes and twinned loops. However, Purkinje did not associate friction ridges to a means of personal identification. Sir William Herschel[34] was the first individual to use fingerprints on a large scale, in 1858. He was a British government official in India. He used the right index and middle fingerprints on every contract made with the locals. At first, the idea was simply that the physical contact with an official document might discourage attempts of cheating. As his fingerprint collections grew, he began to notice that the inked impressions were unique to individuals and remain unchanged throughout the individual's life. At approximately the same time, Dr. Henry Faulds, a Scottish doctor living in Japan, took up the study of *skin-furrows* after noticing finger marks on specimens of prehistoric pottery. He discussed fingerprints as a means of personal identification, and the use of printers ink as a method for obtaining such fingerprints. By chance, he was asked to help investigate a crime and solved it by using the fingerprints that were left at the scene. It was the first time a crime was solved based on fingerprint evidence[54]. In the late nineteenth century, Sir Francis Galton conducted an extensive study of fingerprints after Charles Darwin passed Faulds' discovery to him. In 1888, Sir Francis Galton first introduced the minutiae features for fingerprint matching and

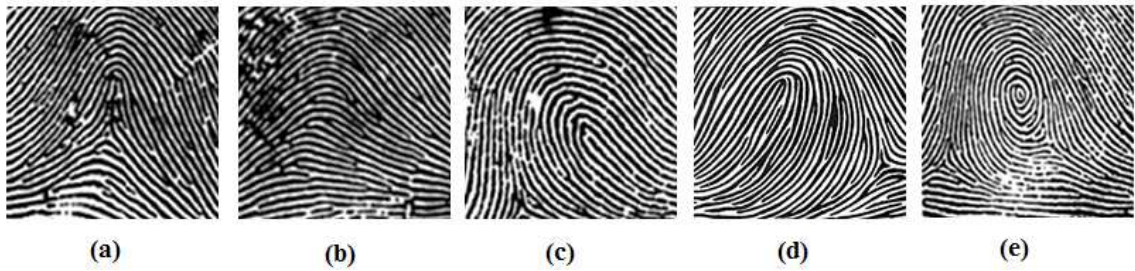


Figure B.1: Example of Fingerprint Classes: (a)Tented Arch (b)Arch (c)Right Loop (d)Left Loop (e)Whorl

the study of the uniqueness of fingerprints[27, 54, 61]. His work also contained the first system for fingerprint classification. He proposed three classes: arch, loop and whorl[27]. An important advance in the study of fingerprint was made by Sir Edward Henry (actually two of his assistants in India) in 1899. He continued Galton's work on fingerprint classification and created the now famous *Henry System* of fingerprint classification, which subdivided the three main classes of Galton's study into more specific sub-classes (Figure B.1) [33, 106]. He also introduced the *core* and *delta* points of fingerprints and used them for fingerprint classification (Figure B.2). Till today, the *Henry System* is still the basis of modern fingerprint classification schemes. In 1901, the first fingerprint office was established by Sir Edward Henry in England and Wales. The first official use of fingerprints was in the USA by the New York City Civil Service Commission in 1902. At that time, fingerprint recognition had been formally accepted as a valid personal identification and became a standard routine in forensics. In the early of twentieth century, the characteristics of fingerprints were well understood, as:



Figure B.2: Core and delta points in a fingerprint. The circle denotes the core point and the triangle denotes the delta point.

- epidermal ridges and valleys have different characteristics for each fingerprint;
- the configurations of every fingerprint vary within a limited range, thus can be classified;
- the fingerprint patterns remain structurally unchanged throughout one's lifetime.

As fingerprint recognition technologies were accepted and developed worldwide, criminal fingerprint databases got established. In early 1960s, the Federal Bureau of Investigation (FBI) started to develop automatic fingerprint identification systems (AFISs) because of the increasing process requests, enlarged databases, and advanced technologies. Their efforts on AFIS were so successful that almost every law enforcement agency worldwide uses

it. Moreover, in the late 1960s, fingerprint technology met one of the most important turning points in the invention of *live-scan* technology. This is the method to obtain the fingerprint image without the use of print ink. The success of *live-scan* technology and AFISs made automatic fingerprint recognition technologies grow rapidly. In 1968, one security company in Wall Street had already used fingerprint recognition technology for secure authentication[41, 61].

Today, automatic fingerprint technologies are used in many fields, such as physical access control, medical, financial, e-business, and forensic applications, for secure and effective identity authentication.

B.2 Fingerprint Acquisition

Fingerprint images can be classified by their acquisition methods as either inked (off-line) or live-scanned (on-line) images. Ink-technique is mainly used in forensic applications. This technique has a possible advantage over *rolled* images, which contain the whole fingerprint pattern with more information than flat impressions. Nowadays, AFIS has already integrated *live-scan* scanners into the system, thus those inked images need be converted into digital form and stored in a database for automatic fingerprint verification.

Live-scan technology is one of the main contributors to the extraordinary progress of fingerprint recognition. Especially the invention of user-friendly, low-cost, reliable, and compact fingerprint scanners, which makes fingerprint recognition technologies rapidly



Figure B.3: Various commercial *live-scan* fingerprint scanners.

expand into civilian applications. *Live-scan* scanners (Figure B.3) are able to obtain fingerprint images in real-time. *Live-scan* fingerprint scanners can be classified as follows:

- **Optical Sensors:** Most of the optical sensors are based on *Frustrated Total Internal Reflection (FTIR)* technique to acquire the fingerprint image. This is the oldest and most widely used technology and is fairly inexpensive. In this technique, a finger touches the top side of a glass prism and a light source illuminates the fingerprint from one side of the prism. On the other side of the prism, a CCD or CMOS image sensor is used to digitize the fingerprint image (Figure B.4). Because of the internal reflection phenomenon, most of the light entering the prism is reflected on the other side, but scattered randomly when it meets the fingerprint surface. Thus, the resulting fingerprint images are dark at ridges and bright at valleys. Several variations, such as using plastic prism or a sheet prism to replace the glass prism exist to reduce the costs and size of the devices. However, the acquired image is usually lower in quality compared to those obtained by a glass-prism sensor. Optical sensors also use fiber-optical platen instead of prisms, but may result in higher cost.

This technique relies on the contact of the finger with sensors to produce the fingerprint image. Hence the skin condition (dry or wet) affects image quality. Because a three-dimensional surface is sensed, it cannot be easily spoofed by presenting a photocopy of a fingerprint. However, fake fingers spoof most commercial sensors.

- **Capacitive Sensors:** This type of sensor utilizes a two-dimensional silicon-based

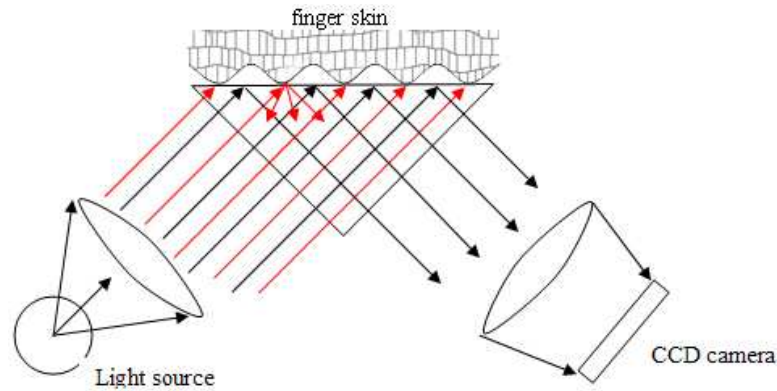


Figure B.4: General schematic for an FTIR based optical sensor

sensor array (Figure B.5). Depending on the distances between the skin surface and each of the silicon plates, varying electrical charges are generated. The sensor reads each capacitor's value and then converts them into an 8-bit grayscale image. Capacitive sensors reduce both the cost and size of a *live-scan* scanner [70], to be used on various electrical devices. Since the user directly touches the surface of a capacitive sensor, the size of the sensor has to be the same as the required fingerprint image. While a large silicon sensor may cost more than an optical one, the very small sensor areas significantly reduce the recognition rate [49]. Because of the direct contact with the skin the sensors need to be cleaned regularly and carefully. The chance of damaging the thin protecting coating of the sensor by electrostatic discharges, chemical corrosion, and physical scratches is increasing.

Like optical sensors, capacitive sensors can be spoofed by a fake finger but not by a photocopy, since the sensing must be performed on a three-dimensional surface.

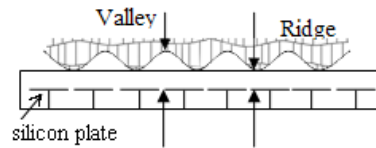


Figure B.5: Capacitive sensing.

-
- **Ultrasound Sensors:** Ultrasonic fingerprint scanners produce high quality images. Ultrasound waves are sent towards the finger and the echo signals bounce back from the finger skin. Due to the penetration ability of a sound wave, ultrasound-based scanners can produce a high quality fingerprint image without artifacts that are introduced by ink, dirt, grease, or moisture on the finger. This technology provides images with very high resolution. Moreover, it can be configured to prevent attacks from a fake finger by identifying a unique ultrasound signature of the human skin (www.ultra-scan.com). However, mechanical parts make the scanners large in size. Hence, the applications on hand-held/portable devices are limited.
 - **Thermal Sensors:** These sensors are made of pyro-electric materials whose properties change with temperature. The miniature size of the scanner makes it useful in many applications. The thermal scanner measures the temperature difference when the finger contacts the sensor. Since the air (valleys) and skin (ridges) have different thermal conductivities, the temperature differences are amplified and used to create the fingerprint image. Thermal equilibrium is reached quickly causing the image to disappear once the temperature is stabilized. Sweeping the finger through the thermal

sensor continuously can break the thermal equilibrium and hence can produce a stable image. However, a first-time user may have difficulties to maintain a steady speed while sweeping the finger. Moreover, the reconstruction of full fingerprint images is time consuming and error prone.

- **Other Types:** Sensors utilize other techniques, such as using high-quality cameras, electric field, or piezoelectric materials exist but are not mature enough for large scale applications.

Bibliography

- [1] A.S. Abutaleb and M. Kamel. A genetic algorithm for the estimation of ridges in fingerprints. *IEEE Transactions on Image Processing*, 8(8):1134–1138, 1999.
- [2] Canada Border Services Agency. CANPASS: streamlines customs clearance for frequent travellers. <http://www.cbsa-asfc.gc.ca/travel/canpass/menu-e.html>, 2004.
- [3] C. Arcelli and G.S.D. Baja. A width independent fast thinning algorithm. *IEEE Transactions on Pattern Analysis and Machine Intelligence*, 4(7):463–474, 1984.
- [4] O. Baruch. Line thinning by line following. *Pattern Recognition Letter*, 8(4):271–276, 1988.
- [5] A.M. Bazen and S.H. Gerez. An intrinsic coordinate system for fingerprint matching. In *Proc. Int. Conf. on Audio- and Video-Based Biometric Person Authentication (3rd)*, pages 198–204, 2001.
- [6] A.M. Bazen and S.H. Gerez. Systematic methods for the computation of the directional fields and singular points of fingerprints. *IEEE Transactions on Pattern*

Analysis and Machine Intelligence, 24(7):905–919, 2002.

- [7] Asker M. Bazen and Sabih H. Gerez. Fingerprint matching by thin-plate spline modeling of elastic deformations. *Pattern Recognition*, 36(8):1859–1867, 2003.
- [8] Christopher M. Brislawn and Jonathan N. Bradley. The FBI compression standard for digitized fingerprint images. In *Proceeding of SPIE*, volume 2847, pages 344–355, August 1995.
- [9] J.H. Chang and K.C. Fan. Fingerprint ridge allocation in direct gray-scale domain. *Pattern Recognition*, 34(10):1907–1925, 2001.
- [10] S.H. Chang, F.H. Cheng, W.H. Hsu, and G.Z. Wu. Fast algorithm for point pattern-matching: Invariant to translations, rotations and scale changes. *Pattern Recognition*, 30(2):311–320, 1997.
- [11] Z. Chen and C.H. Kuo. A topology-based matching algorithm for fingerprint authentication. In *Int. Carnahan Conf. On Security Technology (25th)*, pages 84–87, 1991.
- [12] S. Chikkerur, C. Wu, and V. Govindaraju. A systematic approach for feature extraction in fingerprint images. In *International Conference on Biometric Authentication*, 2004.
- [13] Sharat S. Chikkerur. Online fingerprint verification. Master’s thesis, University at Buffalo, the State University of New York, 2005.

- [14] Roger Clarke. Human identification in information systems: management challenges and public policy issues. *Information Technology & People*, 7(4):6–37, December 1994.
- [15] L. Coetzee and E. C. Botha. Fingerprint recognition in low quality images. *Pattern Recognition*, 26(10), 1993.
- [16] Thomas H. Cormen, Charles E. Leiserson, and Ronald L. Rivest. *Introduction to algorithms*. McGraw-Hill Book Company, New York, 1998.
- [17] H. Cummins and R. Kennedy. Purkinjes' observations (1832) on fingerprints and other skin features. *American Journal of Police Science*, 31(3), 1940.
- [18] Joseph M. Cychosz. Efficient binary image thinning using neighborhood maps. *Graphics gems IV*, pages 465–473, 1994.
- [19] J.G. Daugman. Two-dimensional spectral analysis of cortical receptive field profiles. *Vision Research*, 20:847–856, 1980.
- [20] C. Domeniconi, S. Tari, and P. Liang. Direct gray scale ridge reconstruction in fingerprint images. In *Int. Conf. Acoustic Speech and Signal Processing*, 1998.
- [21] Liju Dong and Ge Yu. An optimization-based approach to image binarization. In *Computer and Information Technology, 2004. CIT '04. The Fourth International Conference on*, pages 165–170, Sept. 2004.

- [22] Richard O. Duda, Peter E. Hart, and David G. Stork. *Pattern Classification*. John Wiley & Sons Pte. Ltd., 2nd edition, 2002.
- [23] J. Edmonds and R. Karp. Theoretical improvements in algorithmic efficiency for network flow problems. *Journal of ACM*, pages 248–264, 1972.
- [24] A.P. Fitz and R.J. Green. Fingerprint classification using hexagonal fast fourier transform. *Pattern Recognition*, 29(10):1587–1597, 1996.
- [25] L. R. Ford and D. R. Fulkerson. *Flows In Networks*. Princeton University Press, Princeton NJ, 1962.
- [26] D. Gabor. Theory of communication. *Journal of IEE*, 93:429–457, 1946.
- [27] Francis Galton. *Finger Prints*. McMillan, London, 1892.
- [28] M. D. Garris, C. I. Watson, R. M. McCabe, and C. L. Wilson. User’s guide to nist fingerprint image software (NFIS). Technical Report NISTIR 6813, National Institute of Standards and Technology, 2002.
- [29] Robert S. Germain, Andrea Califano, and Scott Colville. Fingerprint matching using transformation parameter clustering. *IEEE Computational Science & Engineering*, 4(4):42–49, Oct. 1997.
- [30] A. V. Goldberg. An efficient implementation of a scaling minimum-cost flow algorithm. *Journal of Algorithm*, 22(1):1–29, 1997.

- [31] M. Golfarelli, D. Maio, and D. Malton. On the error-reject tradeoff in biometric verification systems. *IEEE Transactions on Pattern Analysis and Machine Intelligence*, 19(7):786–796, 7 1997.
- [32] Ronald J. Hays. Immigration and naturalization service’s passenger accelerated service system (INSPASS). <http://www.biometrics.org/REPORTS/INSPASS.html>, 1996.
- [33] Edward Henry. *Classification and Uses of Finger Prints*. Routledge, London, 1900.
- [34] William J. Herschel. Skin furrows of the hand. *Nature*, 76, 1880.
- [35] L. Hong, Y. Wang, and A. K. Jain. Fingerprint image enhancement: Algorithm and performance evaluation. *Transactions on PAMI*, 21(4):777–789, August 1998.
- [36] P.V.C. Hough. Machine analysis of bubble chamber pictures. In *Int. Conf. on High Energy Accelerator and Instrumentation*, 1959.
- [37] A. Hrechak and J. McHugh. Automated fingerprint recognition using structural matching. *Pattern Recognition*, 23(8):893–904, 1990.
- [38] Ching-Tang Hsieh, Eugene Lai, and You-Chuang Wang. An effective algorithm for fingerprint image enhancement based on wavelet transform. *Pattern Recognition*, 36(2):303–312, 2003.

- [39] D.C.D Hung. Enhancement and feature purification of fingerprint images. *Pattern Recognition*, 26(11):1661–1671, 1993.
- [40] N. Ideda, M. Nakanishi, K. Fujii, T. Hatano, S. Shigenmatsu, T. Adachi, Y. Okazaki, and H. Kyuragi. Fingerprint image enhancements by pixel-parallel processing. In *Proc. Int. Conf. on Pattern Recognition (16th)*, volume 3, pages 752–755, 2002.
- [41] Raviraj Technologies Inc. India. Biometrics fingerprint technology. http://www.ravirajtech.com/biometrics_fingerprint_technology.html.
- [42] American National Standards Institute. Common biometric exchange file format (<http://www.itl.nist.gov/div895/isis/bc/cbeff/>).
- [43] American National Standards Institute. American national standard for information systems, data format for the interchange of fingerprint information, 1993. Doc# ANSI/NIST-CSL 1-1993.
- [44] A. Jain, Lin Hong, and R. Bolle. On-line fingerprint verification. *IEEE Transactions on Pattern Analysis and Machine Intelligence*, 19(4):302–314, Apr. 1997.
- [45] A. K. Jain, L. Hong, S. Pankanti, and R. Bolle. An identity authentication system using fingerprints. *Proc. IEEE*, 85(9):1365–1388, 1997.
- [46] A.K. Jain, S. Prabhakar, L. Hong, and S. Pankanti. Filterbank-based fingerprint matching. *IEEE Transactions on Image Processing*, 9:846–859, 2000.

- [47] Anil K. Jain, Lin Hong, and Y. Kulkarni. F2ID: a personal identification system using faces and fingerprints. *Fourteenth International Conference on Pattern Recognition*, 2:1373–1375, August 1998.
- [48] Anil K. Jain, Salil Prabhakar, and Sharath Pankanti. Twin test: On discriminability of fingerprints. In *AVBPA '01: Proceedings of the Third International Conference on Audio- and Video-Based Biometric Person Authentication*, pages 211–216, London, UK, 2001. Springer-Verlag.
- [49] Tsai-Yang Jea, Viraj S. Chavan, Venu Govindaraju, and John K. Schneider. Security and matching of partial fingerprint recognition systems. In *Proceeding of SPIE*, volume 5404, pages 39–50, 2004.
- [50] Tsai-Yang Jea and Venu Govindaraju. A minutia-based partial fingerprint recognition system. *Pattern Recognition*, 2005.
- [51] X. Jiang and W.Y. Yau. Fingerprint minutiae matching based on the local and global structures. In *Int. Conf. on Pattern Recognition (15th)*, volume 2, pages 1042–1045, 2000.
- [52] X. Jiang, W.Y. Yau, and W. Ser. Minutiae extraction by adaptive tracing the gray level ridge of the fingerprint image. In *Proc. Int. Conf. on Image Processing*, volume 2, pages 852–856, 1999.

- [53] X. Jiang, W.Y. Yau, and W. Ser. Detecting the fingerprint minutiae by adaptive tracing the gray-level ridge. *Pattern Recognition*, 34(5):999–1013, 2001.
- [54] Eamonn Keogh. An overview of the science of fingerprints. *Anil Aggrawal's Internet Journal of Forensic Medicine and Toxicology*, 2(1), 2001.
- [55] Zsolt Miklós Kovács-Vajna. A fingerprint verification system based on triangular matching and dynamic time warping. *Transactions on Pattern Analysis and Machine Intelligence*, 22(11):1266–1276, 2000.
- [56] M. Kücken and A. C. newell. A model for fingerprint formation. *Europhysics Letters*, 68(1):141–146, 2004.
- [57] Paul Kwok. A thinning algorithm by contour generation. *Commun. ACM*, 31(11):1314–1324, 1988.
- [58] Y. Lamdan and H.J. Wolfson. Geometric hashing: A general and efficient model-based recognition scheme. In *Second International Conf. Computer Vision*, pages 238–249, 1988.
- [59] M.S. Landy, Y. Cohen, and G. Sperling. Hips: a Unix-based image processing system. *Computer Vision, Graphics, and Image Processing*, 25(3):331–347, 1984.
- [60] Dongjae Lee, Kyoungtaek Choi, and Jaihie Kim. A robust fingerprint matching algorithm using local alignment. In *16th International Conference on Pattern Recognition*, volume 3, pages 803–806, 2002.

- [61] H.C. Lee and R.E. Gaensslen. *Advance in Fingerprint Technology*. Elsevier, New York, 2nd edition, 2001.
- [62] M. Leung, W. Engeler, and P. Frank. Fingerprint image processing using neural network. In *Proc. IEEE Region 10 Conf. on Computer and Communication Systems*, volume 2, pages 582–586, 1990.
- [63] J. Liu, Z. Huang, and K. Chan. Direct minutiae extraction from graylevel fingerprint image by relationship examination. In *Proc. Int. Conf. on Image Processing*, volume 2, pages 427–430, 2000.
- [64] Jingping Liu. Algorithms for minimum-cost flows. http://www.csd.uwo.ca/gradstudents/jliu36/min_cost.pdf, 2003.
- [65] X. Luo and J. Tian. Knowledge based fingerprint image enhancement. In *Proc. Int. Conf. on Pattern Recognition (15th)*, volume 4, pages 783–786, 2000.
- [66] X. Luo, J. Tian, and Y. Wu. A minutia matching algorithm in fingerprint verification. In *International Conference on Pattern Recognition*, volume 4, pages 833–836, 2000.
- [67] S. Madhvanath, G. Kim, and V. Gocindaraju. Chain code processing for handwritten word recognition. *IEEE Transactions on Pattern Analysis and Machine Intelligence*, 21:928–932, 1997.

- [68] D. Maio and D. Maltoni. Direct gray scale minutia detection in fingerprints. *IEEE Transactions on Pattern Analysis and Machine Intelligence*, 19(1), 1997.
- [69] D. Maio, D. Maltoni, R. Cappelli, J.L. Wayman, and A.K. Jain. FVC2002: Second fingerprint verification competition. In *Int. Conf. on Pattern Recognition (16th)*, volume 3, pages 811–814, 2002.
- [70] Davide Maltoni, Dario Maio, Anil K. Jain, and Salil Prabhakar. *Handbook of Fingerprint Recognition*. Springer, 2003.
- [71] Amit Mhatre, Srinivasa Palla, Sharat Chikkerur, and Venu Govindaraju. Efficient search and retrieval in biometric databases. In *SPIE Defence and Security Symposium*, 2005.
- [72] Dinesh P. Mital and Eam Khwang Teoh. An automated matching technique for fingerprint identification. In *First Int. Conf. on Knowledge-Based Intelligent Electronic Systems*, volume 1, pages 142–147, 1997.
- [73] B. Moayer and K. Fu. A tree system approach for fingerprint pattern recognition. *IEEE Transactions on Pattern Analysis and Machine Intelligence*, 8(3):376–388, 1986.
- [74] A. Moenssens. *Fingerprint Techniques*. Chilton, London, 1971.
- [75] Christian Neusius and Jan Olszewski. A noniterative thinning algorithm. *ACM Trans. Math. Softw.*, 20(1):5–20, 1994.

- [76] Emma Newham. *The Biometrics Report*. SJB Services, 1995.
- [77] L. O’Gormann and J.V.Nickerson. An approach to fingerprint filter design. *Pattern Recognition*, 22(1):29–38, 1989.
- [78] N. Otsu. A threshold selection method from gray level histograms. *IEEE Transactions on Systems, Man and Cybernetics*, 9:62–66, 1979.
- [79] Sharath Pankanti, Salil Parabhakar, and Anil K. Jain. On the individuality of fingerprint. *IEEE Transactions on Pattern Analysis and Machine Intelligence*, 24(8):1010–1025, 2002.
- [80] Salil Prabhakar, Anil Jain, and Sharath Pankanti. Learning fingerprint minutiae location and type. *Pattern Recognition*, 36(8):1847–1857, 2003.
- [81] A. Ranade and A. Rosenfeld. Point pattern matching by relaxation. *Pattern Recognition*, 12(2):269–275, 1993.
- [82] Nalini K. Ratha, Jonathan H. Connell, , and Ruud M. Bolle. An analysis of minutiae matching strength. In *AVBPA ’01: Proceedings of the Third International Conference on Audio- and Video-Based Biometric Person Authentication*, pages 223–228, London, UK, 2001. Springer-Verlag.
- [83] N.K. Ratha, R.M. Bolle, V.D. Pandit, and V. Vaish. Robust fingerprint authentication using local structural similarity. In *Fifth IEEE Workshop on Applications of Computer Vision*, pages 29–34, 2000.

- [84] N.K. Ratha, S.Y. Chen, and A.K. Jain. Adaptive flow orientation-based feature extraction in fingerprint images. *Pattern Recognition*, 28(11):1657–1672, 1995.
- [85] N.K. Ratha, K. Karu, Shaoyun Chen, and A.K. Jain. A real-time matching system for large fingerprint databases. *IEEE Transactions on Pattern Analysis and Machine Intelligence*, 18:799 – 813, August 1996.
- [86] Arun Ross and Anil K. Jain. Information fusion in biometrics. *Pattern Recognition Letters*, 24:2115–2125, 2003.
- [87] Greenberg S., Aladjem M., Kogan D., and Dimitrov I. Fingerprint image enhancement using filtering techniques. In *International Conference on Pattern Recognition*, volume 3, pages 326–329, 2000.
- [88] M. Sezgin and B. Sankur. Survey over image thresholding techniques and quantitative performance evaluation. *Journal of Electronic Imaging*, 13(1):146–165, Jan. 2004.
- [89] B. G. Sherlock, D. M. Monro, and K. Millard. Fingerprint enhancement by directional fourier filtering. *Vision, Image and Signal Processing, IEE Proceedings*, 141:87–94, April 1994.
- [90] A. Sherstinsky and R. W. Picard. Restoration and enhancement of fingerprint images using m-lattice. In *International Conference on Pattern Recognition*, pages 195–200, 1994.

- [91] Robert Snelick, Mike Indovina, James Yen, and Alan Mink. Multimodal biometrics: issues in design and testing. In *ICMI '03: Proceedings of the 5th international conference on Multimodal interfaces*, pages 68–72, New York, NY, USA, 2003. ACM Press.
- [92] P. T. Sokkalingam, R. K. Ahuja, and J. B. Orlin. New polynomial-time cycle-canceling algorithms for minimum-cost flows. *Networks*, 36:53–63, 2000.
- [93] R.M. Stock and C.W. Swonger. Development and evaluation of a reader of fingerprint minutiae. Technical Report XM-2478-X1:13-17, Cornell Aeronautical Laboratory, 1969.
- [94] D. A. Stoney and J. I. Thornton. A critical analysis of quantitative fingerprint individuality models. *Journal of Forensic Sciences*, 31(4):1187–1216, October 1986.
- [95] M. Tico and P. Kuosmanen. A topographic method for fingerprint segmentation. In *Internal Conference on Image Processing*, pages 36–40, 1999.
- [96] O.D. Trier and T. Taxt. Evaluation of binarization methods for document images. *IEEE Transactions on Pattern Analysis and Machine Intelligence*, 17(3):312–315, Mar 1995.
- [97] V. Govindaraju V., Z. Shi, and J. Schneider. Feature extraction using a chaincoded contour representation. In *International Conference on Audio and Video Based Biometric Person Authentication*, 2003.

- [98] M.R. Verma, A.K. Majumdar, and B. Chatterjee. Edge detection in fingerprints. *Pattern Recognition*, 20:513–523, 1987.
- [99] A. Wahab, S.H. Chin, and E.C. Tan. Novel approach to automated fingerprint recognition. *IEE Proceedings Vision Image and Signal Processing*, 145(3):160–166, 1998.
- [100] Craig I. Watson, Michael D. Garris, Elham Tabassi, Charles L. Wilson, R. Michael McCabe, and Stanley Janet. User’s guide to NIST fingerprint image software 2 (NFIS2). Technical report, National Institute of Standards and Technology, 2002.
- [101] D.M. Weber. A cost effective fingerprint verification algorithm for commercial applications. In *Proc. South African Symp. on Communication and Signal Processing*, pages 99–104, 1992.
- [102] J.H. Wegstein. An automated fingerprint identification system. U.S. Government Publication, U.S. Dept. of Commerce, National Bureau of Standards, Washington, DC, 1982.
- [103] Andrew John Willis and L. Myers. A cost-effective fingerprint recognition system for use with low-quality prints and damaged fingertips. *Pattern Recognition*, 34(2):255–270, 2001.
- [104] Haim J. Wolfson and Isidore Rigoutsos. Geometric Hashing: An Overview. *IEEE Computational Science and Engineering*, 4(4):10–21, 1997.

- [105] C. Wu, Z. Shi, and V. Govindaraju. Fingerprint image enhancement using directional median filters. In *Proceeding of SPIE*, volume 5404, pages 66–75, 2004.
- [106] Neil Yager and Adnan Amin. Fingerprint classification: a review. *Pattern Analysis & Applications*, 7(1):77–93, April 2004.
- [107] J. Yang, L. Liu, T. Jiang, and Y. Fan. A modified Gabor filter design method for fingerprint image enhancement. *Pattern Recognition Letter*, 24:1805–1817, August 2003.